Chair of Reservoir Engineering

Master's Thesis

Impact of Fractures Networks on Gas-based EOR Methods

Nouri Alalim

May 2022

MONTANUNIVERSITÄT LEOBEN
www.unileoben.ac.at

AFFIDAVIT

I declare on oath that I wrote this thesis independently, did not use other than the specified sources and aids, and did not otherwise use any unauthorized aids.

I declare that I have read, understood, and complied with the guidelines of the senate of the Montanuniversität Leoben for "Good Scientific Practice".

Furthermore, I declare that the electronic and printed version of the submitted thesis are identical, both, formally and with regard to content.

Date 13.05.2022

Signature Author
Nouri Alalim

Nouri Alalim

Master Thesis 2022

Supervisor: Univ.-Prof. MSc. PhD Riyaz Kharrat

Impact of Fractures Networks on Gas-based EOR Methods

dpe DEPARTMENT PETROLEUM ENGINEERING

MONTAN UNIVERSITÄT

To my beloved family, brothers, sisters

, and my grandmother "Fatima Ender"

Declaration

I hereby declare that except where specific reference is made to the work of others, the contents of this dissertation are original and have not been published elsewhere. This dissertation is the outcome of my own work using only cited literature.

Erklärung

Hiermit erkläre ich, dass der Inhalt dieser Dissertation, sofern nicht ausdrücklich auf die Arbeit Dritter Bezug genommen wird, ursprünglich ist und nicht an anderer Stelle veröffentlicht wurde. Diese Dissertation ist das Ergebnis meiner eigenen Arbeit mit nur zitierter Literatur.

Nouri Alalim, 13 May 2022

Acknowledgments

I would like to thank my supervisor Prof. Riyaz Kharrat for his valuable guidance, time commitment, and encouragement that helped me to finish my research.

I also want to thank OMV Exploration & Production GmbH for giving me the opportunity to study in Austria.

My sincere thanks also go to my friend Milos Pejic for his support.

Finally, I would like to thank all the Petroleum Engineering Department members for the enjoyable experience.

Abstract

A Significant number of reservoirs that highly contribute to the global petroleum production and reserve are considered fractured reservoirs. Generally, to consider a reservoir as a naturally fractured reservoir, the fractures need to form an interconnected network. Dual continuum approaches are commonly used to simplify the modeling process. These models require assigning average properties, such as aperture, permeability, and matrix fracture interaction parameters.

In this study, a low permeability fractured reservoir with well-connected fracture networks (Major, Medium, and Minor) was investigated using the Discrete Fracture Model (DFN) provided in the CMG software. Different systematic models in 2 and 3 dimensions were defined for the gas-based enhanced oil recovery processes to investigate the impact of the different fracture network types on the recovery. Dimensionless numbers were used to link the properties of these different networks to the properties of the major fractures network.

The increase in the aperture ratios decreased the relative importance of the non-major fracture networks. Moreover, the magnitude of the impact was increased with the increase in the reservoir height for the assisted-gravity drainage mode. However, the increase in the intensity ratio decreased the relative importance of including the non-major fracture networks.

The results of the fracture networks indicated that the Foam Assisted Water Alternating Gas (FAWAG) process was more sensitive than the Assisted Water Alternating Gas (WAG) and the continuous gas injection (GI) process. Hence, the magnitude of the impact is process deepening. However, the impact magnitude for excluding these non-major fracture networks depends on other factors, such as the properties of reservoir fluids.

The homogenization process results indicated that the explicit representation of the homogenized fractures network provides a better capturing of the flow behavior than the pseudo-matrix option for using the standard dual continuum modeling approach. However, the hybrid modeling approach is recommended if the error is significant.

Zusammenfassung

Eine beträchtliche Anzahl von Lagerstätten, die in hohem Maße zur globalen Erdölförderung und -reserve beitragen, werden als zerklüftete Lagerstätten betrachtet. Um eine Lagerstätte als natürlich zerklüftetes Lagerstätte zu betrachten, müssen die Klüfte im Allgemeinen ein miteinander verbundenes Netzwerk bilden. Dual-Continuum-Ansätze werden häufig verwendet, um den Modellierungsprozess zu vereinfachen. Diese Modelle erfordern die Zuweisung von durchschnittlichen Eigenschaften wie Öffnungsweite, Permeabilität und Matrix-Kluft-Wechselwirkungsparametern.

In dieser Studie wurde eine zerklüftete Lagerstätte mit geringer Permeabilität mit gut verbundenen Kluftnetzwerken (Major, Medium und Minor Klüfte) unter Verwendung des in der CMG-Software bereitgestellten Discrete Fracture Model (DFN) untersucht. Für die gasbasierten Enhanced Oil Recovery-Prozesse wurden verschiedene systematische Modelle in 2D und 3D definiert, um den Einfluss der verschiedenen Kluftnetzwerktypen auf die Gewinnung zu untersuchen. Dimensionslose Kennzahlen wurden verwendet, um die Eigenschaften dieser unterschiedlichen Netzwerke mit den Eigenschaften des Hauptkluftnetzwerks zu verknüpfen.

Eine Erhöhung der Öffnungsweite verringerte die relative Bedeutung aller nicht-Major-Kluftnetzwerke. Darüber hinaus wurde der Einfluss mit der Erhöhung der Lagerstättenhöhe für den unterstützten Schwerkraftmodus (gravity draiange) erhöht. Die Erhöhung des Intensitätsverhältnisses verringerte jedoch die relative Bedeutung der Einbeziehung der nicht-großen Kluftnetzwerke.

Die Ergebnisse der Kluftnetzwerke zeigten, dass das Foam Assisted Water Alternating Gas (FAWAG) Verfahren empfindlicher war als das Assisted Water Alternating Gas (WAG) und das Continuous Gas Injection (GI) Verfahren. Daher ist das Ausmaß der Auswirkung eine Prozessvertiefung. Die Auswirkungsgröße zum Ausschließen dieser nicht-Major-Kluftnetzwerke hängt jedoch von anderen Faktoren ab, wie beispielsweise den Eigenschaften der Lagerstättenfluide.

Die Ergebnisse des Homogenisierungsprozesses zeigten, dass die explizite Darstellung des homogenisierten Kluftnetzwerks eine bessere Erfassung des Strömungsverhaltens bietet als die Pseudo-Matrix-Option für die Verwendung des standardmäßigen Dual-Continuum-

Modellierungsansatzes. Der hybride Modellierungsansatz wird jedoch empfohlen, wenn der Fehler signifikant ist.

Table of Contents

List of Figures

List of Tables

Abbreviations

CO_2	Carbon dioxide
CMG	Computer Modeling Group
DFM	Discrete Fracture Models
DFN	Discrete Fracture Network
DFS	Discrete Fracture Segment
DFU	Discrete Fracture Unite
DK	Dual porosity
DP	Dual permeability
EDFM	Embedded Discrete Fracture Models
EMI	Electrical Micro-Imager
EOR	Enhanced Oil Recovery
GAGD	Gas-assisted gravity drainage
FAWAG	Foam-assisted WAG
FMI	Formation Micro-Imager
PV	Pore Volume
PVT	Pressure-Volume Temperature analysis
Rd	Apertures ratio between primary and secondary fractures
Rd3	Apertures ratio between primary and tertiary fractures
Rn	The ratio between the number of primary fractures to the total number of primary and secondary fractures
SAGD	Steam assisted gravity drainage
WAG	Water alternative gas
3D	Three dimensions
2D	Two dimensions

Chapter 1

Introduction

Reservoir simulation is an essential assessment tool to support decision-making in modern reservoir management. The ability to forecast the reservoir response to the oil and gas recovery processes allows the selection of the most cost-effective method to maximize oil production. Therefore, an accurate fracture network characterization is essential for understanding the fluid flow behavior (Guerriero et al., 2013).

1.1 Background and Context

This research discusses and investigates the fractures networks' characteristics and their impacts on the recovery processes. A numerical model is used to build discrete fracture networks and simulate the gas-based recovery processes with a similar investigation framework presented by Gong & Rossen (2018) in their study on the impact of the fracture networks.

1.2 Scope and Objectives

This work aims to qualitatively investigate the impact of fractures networks sets on the recovery processes. These fracture networks have different fracture characteristics that might have a considerable effect on the flow pathways for the injected fluids; the including or the excluding of these fracture networks can consequently impact the assessment of the recovery process. In the typical and widely used dual continuum modeling approach, fracture characteristics are subjected to upscaling and homogenization processes to obtain the required inputs for the model. Depending on the deployed recovery process, these fracture characteristic inputs might need reconsideration in some cases. In this work, simplistic models are used to describe the impact of these fractures on the recovery by using dimensionless numbers.

1.3 Achievements

The impact of including different sets of fracture networks was investigated for the primary production process and the gas-based EOR processes. The relationship between these fracture networks was defined using dimensionless numbers that can be further developed to link the impact of the fracture's characteristics on the recovery mechanisms for each recovery process and describe the relative importance of considering these fracture sets in the modeling phase of fractured reservoirs.

1.4 Technical Issues

The CMG compositional simulator GEM is a widely used simulator for modeling the chemical EOR processes. However, the foam injection process was challenging to model in fine grids using the discrete fractures modeling approach. Each simulation run is computationally intensive and time-consuming with the normal processing power. In several cases, the simulator could not handle the numerical issues and terminated the simulation runs, consequently limiting the cases and the investigated parameters. Moreover, the limitations of the implicit-texture local-equilibrium approach can make the foam flooding results questionable until the results of an experimental work ascertain its validity.

1.5 Overview of Dissertation

This work starts with a review of the fracture's detection methods and characterization approaches, the main characteristics of the fracture, the impact of the fractures on the recovery processes, and the modeling approaches for the fractured reservoirs. Systematic cases were defined based on dimensionless numbers to investigate the impact of the fracture networks on the gas-based EOR methods that include immiscible gas injection and immiscible FAWAG method. The results and the discussion can provide a better understanding of the required consideration in the modeling process of fractured reservoirs on the field scale.

Chapter 2

Literature Review

2.1 Fractures capturing and detection

Fractures such as joints, faults, veins, and bedding planes are common in subsurface rocks and geological structures. These naturally occurring discontinuities control subsurface rocks' geomechanical and hydrological behavior, often forming complex networks. Therefore, understanding the potential impacts of these fractures is an essential issue in many engineering applications. In addition, the presence of these fractures can result in heterogeneity of the stress fields and channelizing fluid flow pathways. Therefore, reliable fracture models are highly needed. Different data sources are often used to characterize the fractures on different scales (Lei et al., 2017).

2.1.1 Geological detection

Small core samples and borehole logging tools detect the different scale fractures that intersect with the well. In contrast, the surface outcrops analogies allow mapping the fractures in two dimensions. However, the seismic surveys can also detect the relatively large-scale structural fractures in the three dimensions. Still, the current technology cannot identify widely spreading medium and small fractures because of the resolution limits. Therefore, characterizing the fractures geometries is highly subjected to extrapolating the data from these scales to the study domain. However, creating realistic fracture networks remains unresolved (Lei et al., 2017; Ukar et al., 2019).

Recent studies suggested that technologies and practices can improve the accuracy of detecting different fracture characteristics. Ukar et al. (2019), in their study for sandstone outcrops and core samples from Nikanassin formation, proposed guidelines for selecting representative outcrops and showed that additional features could be defined to prove the correspondence

between outcrop and core. These outcrops can then be used to quantify fracture characteristics such as structural location, distributions of height and length, and the relative/absolute fracture intensity, which are difficult to capture on a core scale. Aghli et al. (2020), in their study on the Asmari carbonate formation, have shown that the results of formation micro-imager (FMI) and electrical micro-imager (EMI) for fracture evaluation are more reliable than core data and can be used even if no core is available. The image logs can detect open and closed fractures. Generally, open fractures demonstrate conductive and sinusoidal traces in the electrical imaging logs, where these traces may be continuous or discontinuous. Depending on their aperture appearance and the continuity of the trace across the wellbore, these fractures can be classified into major, medium, and minor open fractures.

2.1.2 Stochastic analysis

The difficulties in measuring the natural-fractured systems in the three dimensions were highlighted in several previous studies. Therefore, statistical approaches are commonly suggested for the fractured network characterization by considering the fracture attributes such as the aperture and fracture density as random variables distributed within the rock volume based on experimentally established statistical models (Lei et al., 2017; Guerriero et al., 2013). The Baecher Stochastic model, also known as the "Poisson" modeling technique, has been implemented in commercial software and many studies. However, the conventional Baecher model tends to have large uncertainty due to the assumption of uniform spatial distribution, the simplification of fracture shape, and the neglection of the correlations between geometrical properties and topological relations. However, an enhanced version is often used (Lei et al., 2017; Gong & Rossen, 2017).

2.1.3 Hybrid Methods

Hybrid models are proposed for better fracture network creation. The models combine the advantages of different methods, such as using the geo-mechanical models. Several comprehensive studies have been carried out to understand the geological past of the natural fractures and the forming processes behind the field observations. The knowledge of fracture mechanics has promoted the creation of geo-mechanical-based models that include fracture growth physics as a response to stress and deformation to simulate fractures networks development. A discrete fracture network (DFN) simulator can replicate a natural fracture pattern that progressively solves stress disorders and captures the discrete fractures' nucleation, propagation, and coalescence using a geologically inferred palaeo-stress/strain condition. However, these hybrid modes are still a potential research area (Lei et al., 2017).

2.2 fractures characteristics

2.2.1 Fracture sets

Fractures can have similar characteristics in the same category, such as the origin of occurrence and the mechanical properties. Therefore, subsurface fractures are usually grouped into different discontinuity sets during the data acquisition stage. In the case of the systematic fracture sets, fractures in one discontinuity set are parallel to one another, which means they have a similar dip and dip direction and making them relatively easy to distinguish. Recognition of fracture sets primarily depends on pattern recognition expertise and capabilities. However, the minor differences in the attributes are typically overlooked to minimize the work complexity, simplify the modeling process, and reduce the required computational power (Wenli et al., 2019). An example of different fracture set identification is shown in Figure 1.

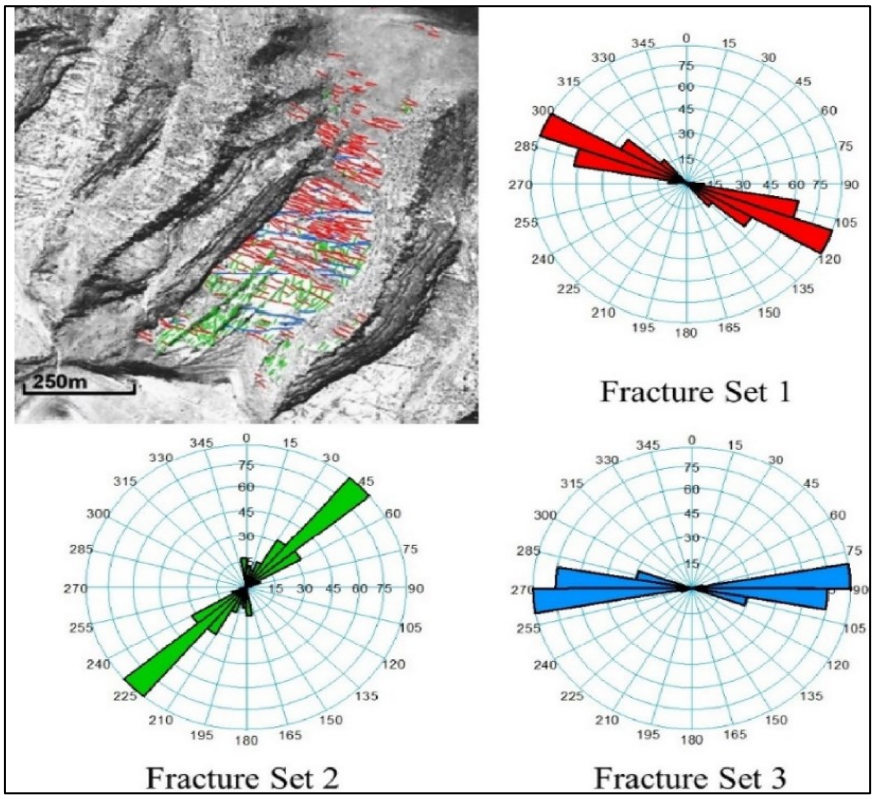

Figure 1: Example for identified fractures sets (Aljuboori et al., 2020)

2.2.2 Fracture orientation

Fracture orientation is an essential part of discrete fracture characteristics since it reflects the position of the joint rock surface. In three-dimensional space, the path of fractures usually consists of dip, dip direction, and rotation angle. The dips direction is an angle measured

clockwise from true north to the discontinuity plane (ranges 0– 360°), while on the other hand, the slope is the angle measured from the horizontal plane (ranges 0– 90°). However, Fractures are generally oriented according to a uniform, bootstrapped distribution or dips (Wenli et al., 2019).

2.2.3 Fracture location and density

Another important parameter for reproducing the discrete fracture networks is the fracture location. Fracture locations usually follow a uniform, gauss, or bootstrapped distribution. If the field data indicates that fractures are uniformly distributed, fracture density becomes the primary factor influencing fracture distribution in the domain. The frequency term is usually used to define the number of fractures and indicate the fractures' existence. However, there are three forms of fracture densities: linear density, areal density, and volumetric density (Wenli et al., 2019). Agada et al. (2016), in their study, for the Amellago Island outcrop as an analogy for Arab D carbonate formation, demonstrated that the fracture intensity could also be a bedding-related property, as shown in Figure 2, and only 30% of fractures have penetrated multiple beds.

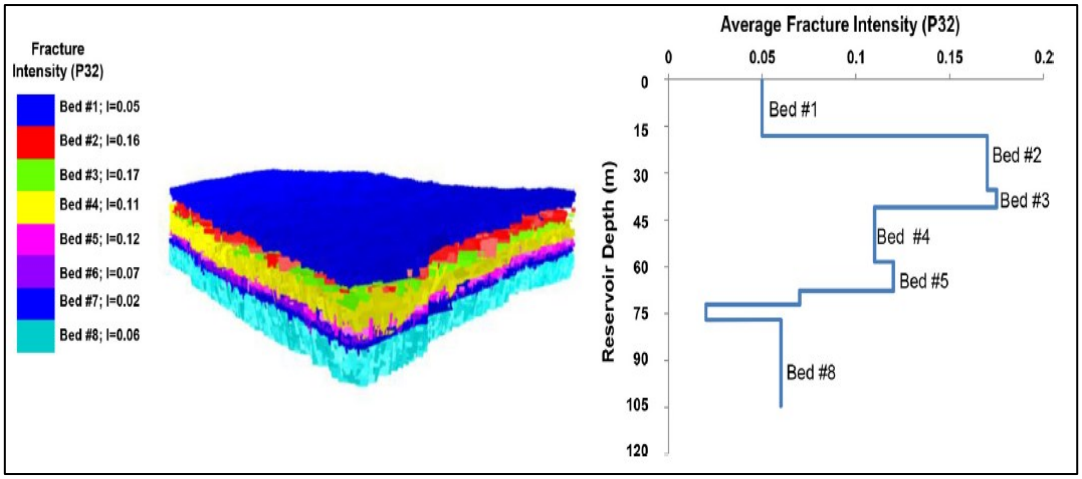

Figure 2: fractures intensity depending on Beds (Agada et al., 2016)

2.2.4 Fracture shape

One of the most challenging properties to be quantified correctly is the fracture shape, representing the fracture extent. Fracture persistence/shape is usually obtained by experience. Furthermore, the size of the fracture is closely related to the shape of the fracture and can be separated into two types: discs and polygons. The polygon shape can be more complex or simply assumed as a rectangle (Wenli et al., 2019; Gong & Rossen, 2017).

2.2.5 Fracture length and aperture

Generally, the flow behavior of fracture networks is controlled by fracture length and aperture. Stochastic models are a common option due to the uncertainties in data and the impact of cutoffs in measurements. Previous studies used the exponential, log-normal, and power-law distribution models to describe the fracture length. However, many researchers highlighted that the power-law distribution is currently the correct model to describe the fracture length (Gong & Rossen, 2017). However, the fracture length is commonly used to estimate the fracture aperture and porosity (Aljuboori et al., 2020).

Various aperture distribution models are commonly used, including log-normal and power-law distributions ranging from narrow to wide. Several studies and Field measurements suggested linking the fracture aperture to the fracture length with linear and non-linear relationships. However, it also follows the power-law distribution when the fracture aperture is proportional to the fracture length. Therefore, the fracture aperture can be used to estimate the fracture permeability by assuming that a fracture is a slit between a pair of smooth, parallel plates, which makes the aperture uniform along the fracture. Then, permeability can be defined as the cross-sectional area of the fracture. However, it is important to note that fracture aperture or length are not the only parameters that impact the flow behavior of the fracture network (Gong & Rossen, 2017).

2.3 Matrix-Fracture interaction

Natural fractures and pore systems have a variety of interaction behaviors, which can create different regions within a reservoir if the interaction of these systems is weak and their conductivity is different. The basis of hydrodynamics for fractured reservoirs is the percolation principle between multiple continuous domains. As a result, the initial production of these reservoirs can reach high levels. However, maintaining the production is difficult because of the complex structure of fracture networks of different levels, where channeling can easily occur in the displacement processes, leading to low recovery (Z.-X. Xu et al., 2020).

The fracture-matrix interaction is determined by the matrix properties such as porosity, permeability, wettability, and fracture network geometry characteristics. In addition, physical processes and displacement mechanisms also influence this interaction. The viscous, gravitational, and capillary forces govern the fracture–matrix fluid transfer during recovery processes such as water injection. The water-wet rock system supports the effective imbibition of water from the fractures to displace oil from the matrix by a counter-current or co-current mechanism, which can be a significant recovery mechanism in fractured reservoirs in some

cases. However, these mechanisms are less effective in a mixed-wettability, or oil-wet system as a faster increase in the water cut usually happens.

Nevertheless, considering the gravity effect can be important in assessing the phase of a recovery process. (Agada et al., 2016). Generally, gravity drainage is the main recovery mechanism from fractured reservoirs with a gas cap or during the gas injection processes. During the depletion process, pressure contrast between matrix blocks and surrounding fractures occurs due to the difference in the oil and gas phases' height resulting from the density difference between the two phases, which eventually promotes the fluid exchange between the two domains to achieve equilibrium conditions. This process enhances the recovery process from the matrix blocks (Aljuboori et al., 2020; Harimi et al., 2019).

The gravitational drainage process is highly subjected to the interaction between the adjacent matrix blocks, which two different phenomena can describe. The first one is the capillary continuity between the blocks. The second phenomenon is the liquid's re-infection from the upper blocks into the lower blocks. The capillary continuity between the blocks is essentially maintained by three mechanisms: porous asperity in fracture, thin liquid films around non-porous asperity, and liquid bridges in fracture. Natural asperities on the fracture surface of real fractured porous media may result in multiple contact points between the adjacent matrix blocks.

Moreover, when the fracture aperture is smaller than a critical value, the advancing liquid drains from the upper matrix block. As a result, it enters the upper face of the lower matrix block before the de-attachment from the upper blocks (Harimi et al., 2019). A recent study by Harimi et al. (2019) investigated the impact of the fracture aperture as the most sensitive parameter for fracture transmissibility. It highlighted that the fracture capillary pressure could reach levels comparable to matrix capillary pressure in narrower fracture apertures due to a liquid bridge. However, to avoid overestimating the transferred volumes between the matrix and fractures, the gravity drainage parameters should be investigated carefully and on a small scale (Aljuboori et al., 2020).

On a Field-scale, several studies and publications have discussed the classification of the fractured reservoirs into four groups: Type 1, Type 2, Type 3, and Type 4, which is also known as Type M. This classification is based on the interaction between the relative porosity and the permeability contributions from the fracture and the matrix systems (Allan & Sun, 2003; Bratton et al., 2006).

2.4 Impact of fractures on recovery processes

Available field data for fractured reservoirs indicated a typical behavior for high initial production flow rates, followed by a rapid decline in production, and low ultimate recovery, with considerable difficulty maintaining the production rates. These production characteristics for the fractured reservoirs often result in considering these reservoirs as difficult for the implementation of the recovery process (Allan & Sun, 2003; Luo & Mohanty, 2021). Moreover, the complexity of the natural fracture networks at various levels often results in the displacement process channeling and fingering for the injected fluid (Z.-X. Xu et al., 2020).

The gas injection has the widest range of applications as an enhanced oil recovery (EOR) process for various reasons, including the gas's availability and good injectivity compared to water or chemical EOR Methods. The miscible and immiscible gas injection can be a successful EOR process depending on reservoir conditions (Mogensen & Masalmeh, 2020).

Silva & Maini (2016) investigated the gas-assisted gravity drainage (GAGD) process using an experimental physical model, as shown in Figure 3. They concluded that the most important properties of this process are the storage and transmissibility capacities and the fracture's direction and intensity. This is because the production potential from the reservoir is determined by the storage and the transmissibility capacity, while the intensity and the direction of the fractures describe the flow pattern in the reservoir. Therefore, they are important factors in the assessment of this recovery mode.

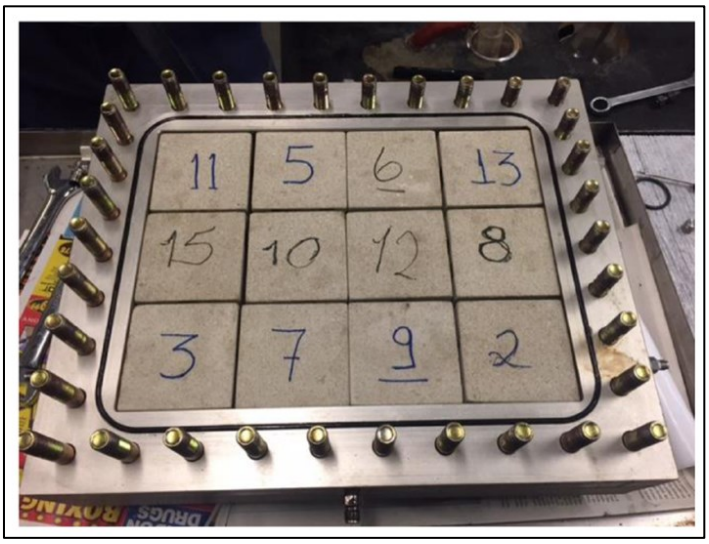

Figure 3: Experimental physical model (Silva & Maini, 2016)

Agada et al. (2016), in their study on CO_2 EOR and storage in a fractured reservoir, noted that fracture intensity is a controlling parameter. When it is above a certain threshold, the simulation results are highly independent of the conceptual geological used to create the fractures network. The high fracture density creates massive continuous flow paths and makes the specific

geometry of the fracture unimportant. However, below this threshold, the simulation results depend on the geological concept

For thermal processes such as steam-assisted gravity drainage (SAGD), the orientation of the fractures affects the steam expansion and oil production from the wells pair. A negative impact on oil production can result from horizontal fractures, while vertical fractures increase production. In addition, more oil volume is produced when fracture spacing is larger because steam has more time to diffuse through the matrix and heat more reservoir volume (Tohidi Hosseini et al., 2017).

However, most gas-based EOR processes suffer from poor sweep efficiency due to the gravity override and unfavorable mobility conditions. Therefore, mobility control is needed to improve the sweep efficiency and successfully implement the gas-based EOR processes. Foam represents a good option to reduce the gas mobility and divert the gas from the fractures into the matrix. However, foam stability is still an issue, especially in oil reservoirs with high temperatures and high salinity (Mogensen & Masalmeh, 2020; Z.-X. Xu et al., 2020).

Previous studies discussed that gas fractional flow, the ratio between the fracture aperture, and the bubble size have an important impact on the sweep efficiency. The apparent foam viscosity is mainly controlled by the number of lamellae per unit length. Moreover, the difference between the pre-generated foam and in-situ foam generation in fracture rock was also investigated. Results indicated that in-situ generation developed four times larger bubble sizes than the pre-generated foam (Haugen et al., 2012). This is directly related to the number of snap-off sites in the fractured system, which means that in some cases, less viscosity can be obtained from the in-situ generated foam. Other studies have also described the reduction of the relative gas permeability due to foam injection, which can also improve sweep efficiency (Haugen et al., 2012; Luo & Mohanty, 2021).

In general, having a good understanding of the reservoir characteristics and the capabilities of the fractures and matrix in providing the storage capacity and the fluid flow pathways can significantly enhance the selection of the recovery process and the efficiency of the recovery process itself.

2.5 Dimensionless numbers

The dimensionless numbers are a common method used to reduce the number of physical parameters through the combination of these interplaying parameters and the physical properties of the fluids and the flow media to describe their impact on the displacement process (Zhou et al., 1997). These numbers include physically related numbers such as gravity number,

capillary number, bond number, and more engineering-related such as develop factor, which also has a physical meaning (Talluru & WuMewbourne, 2017).

A sensitivity analysis can be further performed to investigate the sensitivity of the recovery process to these dimensionless numbers. Some studies claim that higher recovery can be achieved only by a minor tunning of the parameters in these dimensionless numbers. However, other studies discussed that dimensionless numbers are not the only parameters affecting recovery. Further studies are needed to assess governing forces and displacement mechanisms affecting the recovery processes (Kharrat et al., 2021).

Heeremans et al. (2006) have performed a feasibility study for the water alternative gas (WAG) process in the naturally fractured reservoir using a simulation model and dimensionless numbers to generate a proxy model for the sensitivity analysis. As shown in Figure 4, results have demonstrated the possibility of using the proxy models to describe the gas injection and water injection, WAG processes, and the capability to optimize the recovery processes based on this model.

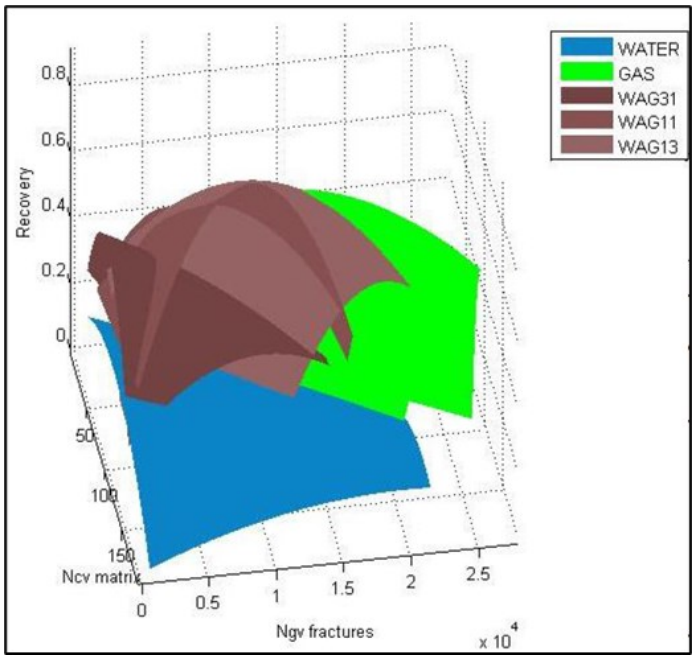

Figure 4: A proxy model for sensitivity analysis (Heeremans et al. 2006)

Kharrat et al. (2021) have also used dimensionless numbers to assess the EOR process in the fractured reservoirs by using the proxy models. They concluded that the Foam and the Foam-assisted WAG (FAWAG) processes are more sensitive than the WAG process to parameters including permeability contrast and matrix-block heights. However, they have highlighted the necessity for developing a new modified dimensionless number to account for the fracture characteristics. The currently used dimensionless numbers lack the capability of capturing the fracture characteristics, which is a major deficiency.

2.6 Modeling of the fractured reservoirs

2.6.1 Continuum approach

In the continuum approach, two independent continuums for matrix blocks and fracture networks are generated, and each continuum has a separate set of properties. The fracture-matrix interaction is conducted through the transfer function. The widely used models for this approach are the Dual-porosity model (DP) and the Dual-permeability model (DK) (Ghaedi et al., 2015).

The main difference between these two models is that the exchange of fluids is only allowed between the matrix block and the fracture in the dual-porosity model. At the same time, the dual permeability model also allows for inter blocks flow. However, several transfer functions have been proposed over the years to improve the matrix and fracture interaction description. Table 1 summarizes these equations (Bourbiaux, 2010; Wong et al., 2020).

Table 1: Transfer functions summary (Wong et al., 2020)

Transfer function	Description
Warren & Root (1963)	The first transfer function
Gilman & Kazemi (1983)	To account for the gravity forces
Quandalle & Sabathier (1989)	Accounts for exchange mechanisms in each matrix block surface

The fundamental advantage of the continuum approach is that the upscaling process can considerably simplify fracture networks' complexity to be suitable for field-scale studies. However, this simplification is not always convenient because it might lead to unreliable simulation results (Ghaedi et al., 2015; Wong et al., 2020).

2.6.2 Discrete Fractures approach

This approach was introduced as an alternative to the dual continuum approach with explicit representation for fractures as elements or control volumes (Y. Xu & Sepehrnoori, 2019). When the reservoir matrix is impermeable or has a negligible permeability, the discrete fracture network models (DFN) can be utilized to simulate the fluid flow through these fractures. while other discrete fracture models (DFM) need to be utilized in case of fracture matrix interaction. (Wong et al., 2020). Generally, it is important to highlight that the DFN term has become a

general term to describe the discrete fracture networks regardless of the matrix contribution in the last years.

The DFM models conveniently describe the fractures' structural features, such as fracture geometry, and eliminate the need for special treatment to describe the fracture matrix interaction, such as the transfer function (Bosma et al., 2017). The majority of the DFM models demand the fractures align with the internal boundaries of the matrix grids, which means that unstructured grids are necessary for the geometrical representation of the fractures and the decentralization of the matrix domain. However, when the distance between the fracture is small, it cannot be easy to have a good gridding quality (Yan et al., 2016). Moreover, the application of field scale DFM models is computationally intensive and beyond the scope of the classical solution methodologies (Bosma et al., 2017).

Another modeling technique in this approach is the embedded discrete fracture model (EDFM), which uses a non-conforming grid to discretize the matrix domain without initial consideration for the fracture's locations. However, the intersection between the fracture polygons and matrix grids is defined after placing the fractures in the matrix grids. In this model, fractures are discretized by the matrix grid boundaries, ensuring that only one fracture segment is created for each penetrated matrix grid by a fracture. This makes the domain suitable for the setup of the connections and the evaluation of transmissibility (Y. Xu & Sepehrnoori, 2019). This advantage makes the model compatible with the common commercial flow simulators (Wong et al., 2020).

2.6.3 Hybrid approach

The explicit representation of all fractures can make the simulation process impractical and computationally intensive, especially for field-scale studies. Therefore, a hybrid approach where the continuum approach and the discrete fracture approach are combined with having the advantage of both the explicit and the implicit representations. This approach captures large fracture effects and simultaneously simplifies the flow process in small fractures. However, the construction phase of the hybrid models includes two essential processes: partitioning and lumping. The fracture network is divided into two sets in the partitioning process, based on a defined partitioning cutoff. The discrete fracture approach will explicitly represent a large fracture set. In contrast, the continuum approach will implicitly represent the small fractures set. After the partitioning process, the lumping process is performed where the implicitly represented fractures need to be additionally subdivided into fracture groups that can be integrated into a continuum (Wong et al., 2020).

Chapter 3

Models' buildup and Simulation work

3.1 Overview of the related Simulation studies

Gong & Rossen (2018) argued that when the aperture distribution is wide enough, most fractures can be neglected without substantially influencing the flow through the naturally fractured reservoir, even if the fracture network is perfectly interconnected. All open fractures provide an effective flow path in the primary production process. In contrast, the amount of injection water or EOR agent determines how much oil is produced during a waterflood or EOR process. Moreover, they suggested that the input fracture parameters for the homogenized dual-porosity and permeability models depend on the recovery process. They used a simple two-dimensional conceptual model with perfectly connected fracture sets to raise this issue. However, their study did not investigate the effect on the gas-based EOR method or gravity-driven flow.

3.2 Simulation Models

3.2.1 Modeling of the Fractures Networks

The recent version of CMG 2020.1 provides an option for modeling different discrete fracture networks without further upscaling processes. After defining the explicit location of the discrete fractures network, the intersection between each fracture plane and the relevant matrix grid will automatically introduce additional embedded control volume segments that directly connect to the matrix grid. This means that in this model, the discrete fractures network (DFN) is discretized based on the shape, orientation, fracture aperture, and permeability into a discrete fracture unit (DFU). And each DFU is further discretized into a discrete fracture segment (DFS) based on the intersection with the matrix grid. The flow capability of the fracture is then

determined based on the fracture aperture and fracture permeability. This modeling option provides a numerical efficiency with the standard neighboring connections in the single porosity model. However, this option can also be used with dual continuum models (CMG, 2020).

Therefore, this study utilized this software to investigate the effect of different fracture network sets on the recovery processes. A simplistic 2D single porosity model was created using CMG-Builder with a similar dimension and matrix properties used in Gong & Rossen's study. However, in this study, the model was created vertically rather than horizontally to investigate the gravitational effect related to the gas-based EOR methods. Moreover, two additional models were created in this study: the first was vertically extended, and the second was a 3D cube. These models can provide an additional validation tool to the observed results in the original Gong & Rossen (2018) 2D model. A description of these models and their related properties is shown in Table 2.

Table 2: Models configurations and description

Model name	Dimensions			Grids number in each direction			Porosity	Permeability		
	m						%	mD		
	X	Y	Z	X	Y	Z	-	X	Y	Z
2D Vertical slice	15	1	15	67	1	67	0.2	1	1	1
Extended 2D Vertical slice	15	1	30	67	1	134	0.2	1	1	1
3D cube	15	15	15	31	31	31	0.2	1	1	1

In their study, Gong & Rossen (2018) categorized the fracture network sets into three types: Primary, secondary, and tertiary. In this study, these are renamed: major fractures set, medium fractures set, and Minor fractures set, respectively. The explicit location of the fractures and the used well's locations are shown in Figure 5.

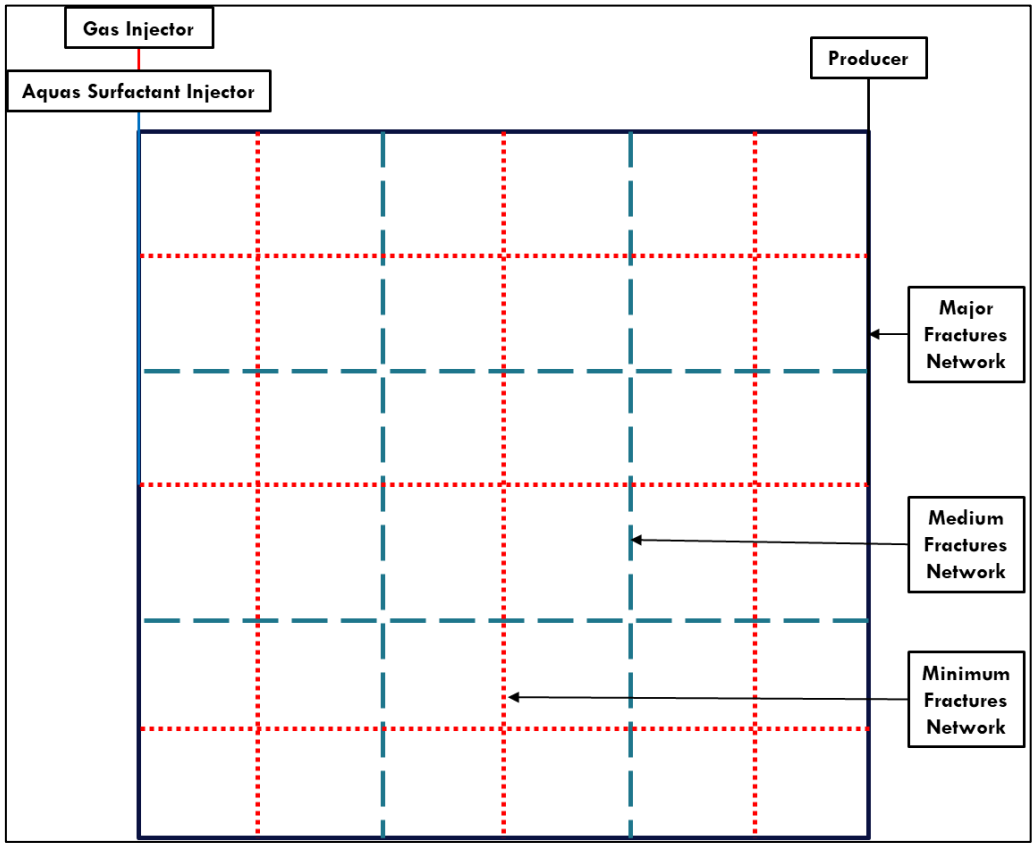

Figure 5: The explicit location of the fracture's networks

To define these sets, they have created new dimensionless numbers to describe the relationship between these discrete fracture networks, allowing for a qualitative description of the changes in the fracture properties and the resulting changes in the recovery factor for each recovery process.

$$R_d = \frac{Primary\ fracture\ apeature}{Secondary\ fracture\ apeature} \quad (1)$$

$$R_{d3} = \frac{Primary\ fracture\ apeature}{Tertiary\ fracture\ apeature} \quad (2)$$

$$R_n = \frac{Number\ of\ Primary\ fractures}{Total\ number\ of\ Primary\ and\ Secondary\ fractures} \quad (3)$$

To avoid the numerical issues, Gong & Rossen (2018) have assumed a constant fracture aperture for all fractures and have only changed the fracture permeability to obtain the changes in their dimensionless numbers. This argument is based on the derivation of the cubic law for fracture permeability calculation from the fracture aperture. However, the results have indicated that using this assumption will lead to inaccurate results. Therefore, the fracture aperture was changed along with the fracture permeability for each case in this work. Similar to the fracture aperture, the ratio for the fracture permeabilities is defined by Rk and Rk3. Rk represents the ratio between the primary fracture permeability and the secondary fracture permeability. The

Rk3 represents the ratio between the primary fracture permeability and the tertiary fracture permeability.

Based on these described equations, three categories of fracture properties were defined to cover a wider range of properties for each set of fracture networks. The fracture properties for each set in the defined categories are summarized in Table 3.

However, in this fractures modeling approach, no additional relative permeability and capillary pressure curves are needed to describe the flow in the fractures. It is important to highlight that in all the cases, the Major fractures aperture and permeability are constant. The fracture permeability for all the cases is higher than the matrix to avoid any issues highlighted by Wong et al. (2020) in similar EDFM models when the permeability of the fracture is less than the permeability of the fracture.

Table 3: Fractures apertures and permeabilities for the three defined categories

properties	**Fractures Aperture**			**Dimensionless numbers**		**Fractures Permeability**			**Dimensionless numbers**	
	mm					**Darcy**				
Category	**Maj**	**Med**	**Min**	**Rd**	**Rd3**	**Maj**	**Med**	**Min**	**Rk**	**Rk3**
1	2.00	1.60	0.80	1.25	2.50	4.00	2.56	0.64	1.5625	6.250
2	2.00	0.80	0.40	2.50	5.00	4.00	0.64	0.16	6.2500	25.00
3	2.00	0.40	0.20	5.00	10.00	4.00	0.16	0.04	25.000	100.00

3.2.2 Modeling of the recovery processes

This study investigated three recovery processes: primary production, immiscible gas injection, and immiscible foam flooding. For modeling the primary production process and the immiscible gas injection process, the CMG black oil simulator IMEX was utilized. In the black oil model, the multi-component multi-phase system is described only by three pseudo components to form three phases: aqueous phase for water, gaseous phase for gas component, and oleic phase that contain oil and dissolved gas (Agada et al., 2016). The fluid properties used in this study are based on G field PVT data located in the middle east. A summary of the data is demonstrated in Table 4.

Table 4: The Black oil Fluid Model for gas injection cases

Parameter	Value	unite
GOR	155	m^3/m^3
Pb	25	bar
Bg	0.0043	m^3/sm^3
Bo	1.42	m^3/sm^3
µg	0.042	cp
µo	0.76	cp

Several approaches have been developed to model the foam flow through the porous media. Ma et al. (2015) have reviewed and categorized these approaches into three main groups: implicit-texture local-equilibrium models, population-balance local-equilibrium models, and population-balance dynamic-texture models. They have also highlighted the challenges incorporated with the modeling of the foam flooding process and the capabilities of the current models to capture the relevant physical effects. In this study, the CMG compositional simulator GEM was used. The foam injection process is modeled using the implicit-texture local-equilibrium approach in this model. The foam quality is defined as the ratio of the gas rate to the total fluid rate (Luo & Mohanty, 2021).

To simulate the foam presence in the empirical model, the relative permeability of the gas phase is adjusted by the dimensionless foam parameter (FM), which is computed by this formula:

$$FM = \frac{1}{1+FMMOB*F1*F2*F3*F4*F5*F6*F7*FDRY} \quad \text{(4)}$$

As seen in equation (4), the FM represents the inverse of the reference foam mobility reduction factor (FMMOB) when no other parameters influence the foam mobility. It can vary between FM=1, which means no Foam has formed, and FM=0, where a strong foam has formed. The foam mobility reduction factor ranges between 5 and 100. However, the FMMOB factor is multiplied by other factors to represent the dependency on these effects to account for other effects (CMG, 2020). These factors are calculated based on the following formulas:

$$F1 = \left(\frac{Mole\ Fraction\ (Surfactant)}{FMSURF}\right)^{EPSURF} \quad \text{(5)}$$

$$F2 = \left(\frac{FMOIL-S_o}{FMOIL-FLOIL}\right)^{EPOIL} \quad \text{(6)}$$

$$F3 = \left(\frac{FMCAP}{Capillary\ Number}\right)^{EPCAP} \quad \text{(7)}$$

$$F4 = \left(\frac{Capillary\ Number - FMGCP}{FMGCP}\right)^{EPGCP} \quad \text{(8)}$$

$$F5 = \left(\frac{FMOMF - X_{comp\_name}}{FMOMF}\right)^{EPOMF} \quad \text{(9)}$$

$$F6 = \left(\frac{X_{salt} - FLSALT}{FMSALT - FLSALT}\right)^{EPSALT} \quad \text{(10)}$$

$$F7 = \frac{1}{FMPERM1} * \ln\left(\frac{PERMAV}{FMPERM2} + 1\right) \quad \text{(11)}$$

F1: represents the effect of surfactant concentration

F2: represents the effect of oil saturation

F3: represents the effect of shear-thinning

F4: represents the effect of limited capillary pressure

F5: represents the effect of oil components

F6: represents the effect of salt concentration

F7: represents the effect of permeability dependence

The equation (12) describes the foam dry-out as FDRY, which rescales foam relative permeability to the original or no foam gas relative permeability. The dry-out factor (SF) ranges between SF=1, which means no foam, and SF= 0, which means no dry-out. More information is available in the CMG GEM user manual.

$$FDRY = 0.5 + \frac{\arctan\left(SFBET(S_w - SF)\right)}{\pi} \quad \text{(12)}$$

This study used the relative permeability and capillary curves from the G field as input, as shown in Figure 6 and Figure 7.

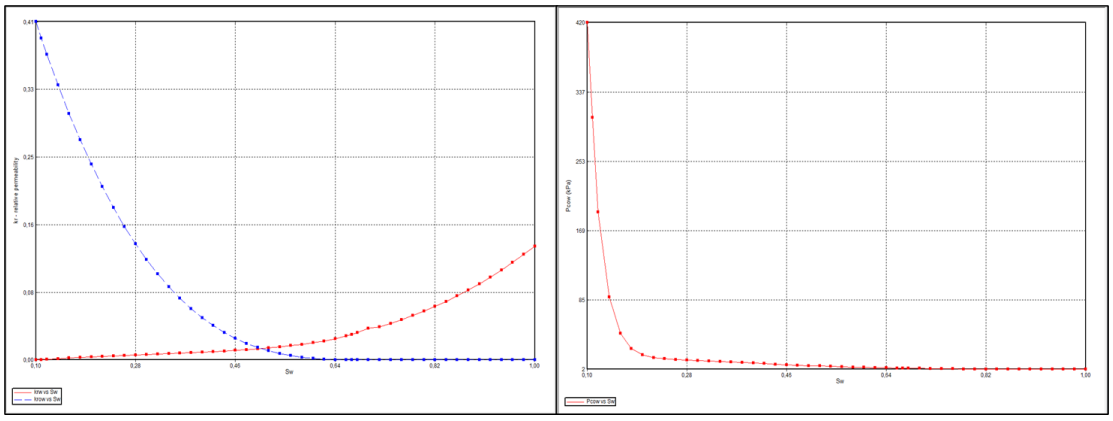

Figure 6: Relative permeability model and capillary pressure for the oil-water system

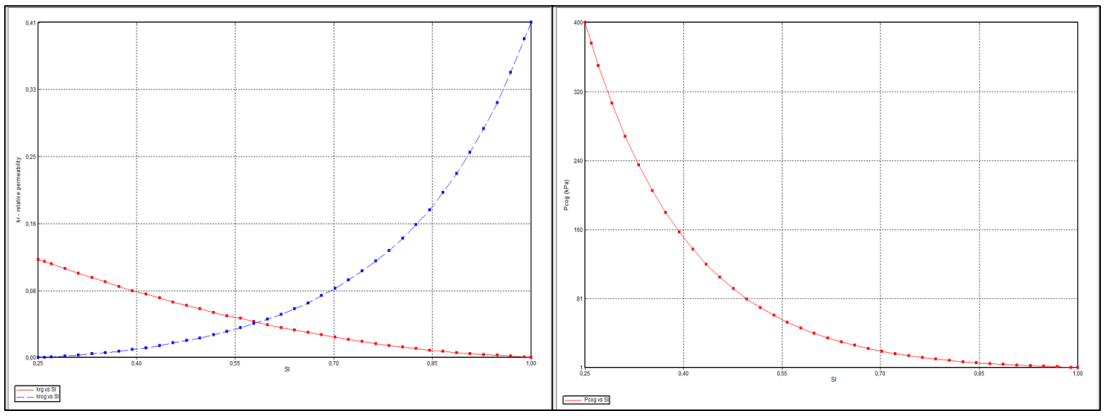

Figure 7: Relative permeability model and capillary pressure for the gas-liquid system

However, for foam modeling, data from the GMSMO85 CMG provided templet model was adjusted and used to simplify the modeling process and maintain the main target of this study in investigating the effect of the fracture networks on the recovery process. The foam model was used to simulate three cycles of the FAWAG process with a WAG ratio of 1:2.

Based on these defined models, systematic cases were created and simulated to investigate the fracture networks' effect on the recovery processes, as shown in Figure 8.

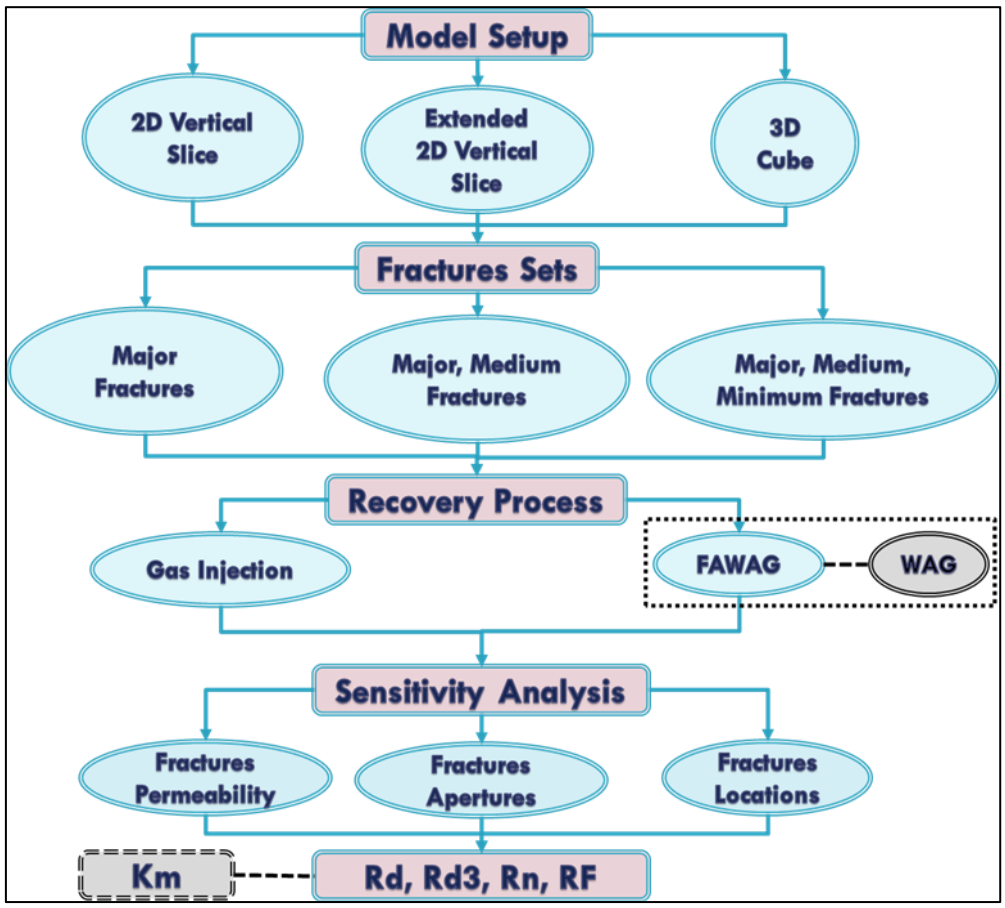

Figure 8: Investigation workflow for the effect of the fracture's networks

However, two injection schemes were used for the gas injection process: vertical injection scheme and horizontal injection scheme to investigate if the effect of the fractures networks is sensitive to the propagation direction. A summary for the 54 cases is shown in Table 5 to Table 7, with a brief description given in Table 8 to Table 10

Table 5: Defined cases for the first category (Rd=1.25 and Rd3=2.5)

Case number	Case name	Model name
1	1_2D_Vs_Vw_GI_Maj	2D Vertical slice
2	1_2D_Vs_Vw_GI_MajMed	2D Vertical slice
3	1_2D_Vs_Vw_GI_MajMedMin	2D Vertical slice
4	1_2D_Vs_Hw_GI_Maj	2D Vertical slice
5	1_2D_Vs_Hw_GI_MajMed	2D Vertical slice
6	1_2D_Vs_Hw_GI_MajMedMin	2D Vertical slice
7	1_2D_EVs_Hw_GI_Maj	Extended 2D Vertical slice
8	1_2D_EVs_Hw_GI_MajMed	Extended 2D Vertical slice
9	1_2D_EVs_Hw_GI_MajMedMin	Extended 2D Vertical slice
10	1_3D_Vs_Vw_GI_Maj	3D cube
11	1_3D_Vs_Vw_GI_MajMed	3D cube
12	1_3D_Vs_Vw_GI_MajMedMin	3D cube
13	1_2D_Vs_Vw_WAG_Maj	2D Vertical slice
14	1_2D_Vs_Vw_WAG_MajMed	2D Vertical slice
15	1_2D_Vs_Vw_WAG_MajMedMin	2D Vertical slice
16	1_2D_Vs_Vw_FAWAG_Maj	2D Vertical slice
17	1_2D_Vs_Vw_FAWAG_MajMed	2D Vertical slice

18	1_2D_Vs_Vw_FAWAG_MajMedMin	2D Vertical slice
19	1_3D_Vs_Vw_FAWAG_Maj	3D cube
20	1_3D_Vs_Vw_FAWAG_MajMed	3D cube
21	1_3D_Vs_Vw_FAWAG_MajMedMin	3D cube

Table 6: Defined cases for the second category (Rd=2.5 and Rd3=5)

Case number	**Case name**	**Model name**
22	2_2D_Vs_Vw_GI_MajMed	2D Vertical slice
23	2_2D_Vs_Vw_GI_MajMedMin	2D Vertical slice
24	2_2D_Vs_Hw_GI_MajMed	2D Vertical slice
25	2_2D_Vs_Hw_GI_MajMedMin	2D Vertical slice
26	2_2D_EVs_Hw_GI_MajMed	2D Vertical slice
27	2_2D_EVs_Hw_GI_MajMedMin	2D Vertical slice
28	2_2D_Vs_Vw_FAWAG_MajMed	2D Vertical slice
29	2_2D_Vs_Vw_FAWAG_MajMedMin	2D Vertical slice

Table 7: Defined cases for the third category (Rd=5 and Rd3=10)

Case number	**Case name**	**Model name**
30	3_2D_Vs_Vw_GI_MajMed	2D Vertical slice
31	3_2D_Vs_Vw_GI_MajMedMin	2D Vertical slice
32	3_2D_Vs_Hw_GI_MajMed	2D Vertical slice
33	3_2D_Vs_Hw_GI_MajMedMin	2D Vertical slice

34	3_2D_EVs_Hw_GI_MajMed	2D Vertical slice
35	3_2D_EVs_Hw_GI_MajMedMin	2D Vertical slice
36	3_2D_Vs_Vw_FAWAG_MajMed	2D Vertical slice
37	3_2D_Vs_Vw_FAWAG_MajMedMin	2D Vertical slice

Table 8: Cases description for the first category (Rd=1.25 and Rd3=2.5)

Case number	**Case description**
1	Gas injection process with only Major fractures are included in the vertical injection scheme
2	Gas injection process with Major & Medium fractures are included in the vertical injection scheme
3	Gas injection process with Major, Medium & Minor fractures are included in the vertical injection scheme
4	Gas injection process with only Major fractures are included in the horizontal injection scheme
5	Gas injection process with Major & Medium fractures are included in the horizontal injection scheme
6	Gas injection process with Major, Medium & Minor fractures are included in the horizontal injection scheme
7	Gas injection process with only Major fractures are included in the horizontal injection scheme
8	Gas injection process with Major & Medium fractures are included in the horizontal injection scheme
9	Gas injection process with Major, Medium & Minor fractures are included in the horizontal injection scheme
10	Gas injection process with only Major fractures are included in the vertical injection scheme

11	Gas injection process with Major & Medium fractures are included in the vertical injection scheme
12	Gas injection process with Major, Medium & Minor fractures are included in the vertical injection scheme
13	Gas injection process with only Major fractures are included in the vertical injection scheme
14	Gas injection process with Major & Medium fractures are included in the vertical injection scheme
15	Gas injection process with Major, Medium & Minor fractures are included in the vertical injection scheme
16	FAWAG injection process with only Major fractures are included for the vertical injection scheme, and three cycles of injection of 1:2 ratio
17	FAWAG injection process with Major & Medium fractures are included for the vertical injection scheme, and three cycles of 1:2 aqueous to gas ratio
18	FAWAG injection process with Major, Medium & Minor fractures are included for the vertical injection scheme, and three cycles of 1:2 aqueous to gas ratio
19	FAWAG injection process with only Major fractures are included for the vertical injection scheme, and three cycles of injection of 1:2 ratio
20	FAWAG injection process with Major & Medium fractures are included for the vertical injection scheme, and three cycles of 1:2 aqueous to gas ratio
21	FAWAG injection process with Major, Medium & Minor fractures are included for the vertical injection scheme, and three cycles of 1:2 aqueous to gas ratio

Table 9: Cases description for the second category (Rd=2.5 and Rd3=5)

Case number	Case description
22	Gas injection process with Major & Medium fractures are included in the vertical injection scheme
23	Gas injection process with Major, Medium & Minor fractures are included in the vertical injection scheme
24	Gas injection process with Major & Medium fractures are included in the horizontal injection scheme
25	Gas injection process with Major, Medium & Minor fractures are included in the horizontal injection scheme
26	Gas injection process with Major & Medium fractures are included in the horizontal injection scheme
27	Gas injection process with Major, Medium & Minor fractures are included in the horizontal injection scheme
28	FAWAG injection process with Major & Medium fractures are included for the vertical injection scheme, and three cycles of 1:2 aqueous to gas ratio
29	FAWAG injection process with Major, Medium & Minor fractures are included for the vertical injection scheme, and three cycles of 1:2 aqueous to gas ratio

Table 10: Cases description for third category (Rd=5 and Rd3=10)

Case number	Case description
30	Gas injection process with Major & Medium fractures are included in the vertical injection scheme
31	Gas injection process with Major, Medium & Minor fractures are included in the vertical injection scheme
32	Gas injection process with Major & Medium fractures are included in the horizontal injection scheme

33	Gas injection process with Major, Medium & Minor fractures are included in the horizontal injection scheme
34	Gas injection process with Major & Medium fractures are included in the horizontal injection scheme
35	Gas injection process with Major, Medium & Minor fractures are included in the horizontal injection scheme
36	FAWAG injection process with Major & Medium fractures are included for the vertical injection scheme, and three cycles of 1:2 aqueous to gas ratio
37	FAWAG injection process with Major, Medium & Minor fractures are included for the vertical injection scheme, and three cycles of 1:2 aqueous to gas ratio

The sensitivity analysis and the homogenization cases are also summarized in Table 11 and Table 12.

Table 11: Defined cases for Sensitivity Analysis and Homogenization

Case number	**Case name**	**Model name**
38	1_2D_Vs_Vw_GI_MajMedMin_same_d	2D Vertical slice
39	2_2D_Vs_Vw_GI_MajMedMin_same_d	2D Vertical slice
40	3_2D_Vs_Vw_GI_MajMedMin_same_d	2D Vertical slice
41	1_2D_Vs_Vw_GI_All_Maj	2D Vertical slice
42	1_2D_Vs_Vw_GI_All_Med	2D Vertical slice
43	1_2D_Vs_Vw_GI_All_Min	2D Vertical slice
44	1_2D_Vs_Vw_GI_MajMed_All_Maj	2D Vertical slice
45	1_2D_Vs_Vw_GI_MajMed_All_Med	2D Vertical slice
46	1_2D_Vs_Vw_GI_Maj_Matrix_2mD	2D Vertical slice
47	1_2D_EVs_Hw_GI_MajMed_All_Maj	Extended 2D Vertical slice
48	1_2D_EVs_Hw_GI_MajMed_All_Med	Extended 2D Vertical slice
49	1_2D_EVs_Hw_GI_Maj_Matrix_2mD	Extended 2D Vertical slice

50	1_3D_Vw_GI_MajMed_All_Maj	3D cube
51	1_3D_Vw_GI_Maj_Matrix_2mD	3D cube
52	1_2D_Vs_Vw_FAWAG_MajMed_All_Maj	2D Vertical slice
53	1_2D_Vs_Vw_FAWAG_Maj_Matrix_2mD	2D Vertical slice
54	1_3D_Vw_FAWAG_MajMed_All_Maj	3D cube

Table 12: Cases description for Sensitivity Analysis and Homogenization

Case number	**Case description**
38	Gas injection process with Major, Medium & Minor fractures are included but with the same aperture for the vertical injection scheme
39	Gas injection process with Major, Medium & Minor fractures are included but with the same aperture for the vertical injection scheme
40	Gas injection process with Major, Medium & Minor fractures are included but with the same aperture for the vertical injection scheme
41	Gas injection process when all fractures are considered as Major for the vertical injection scheme
42	Gas injection process when all fractures are considered as Medium for the vertical injection scheme
43	Gas injection process when all fractures are considered as Minor for the vertical injection scheme
44	Gas injection process by using the vertical injection scheme where the Minor fractures are excluded, and Medium considered to be Major fractures
45	Gas injection process by using the vertical injection scheme where the Minor fractures are excluded, and Major considered being Medium fractures
46	Gas injection process by using the vertical injection scheme where Medium and Minor fractures networks are excluded, and Matrix adjusted to compensate for the effect of the fractures

47	Gas injection process by using the Horizontal injection scheme where the Minor fractures are excluded, and Medium considered to be Major fractures
48	Gas injection process by using the Horizontal injection scheme where the Minor fractures are excluded, and Major considered being Medium fractures
49	Gas injection process by using the Horizontal injection scheme where Medium and Minor fractures networks are excluded, and Matrix adjusted to compensate for the effect of the fractures
50	Gas injection process by using the Vertical injection scheme where the Minor fractures are excluded, and Medium considered to be Major fractures
51	Gas injection process by using the vertical injection scheme where Medium and Minor fractures networks are excluded, and Matrix adjusted to compensate for the effect of the fractures
52	FAWAG injection process with 1:2 aqueous to gas ration and by using the Vertical injection scheme where the Minor fractures are excluded, and Medium considered being Major fractures
53	FAWAG injection process with 1:2 aqueous to gas ration and by using the Horizontal injection scheme where Medium and Minor fractures networks are excluded, and Matrix adjusted to compensate for the effect of the fractures
54	FAWAG injection process with 1:2 aqueous to gas ration and by using the Vertical injection scheme where the Minor fractures are excluded, and Medium considered being Major fractures

Chapter 4

Results and Discussion

4.1 Results and Discussion

Excluding or including fractures is a very common procedure and practice to simplify the modeling process of fractured reservoirs. Typically, it is subjected to a statistical or pre-defined cut-off limit. However, a heterogeneous distribution of fracture apertures can affect the fluid flow behavior and, consequently, the recovery factor. Moreover, the estimated behavior for produced volumes of different fluids can also be affected over the injection period. The impact of excluding or including additional fracture networks to the Major fractures network will be presented in this section.

4.1.1 Primary production

For an undersaturated oil reservoir produced by natural depletion and in the absence of an aquifer, oil is the only flowing phase in the fracture's networks. Under these conditions that correspond to the early stages of reservoir life, the recovery factor is less sensitive to the impact of excluding or including the fractures network, as Gong & Rossen (2018) highlighted. The main focus of this study is the gas-based EOR methods; hence, the primary stage is not considered.

4.1.2 Gas injection

The gas injection results of the different cases are discussed in the following sections.

4.1.2.1 2D Vertical Slice (Vertical Wells)

For the first category of fracture networks, the difference in the estimated recovery factor can be significant along the injection period between the cases when the Major fractures network is only included and the other cases when the Major and the Medium fractures networks are

both included (Figure 9). Including only the Major fractures network has resulted in underestimation; the maximum difference at the end of the injection period of 2 pore volumes has reached 10%. However, the Minor fractures network also slightly differs from the Medium fractures network.

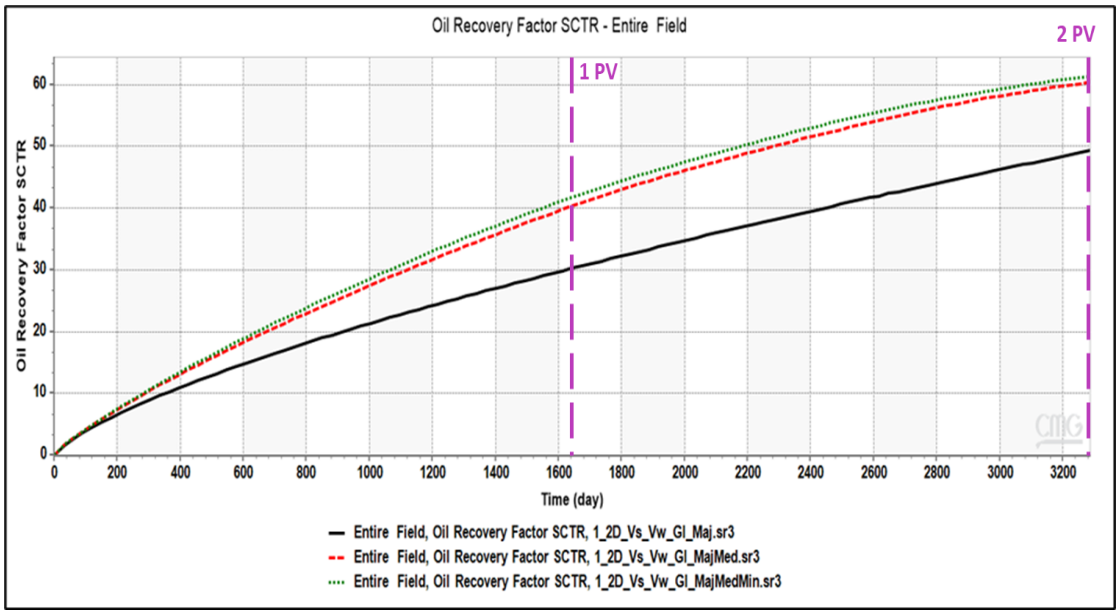

Figure 9: Oil Recovery factor for gas injection process in the first category of fractures networks (2D model & Vertical wells)

The gas-oil ratio (GOR) demonstrates a considerable difference in the overall behavior, as shown in Figure 10. Including only the Major fractures network results in an overestimation of produced gas volume during the early injection period, extending from the gas breakthrough to 1.6 pore volumes. In contrast, this underestimates the produced gas amount in the later period. However, the highest difference in the GOR can be observed when the Minor fractures network is included in addition to the Medium fractures network. Moreover, the additional impact of including the Minor fractures network is smaller than the impact of including the Medium fractures network.

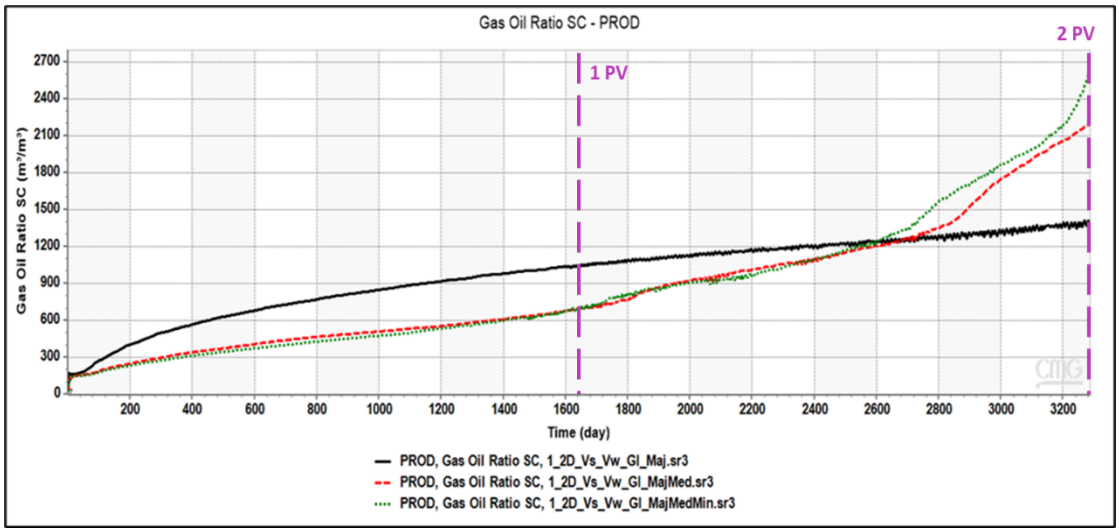

Figure 10: GOR for gas injection process in the first category of fractures networks (2D model & Vertical wells)

As shown in Figure 11, the saturation profile for the three cases demonstrates the gas flow behavior in the fracture networks, where the red color represents the oil phase, and the green color represents the gas phase. The gas flows in the Major fractures network and surrounds the matrix block, where it is slowly draining the matrix. When the Medium fractures network is additionally included, the gas flow in the horizontal fractures can be observed as it is parallel to the flow direction. The gas flow in the vertical fractures is subjected to multiple effects that include the re-infiltration of the oil from the matrix block to another, in addition to the gravity effect. However, as the gas saturation increase in the fractures, the matrix block is surrounded and slowly drained. When the Minor fractures network is included, few differences can be observed in the gas flow behavior, explaining the low impact of the Minor fractures network on the recovery factor and gas-oil ratio.

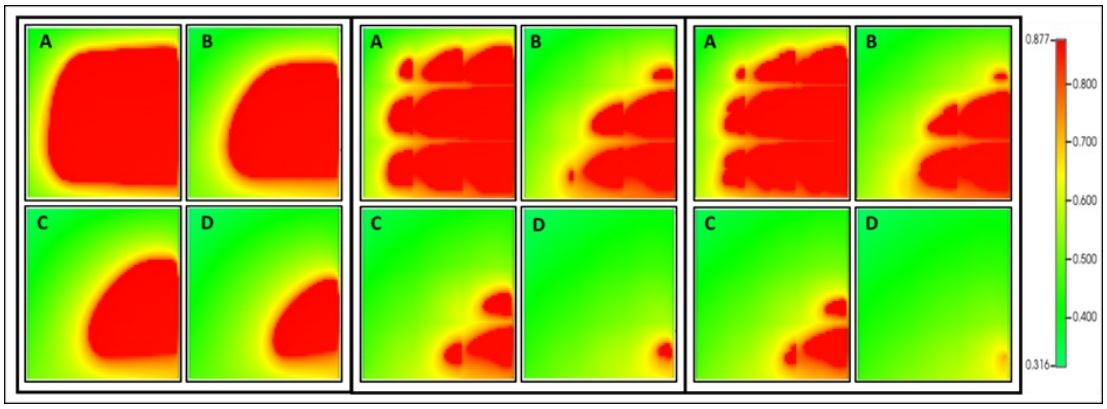

Figure 11: Oil saturation profile (oil in red & gas in green color) for gas injection process in the first category of fractures networks (2D model & Vertical wells) left: Only Major fractures network, Middle: Major & Medium fractures networks, right: Major, Medium & Minor fractures networks, at A:0.5 PV, B:1 PV, C:1.5 PV, D:2 PV.

For the second category of fracture networks, the difference in the recovery factor estimation tends to be smaller between the Major and the case of the Major and Medium fracture compared to the first category of fracture networks (Figure 12). Moreover, the Minor fractures network has a neglectable impact than the Major and Medium fractures networks case.

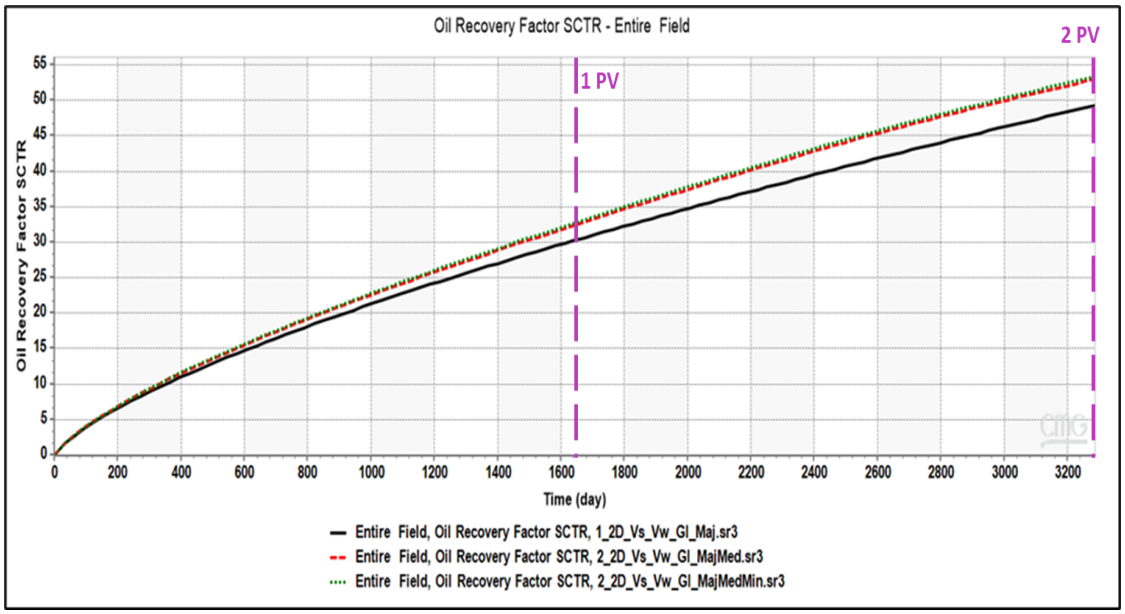

Figure 12: Oil Recovery factor for gas injection process in the second category of fractures networks (2D model & Vertical wells)

The GOR of the second category indicates a similar behavior to the GOR of the first category. Where excluding the additional fracture networks results in an overestimation of the produced gas amount during the early period and up to 1.5 pore volumes, as shown in Figure 13. However, the difference in the magnitude in the second category tends to be smaller. After 1.5 pore volumes, the difference starts to decrease. Moreover, no differences were indicated by including the Minor fracture networks in this category.

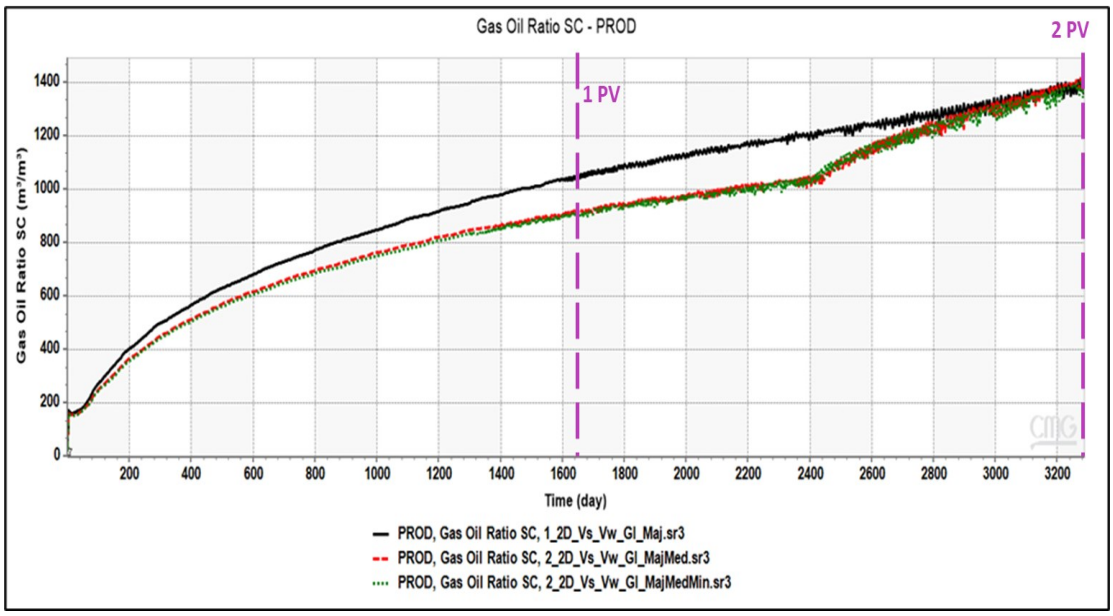

Figure 13: GOR for gas injection process in the second category of fractures networks (2D model & Vertical wells)

The saturation profile shown in Figure 14 demonstrates the gas flow behavior in the fracture networks. When the Medium fractures network is additionally included, the horizontal fractures have slightly impacted the gas flow behavior as it is parallel to the flow direction. However, the vertical fractures have not affected the flow as it can also be seen that including the Minor fractures network has not affected the gas flow behavior.

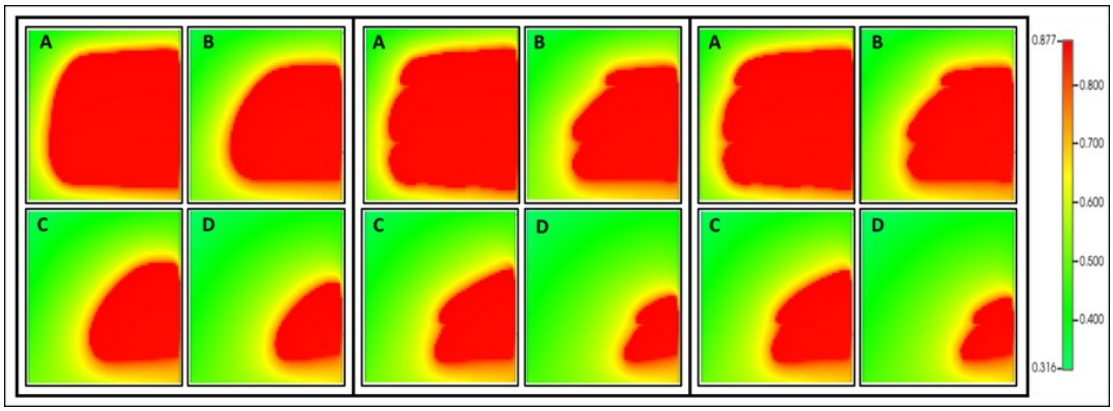

Figure 14: Oil saturation profile (oil in red & gas in green color) for gas injection process in the second category of fractures networks (2D model & Vertical wells) left: Only Major fractures network, Middle: Major & Medium fractures networks, Right: Major, Medium & Minor fractures networks, at A:0.5 PV, B:1 PV, C:1.5 PV, D:2 PV.

In the third category of fracture networks, almost no differences can be observed in estimating the recovery factor between the case when only the Major fractures network is included and the cases when the Medium fractures networks and the Minor fractures network are included (Figure 15).

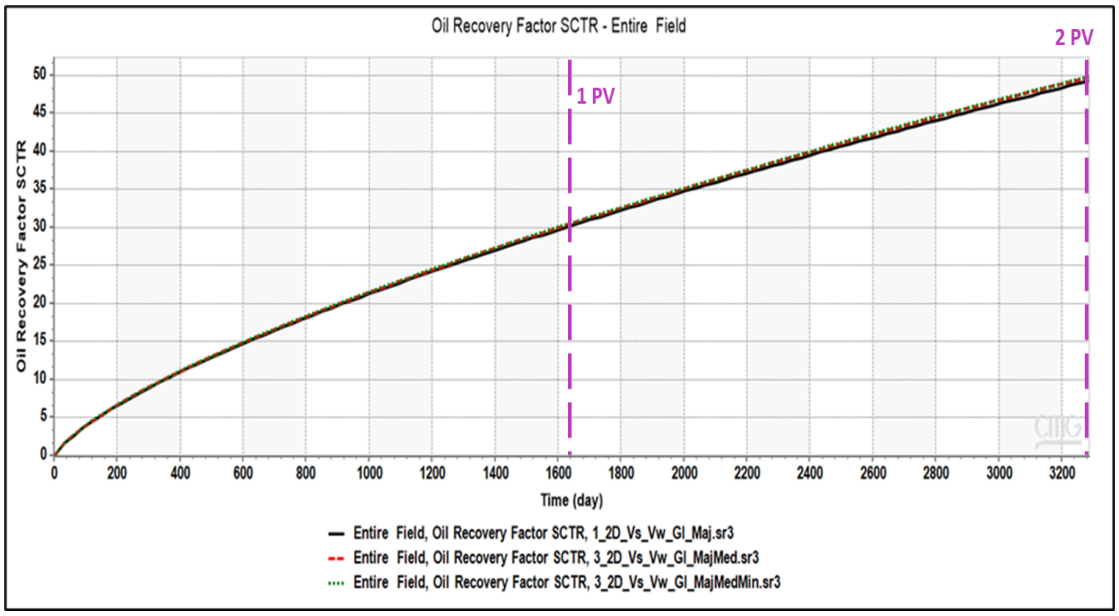

Figure 15: Oil Recovery factor for gas injection process in the third category of fractures networks (2D model & Vertical wells).

Similar to the recovery factor, the GOR for all the cases shows an identical behavior, as shown in Figure 16. This means that the medium and Minor fracture networks have no important effect on estimating the produced fluids volumes.

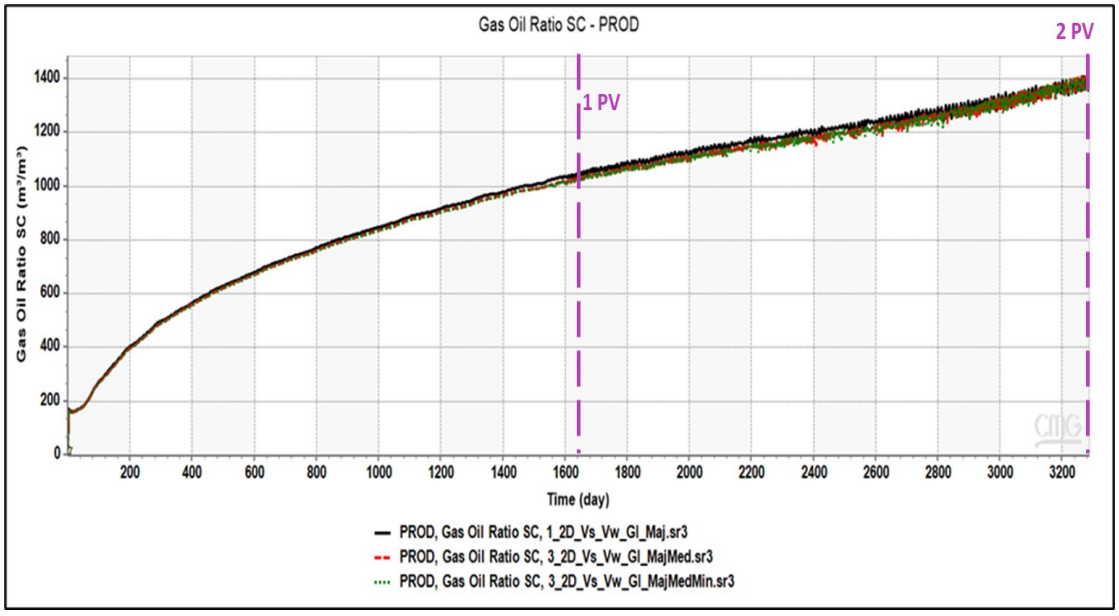

Figure 16: GOR for gas injection process in the third category of fractures networks (2D model & Vertical wells)

As shown in Figure 17), the saturation profile demonstrates the gas flow behavior in the fracture networks. It can be seen that including the Medium and Minor fracture networks has not affected the gas flow behavior. This observation indicates that fractures in this category have similar flow characteristics to the matrix.

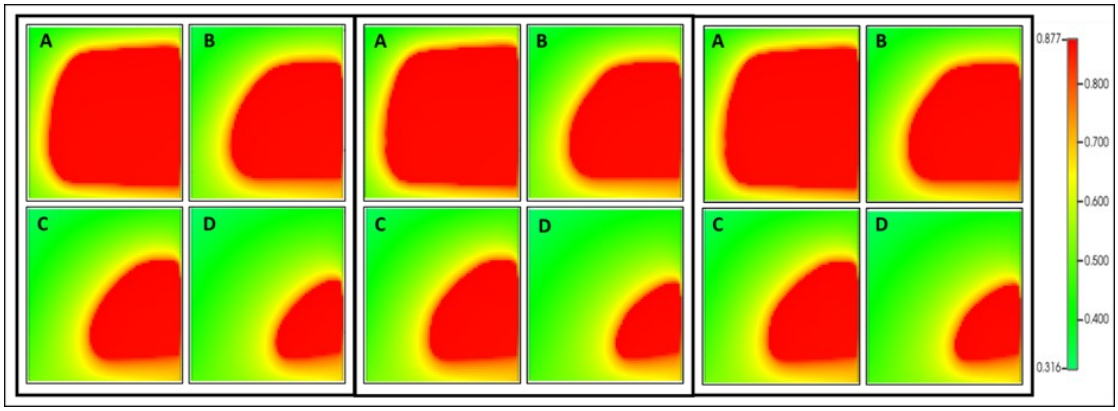

Figure 17: Oil saturation profile(oil in red & gas in green color) for gas injection process in the third category of fractures networks (2D model & Vertical wells) left: Only Major fractures network, Middle: Major & Medium fractures networks, Right: Major, Medium & Minor fractures networks, at A:0.5 PV, B:1 PV, C:1.5 PV, D:2 PV

These results for the three defined categories of the fracture networks have clearly demonstrated the relative importance of including different sets of fracture networks in certain cases. In other cases, excluding these fracture networks has no impact on the estimated produced volumes during the gas injection process. Relevant observations were discussed by Harimi et al. (2019) for narrow fractures as they can have comparable capillary pressures to the matrix due to the liquid bridging.

4.1.2.2 2D Vertical Slice (Horizontal Wells)

Horizontal wells injection scheme was used to investigate the impact of the fracture networks on the gas-assisted gravity drainage. As shown in Figure 18, the recovery factor estimations demonstrate similar trends to the vertical injection scheme for each category of fracture networks. The impact of excluding these networks on the estimation of the recovery factor decreases with decreasing the fracture aperture and the fracture permeability.

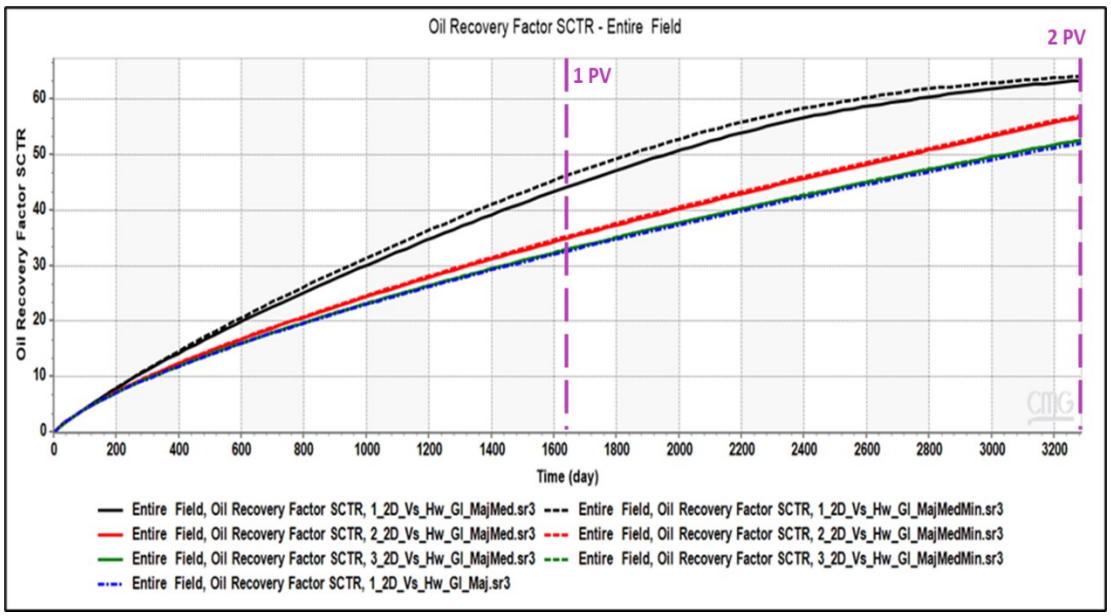

Figure 18: Oil Recovery factor for gas injection process in the three defined categories of fractures networks (2D model, Comparison between Vertical and Horizontal wells)

Similar to the recovery factor, the GOR also shows that the highest difference can be observed in the first category of fracture networks (Figure 19). However, the volume estimation difference of the second recovery continuously increases from the time of breakthrough up to the end of the injection period.

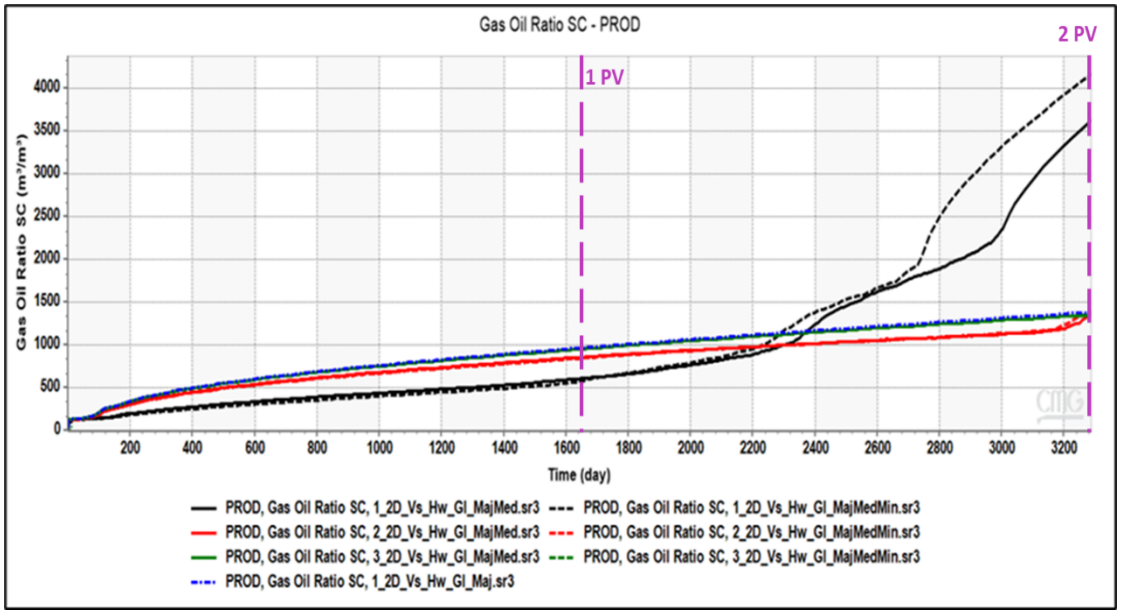

Figure 19: GOR for gas injection process in the three defined categories of fractures networks (2D model Comparison between Vertical and Horizontal wells)

Figure 20 shows that the saturation profile demonstrates a similar observation for gas flow behavior in the fracture networks in vertical wells cases. The gas flows in the Major fractures

network and surrounds the matrix block, where it is slowly draining the matrix. When the Medium fractures network is additionally included, the gas flow in the vertical fractures can be clearly observed as it is parallel to the flow direction. The gas flow in the horizontal fractures is subjected to multiple effects that include the capillary continuity and the re-infiltration of the oil from the matrix block to another, in addition to gravity. However, as the gas saturation increase in the fractures, the matrix block is surrounded and slowly drained afterward.

When the Minor fractures network is additionally included, few differences can be observed in the gas flow behavior, which explains the observations on the recovery factor and the gas-oil ratio.

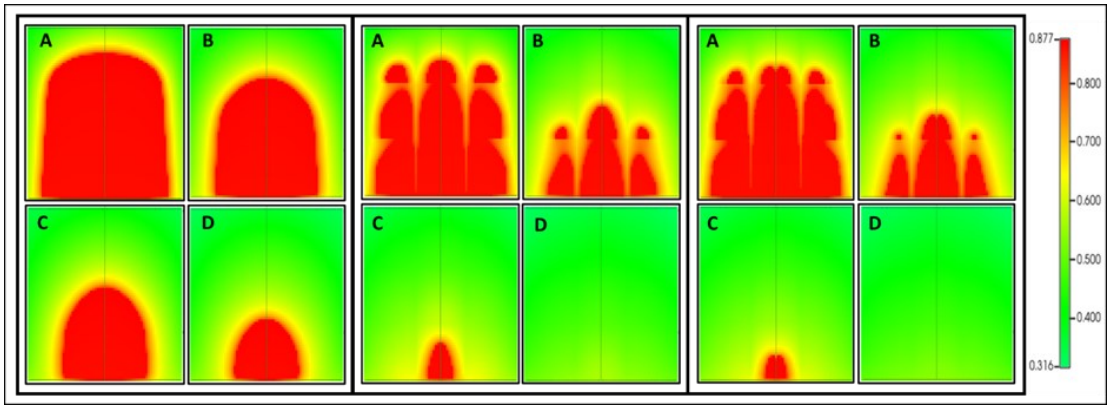

Figure 20: Oil saturation profile (oil in red & gas in green color) for gas injection process in the first category of fractures networks (2D model & Horizontal wells) left: Only Major fractures network, Middle: Major & Medium fractures networks, Right: Major, Medium & Minor fractures networks, at A:0.5 PV, B:1 PV, C:1.5 PV, D:2 PV

4.1.2.3 Extended 2D Vertical Slice

An extended vertical model was also used to represent two-unit cells to investigate the impact of the reservoir height on the Gas-assisted gravity drainage when a different fractures network is included. Also, to confirm the observations and the capability of the standard model to capture the production behavior. However, as shown in Figure 21, results demonstrated similar behavior to the standard model, where excluding the Medium fractures results in a significant underestimation of the recovery factor.

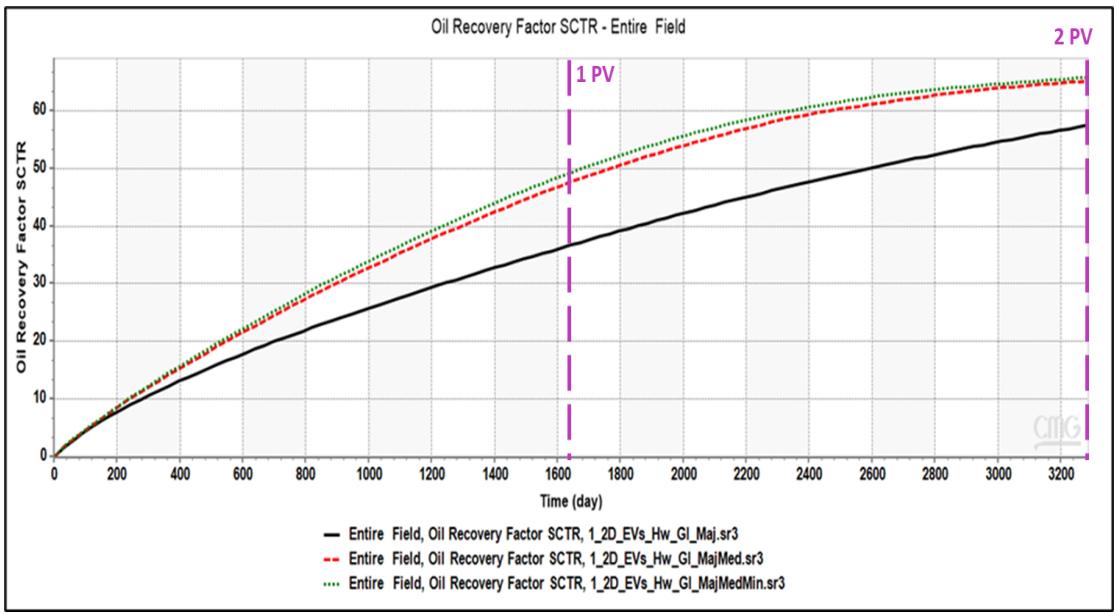

Figure 21: Oil Recovery factor for gas injection process in the first category of fractures networks (Extended 2D model & Horizontal wells)

Similar to the standard 2D model and as shown in Figure 22, the GOR behavior indicates that excluding the Medium fractures networks results in overestimating the produced gas amount in the early period and up to 1.25 pore-volumes. After that, the trend changed to underestimate the produced gas amount.

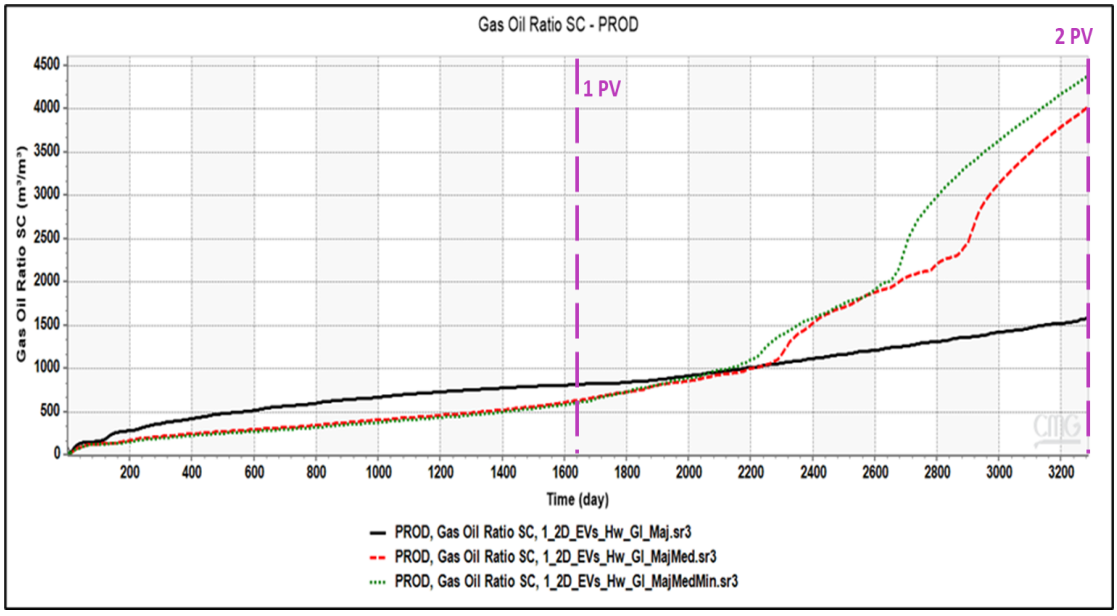

Figure 22: GOR for gas injection process in the first category of fractures networks (Extended 2D model & Horizontal wells)

The saturation profile for the extended 2D model, as shown in Figure 23, can provide a better demonstration of the effects that include the capillary continuity and gas breakthrough across

the different sets of fractures. If no other network is included, the capillary continuity between the upper and the lower major matrix block is maintained for a longer time frame. It can still be observed even after the injection of 1 PV due to the liquid bridging. The high oil saturation can indicate this at the bottom of the upper block and across the fracture into the upper part of the lower block. When the other fracture networks are included, the capillary continuity disrupts faster.

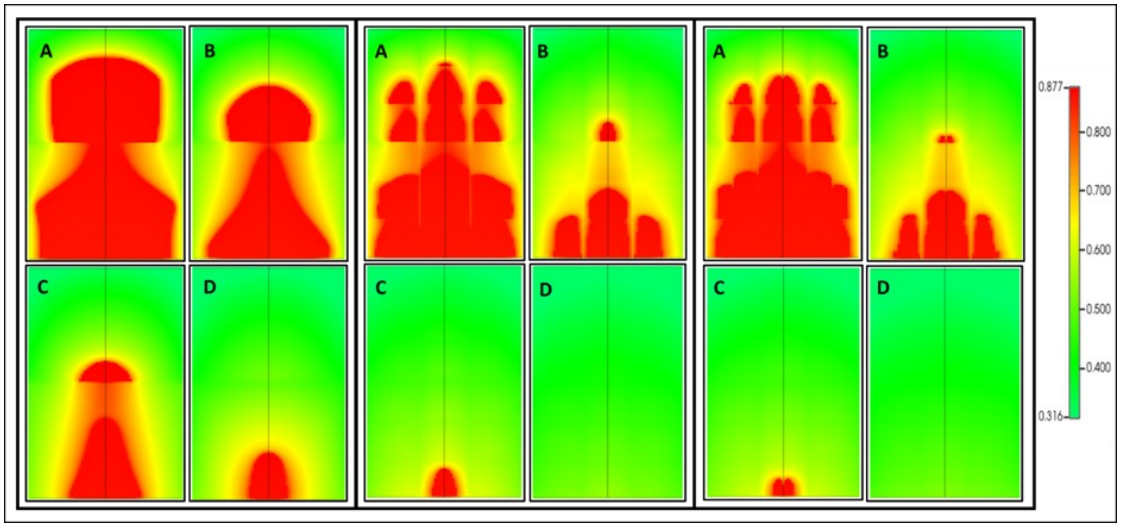

Figure 23: Oil saturation profile (oil in red & gas in green color) for gas injection process in the first category of fractures networks (Extended 2D model & Horizontal wells) left: Only Major fractures network, Middle: Major & Medium fractures networks, right: Major, Medium & Minor fractures networks, at A:0.5 PV, B:1 PV, C:1.5 PV, D:2 PV

4.1.2.4 3D Cube

A 3D cube was also used to investigate the potential behavior change when the fracture networks are included in the three dimensions and when a different number of grids is used. Generally, the results have indicated a similar behavior to the 2D model during the early period. However, the difference between the three cases starts to decrease after the injection of the first pore volume, as shown in Figure 24. This difference in the behavior for the later period between the 2D and 3D models is mainly related to the difference in the Rn or the intensity of the fractures, as additional two Major fractures are defined for the Major fractures network to form a cube. This increases the Rn from 0.5 in the 2D model to 0.6 in the 3D model. Moreover, this observation can be linked to similar observations in previous studies. Agada et al. (2016) highlighted that when the intensity of the fracture is above a certain threshold, the simulation results can be independent of the fundamental geological concept deployed to represent the fracture network. In our case, increasing the intensity of the Major fracture decreased the relative importance of the other fracture networks.

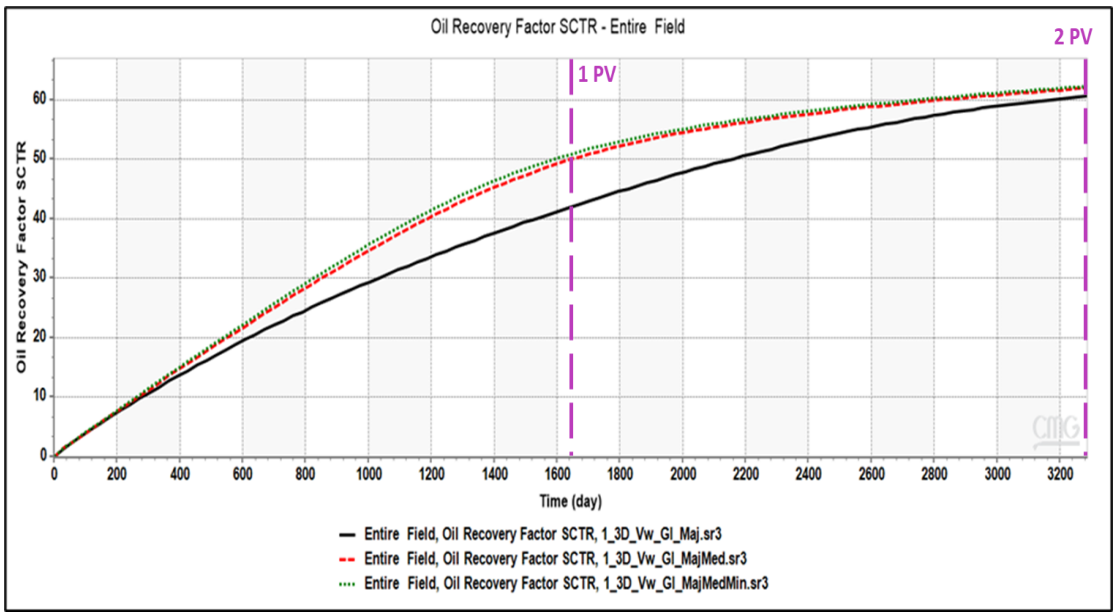

Figure 24: Oil Recovery factor for gas injection process in the first category of fractures networks (3D Cube model)

The GOR behavior demonstrates a similar trend to the standard 2D model and the Extended 2D model for overestimation and underestimation with minor differences in the magnitude (Figure 25).

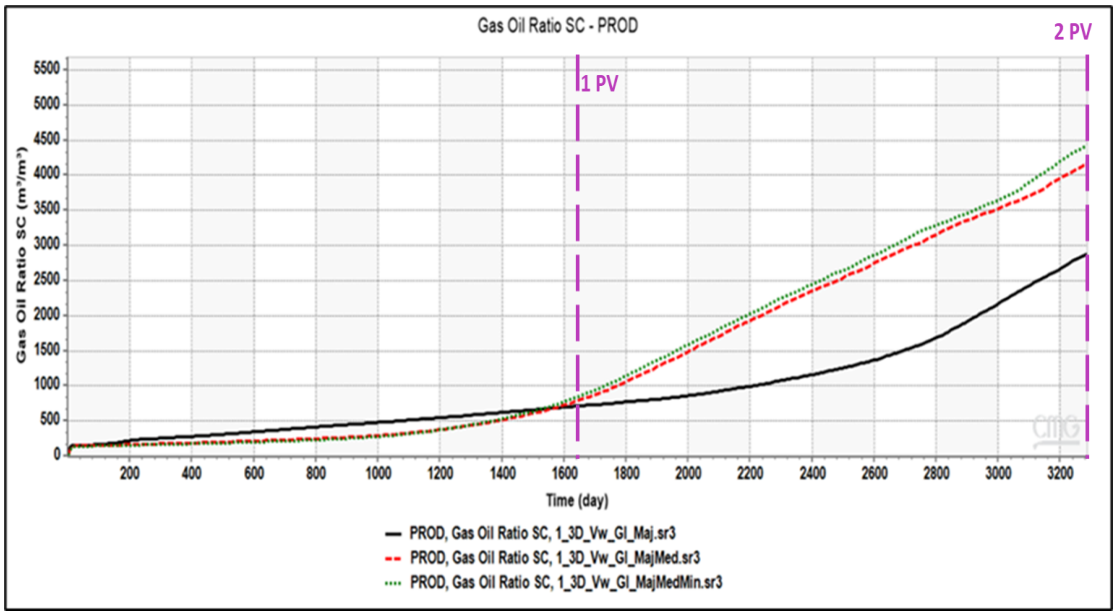

Figure 25: GOR for gas injection process in the first category of fractures networks (3D Cube model)

4.1.3 Foam-Assisted WAG

4.1.3.1 2D vertical Slice (Vertical Wells)

For the first category of fracture networks, results indicated that the differences in the estimations of recovery factor could be observed in the middle period of injection between 0.37 pore volumes and 1.58 pore volumes (Figure 26). Which also cross-pond to the gas phase injection in the first cycle and gas-phase injection in the third cycle, respectively.

When additional fracture networks are included, the maximum difference observed after the complete injection of 0.75 pore volumes is 10% reached during the aqueous phase injection in the second cycle. However, the reduction in the difference in the later period is mainly related to reducing the oil saturation to reach the residual oil saturation.

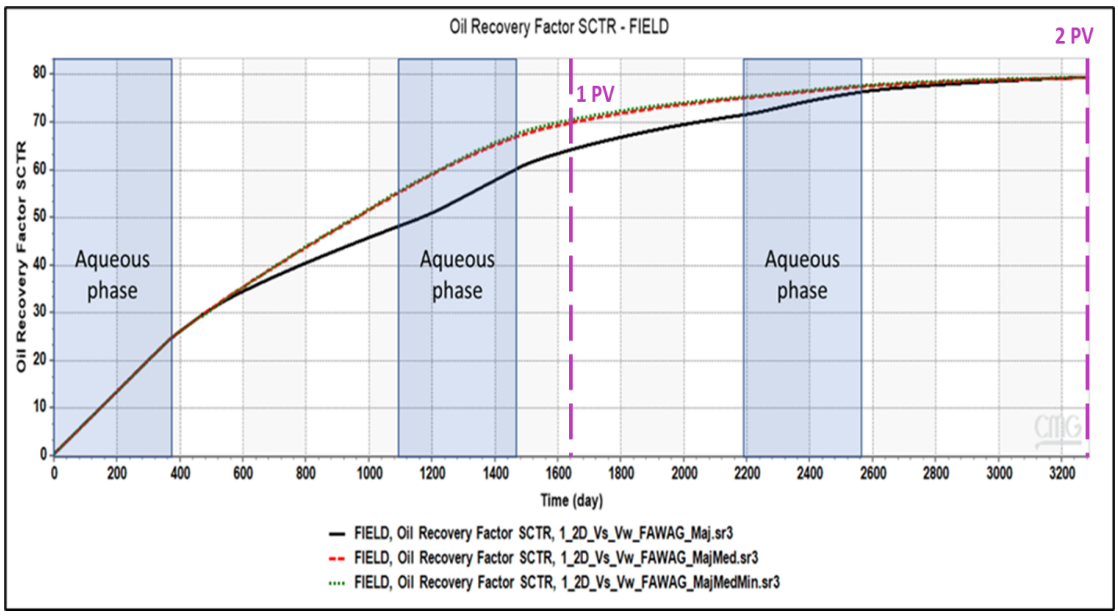

Figure 26: Oil Recovery factor for FAWAG process in the first category of fractures networks (2D Cube model)

The GOR behavior, as can be seen in Figure 27, demonstrates that excluding the additional fracture networks results in an overestimation of the produced gas volume during the first cycle. At the beginning of the second cycle, the opposite behavior can be observed where the produced gas volume starts to be underestimated until the end of the injection period. However, including the Minor fractures network has a smaller impact than the impact of including the Medium fractures network.

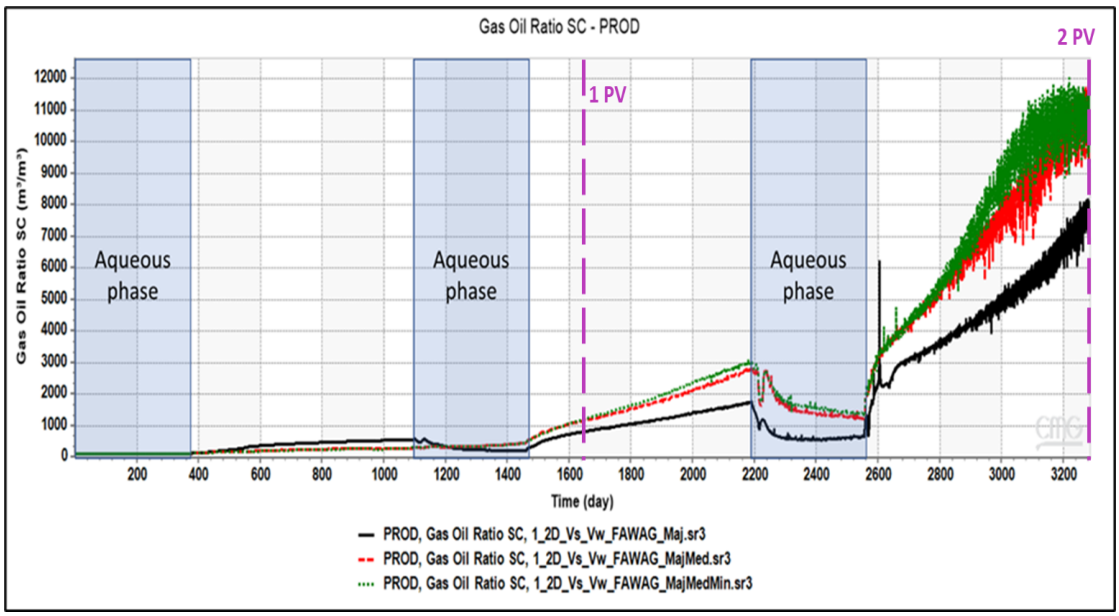

Figure 27: GOR for FAWAG process in the first category of fractures networks (2D Cube model)

As shown in Figure 28, a difference in the overall behavior for the water cut can be observed. Excluding the additional fracture networks result in slight water production in the first cycle as the aqueous phase flows directly through the Major fractures to reach the producer. On the other hand, water production only starts after the aqueous phase injection in the second cycle when the additional fracture networks are included. Moreover, the water cut increasing behavior tends to be linear, while when the additional networks are excluded, the behavior has an increasing curved trend. However, at the end of the aqueous phase injection in the second cycle, the trend of overestimating the water cut is inversed to underestimating the water cut. In the third cycle, the three cases have a similar increasing trend. These observations are mainly related to the fact that the presence of different phases in the fracture networks results in diverting the flow of other phases in the fracture networks.

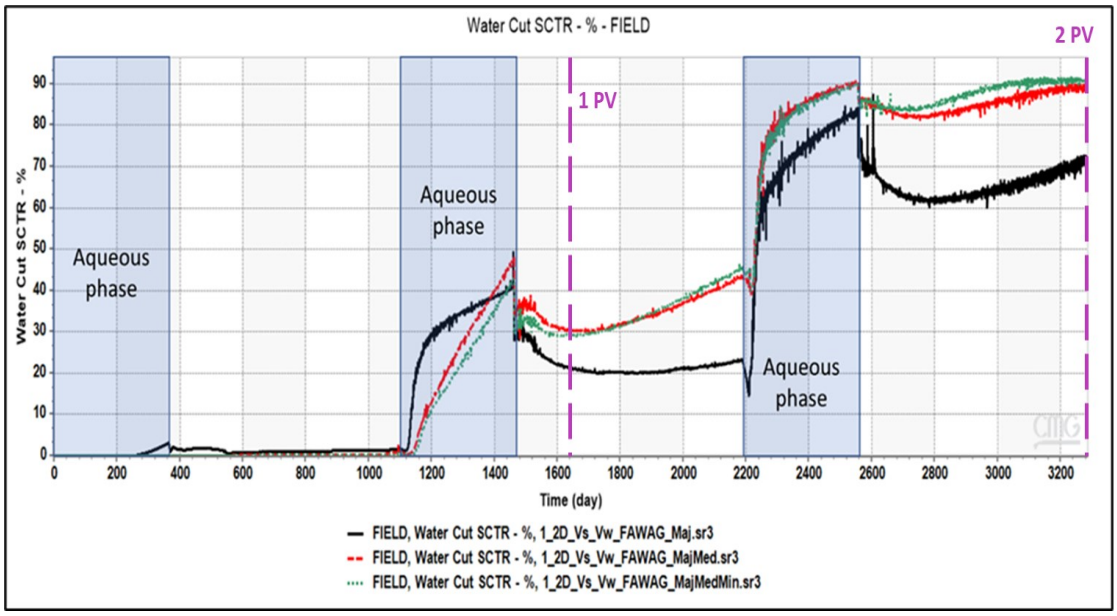

Figure 28: Water cut for FAWAG process in the first category of fractures networks (2D Cube model)

As shown in Figure 29, the gas saturation profile demonstrates the gas flow behavior in the fracture networks where the red color represents the gas phase, and the green color represents the oil phase. It can be seen that injection of the aqueous phase diverts the gas flow path in the fracture networks and into the matrix blocks.

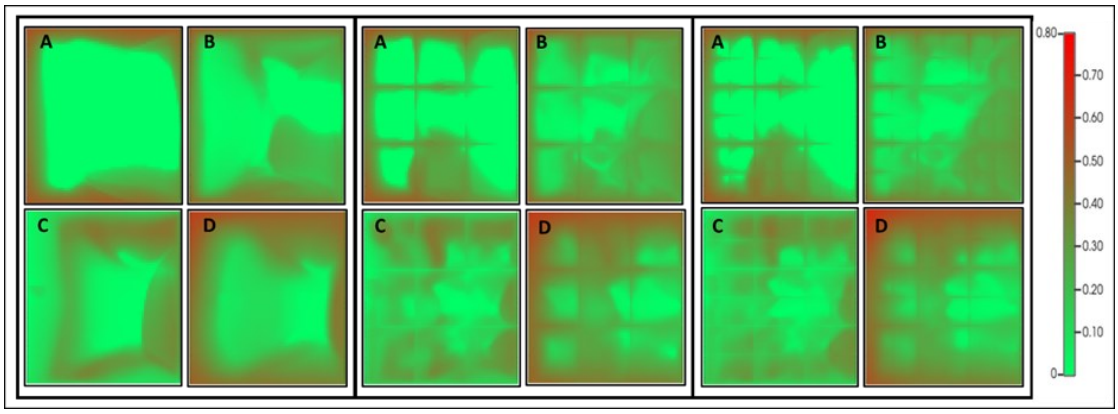

Figure 29: Gas saturation profile (gas in red & oil in green color) for FAWAG process in the first category of fractures networks (2D model) left: Only Major fractures network, Middle: Major & Medium fractures networks, right: Major, Medium & Minor fractures networks, at A:0.5 PV, B:1 PV, C:1.5 PV, D:2 PV

The aqueous phase (in blue) also flows through the Major, Medium, and Minor fractures networks and into the matrix blocks, as seen in the water saturation profile in Figure 30.

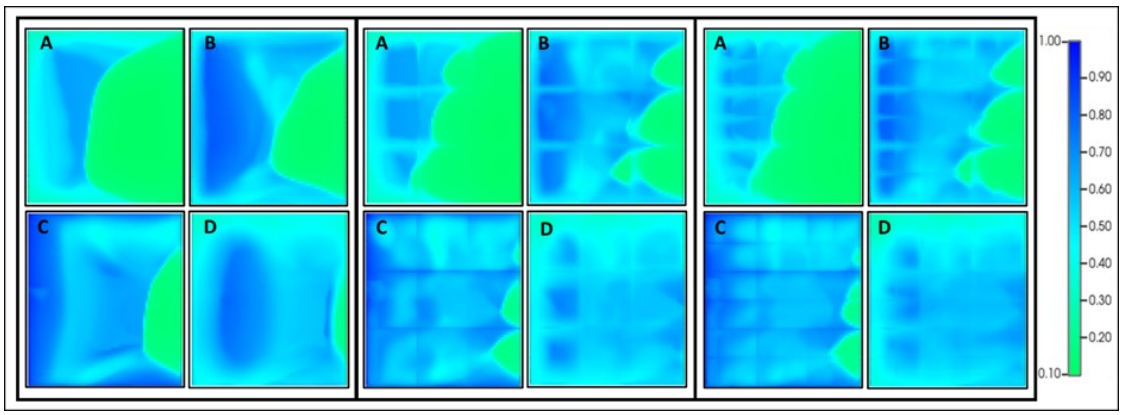

Figure 30: Water saturation profile (water in blue & oil in green color) for FAWAG process in the first category of fractures networks (2D model) left: Only Major fractures network, Middle: Major & Medium fractures networks, right: Major, Medium & Minor fractures networks, at A:0.5 PV, B:1 PV, C:1.5 PV, D:2 PV

Based on the defined foam model, the foam generation can be indicated through the relative permeability interpolator, as shown in Figure 31. The red color indicates that the required conditions for foam generation have not formed yet. Over time the turn of the red color into blue indicates that the necessary condition for foam generation has started to form, and the relative permeability for the gas phase will be modified consequently. However, it is important to highlight that the fluid saturation changes mainly control the conditions defined in this study.

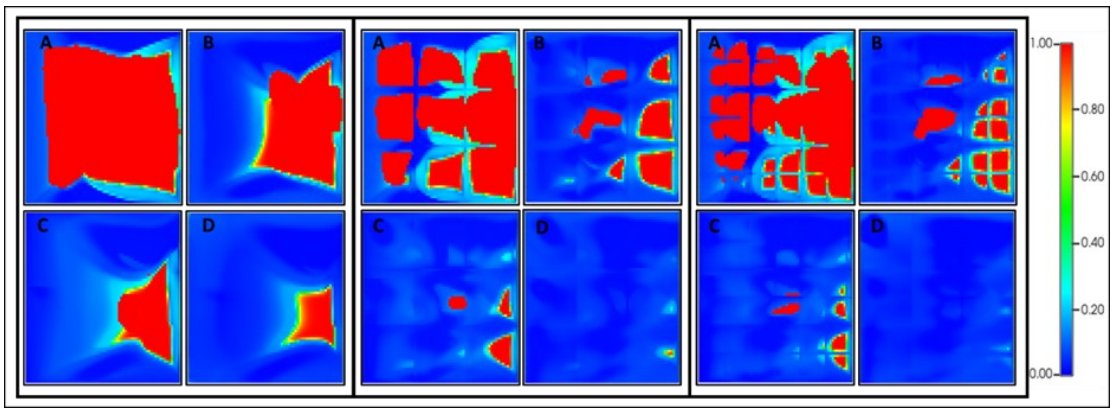

Figure 31: Relative permeability interpolator profile (in blue) for FAWAG process in the first category of fractures networks (2D model) left: Only Major fractures network, Middle: Major & Medium fractures networks, right: Major, Medium & Minor fractures networks, at A:0.5 PV, B:1 PV, C:1.5 PV, D:2 PV.

Figure 32 shows that the dry-out effect can also be indicated through the dry-out interpolation parameter, where the original gas relative permeability is restored. The red color indicates the dry-out location, while the green indicates that the dry-out conditions have not formed. The blue regions are cross-pond to locations where foam has not formed yet.

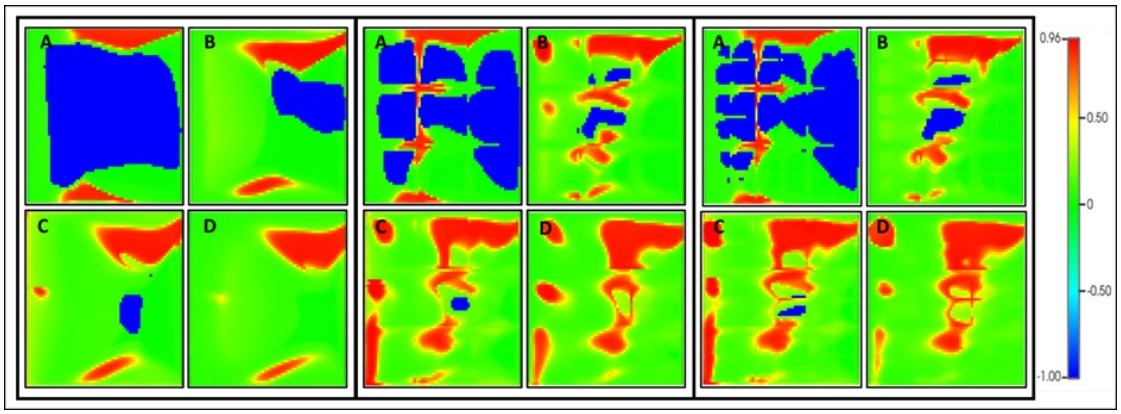

Figure 32: Dry-out interpolation parameter profile (in red) for FAWAG process in the first category of fractures networks (2D model) left: Only Major fractures network, Middle: Major & Medium fractures networks, Right: Major, Medium & Minor fractures networks, at A:0.5 PV, B:1 PV, C:1.5 PV, D:2 PV.

It is important to highlight that the fracture networks and the snap-off points impact foam generation. Prevues experimental studies discussed that the in-situ foam generation results in a larger bubble size than pre-foamed foam (Haugen et al., 2012). However, the used simulation model in this study cannot be used to indicate the size of the bubble.

For the second category of fracture networks, results indicate slight differences in the estimations of recovery factors observed in the middle period, similar to the first category cases (Figure 33).

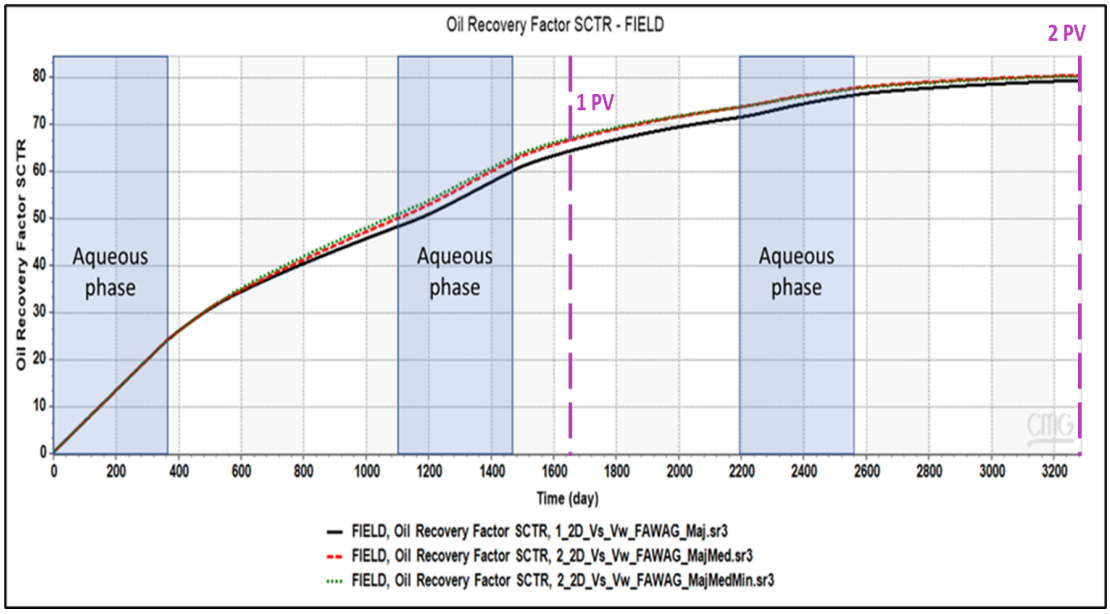

Figure 33: Oil Recovery factor for FAWAG process in the second category of fractures networks (2D Cube model)

Similar to the recovery factor, the GOR behavior, as shown in Figure 34, demonstrates a very slight difference over the injection period when the Medium and the Minor fractures networks are excluded.

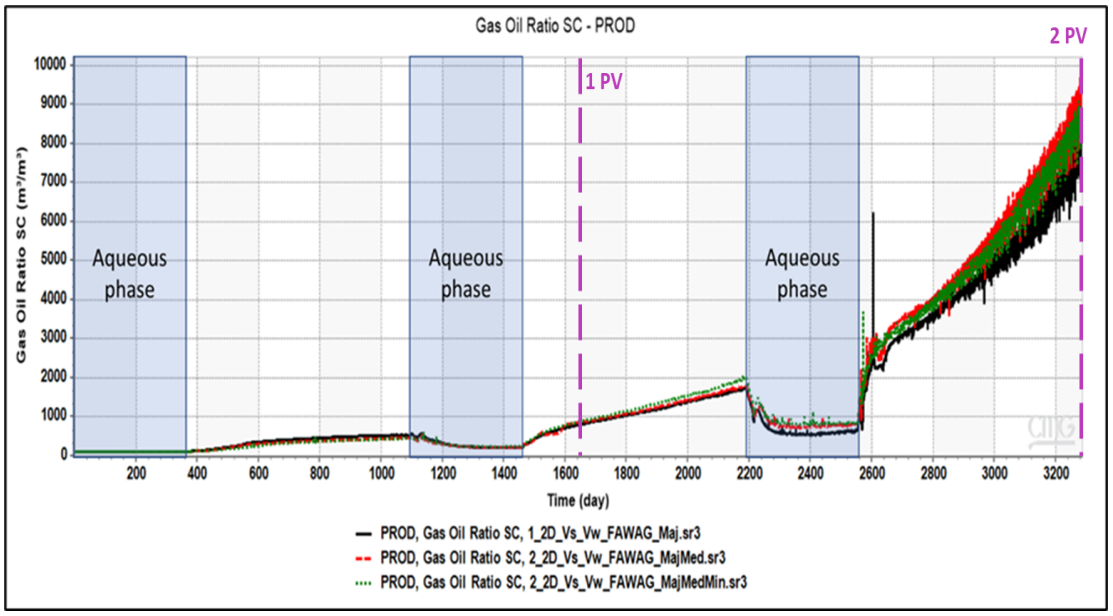

Figure 34: GOR for FAWAG process in the second category of fractures networks (2D Cube model)

The water cut behavior for the second category of fracture networks, as shown in Figure 35, demonstrates a similarity in the overall behavior in contrast to the first category of fracture networks. However, a slight difference in the water cut magnitude can still be observed from the start of the second cycle.

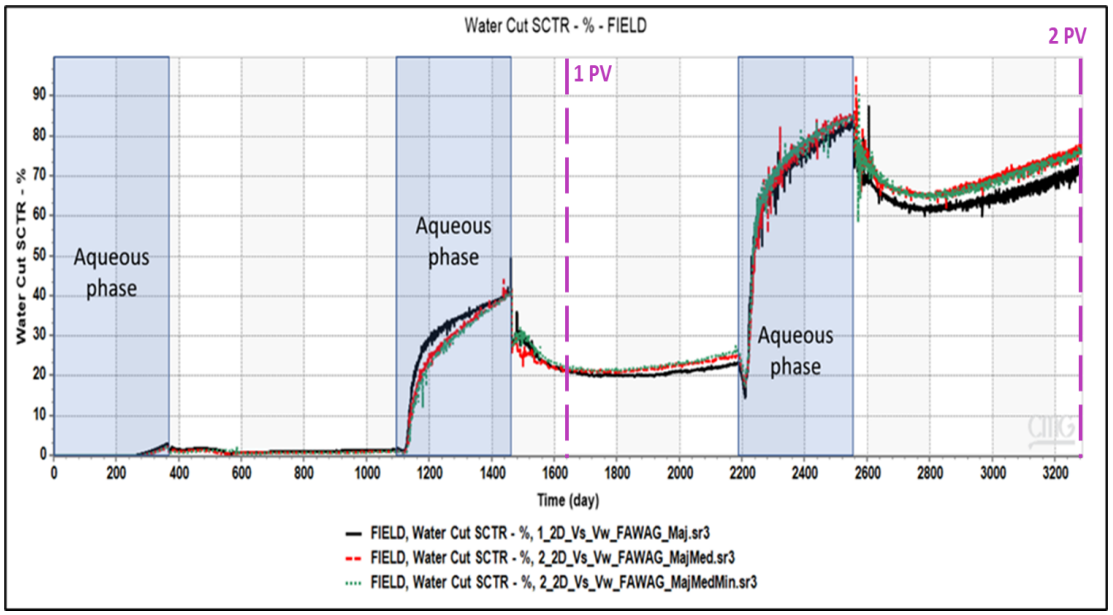

Figure 35: Water cut for FAWAG process in the second category of fractures networks (2D Cube model)

The gas flow behavior in the fracture networks is shown in Figure 36. It can be seen that including the Minor fracture networks has no additional impact on the flow behavior, while including the Medium fracture networks can still impact the gas flow behavior.

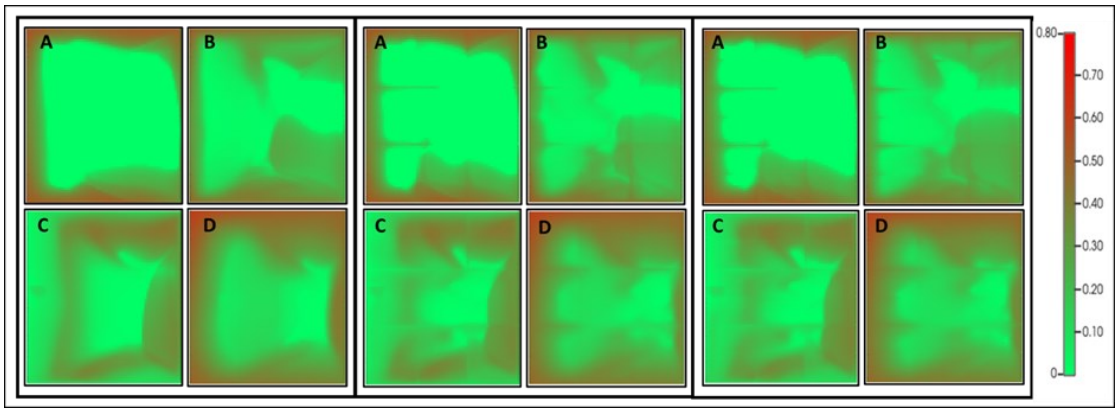

Figure 36: Gas saturation profile (gas in red & oil in green color) for FAWAG process in the second category of fractures networks (2D model) left: Only Major fractures network, Middle: Major & Medium fractures networks, right: Major, Medium & Minor fractures networks, at A:0.5 PV, B:1 PV, C:1.5 PV, D:2 PV

Figure 37 shows that the water phase saturation profile indicates a similar observation to the gas phase. The Minor fractures network has a neglectable impact on the flow behavior, and the Medium fractures network has a very slight impact.

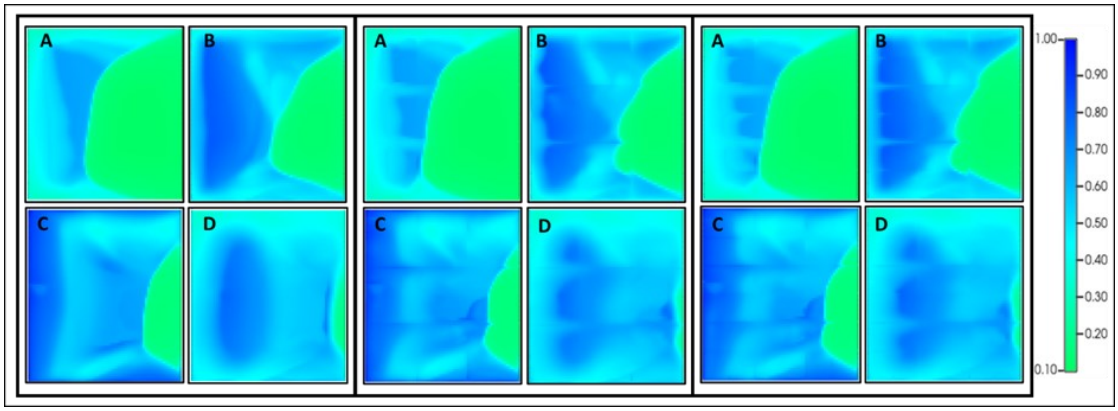

Figure 37: Water saturation profile (water in blue & oil in green color) for FAWAG process in the second category of fractures networks (2D model) left: Only Major fractures network, Middle: Major & Medium fractures networks, right: Major, Medium & Minor fractures networks, at A:0.5 PV, B:1 PV, C:1.5 PV, D:2 PV

As shown in Figure 38, the relative permeability interpolator also indicates that including the Minor fractures network will not affect the predicted location for foam generation compared to the case where the Medium fractures network is included in addition to the Major fractures Network.

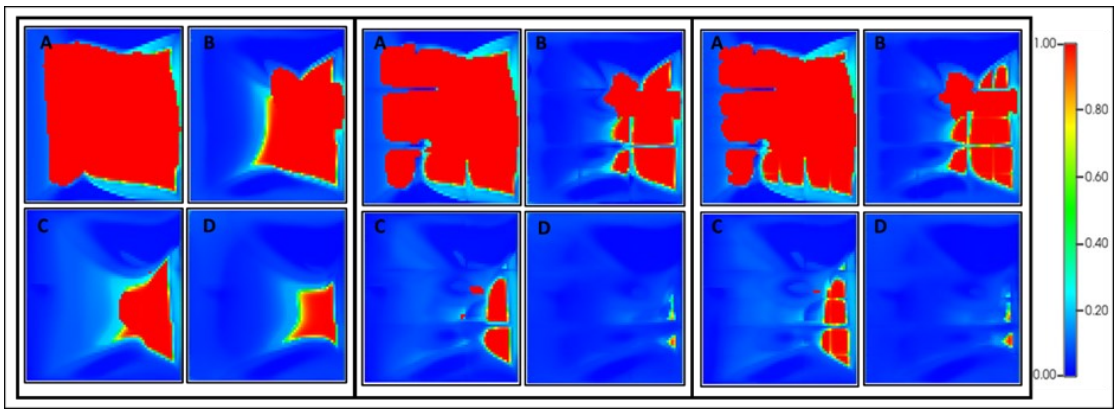

Figure 38: Relative permeability interpolator profile (in blue) for FAWAG process in the second category of fractures networks (2D model) left: Only Major fractures network, Middle: Major & Medium fractures networks, right: Major, Medium & Minor fractures networks, at A:0.5 PV, B:1 PV, C:1.5 PV, D:2 PV.

As shown in Figure 39, and similar to the relative permeability interpolator, the dry-out interpolation parameter indicates that excluding the Minor fractures network will not affect the predicted location for the dry-out.

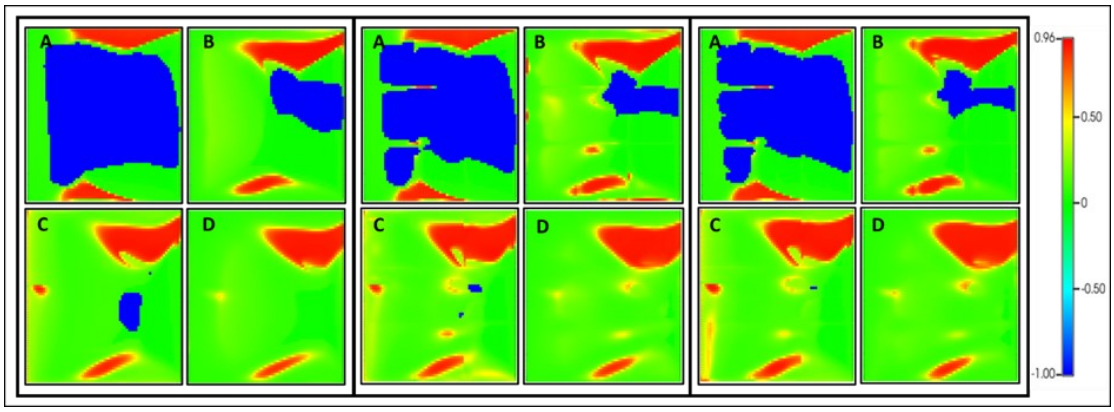

Figure 39: Dry-out interpolation parameter profile (in red) for FAWAG process in the second category of fractures networks (2D model) left: Only Major fractures network, Middle: Major & Medium fractures networks, right: Major, Medium & Minor fractures networks, at A:0.5 PV, B:1 PV, C:1.5 PV, D:2 PV.

In the third category for fracture networks, no major differences can be indicated from the demonstrated results for the recovery factors (Figure 40). This means that the Medium and the Minor fractures network have not affected the flow behavior.

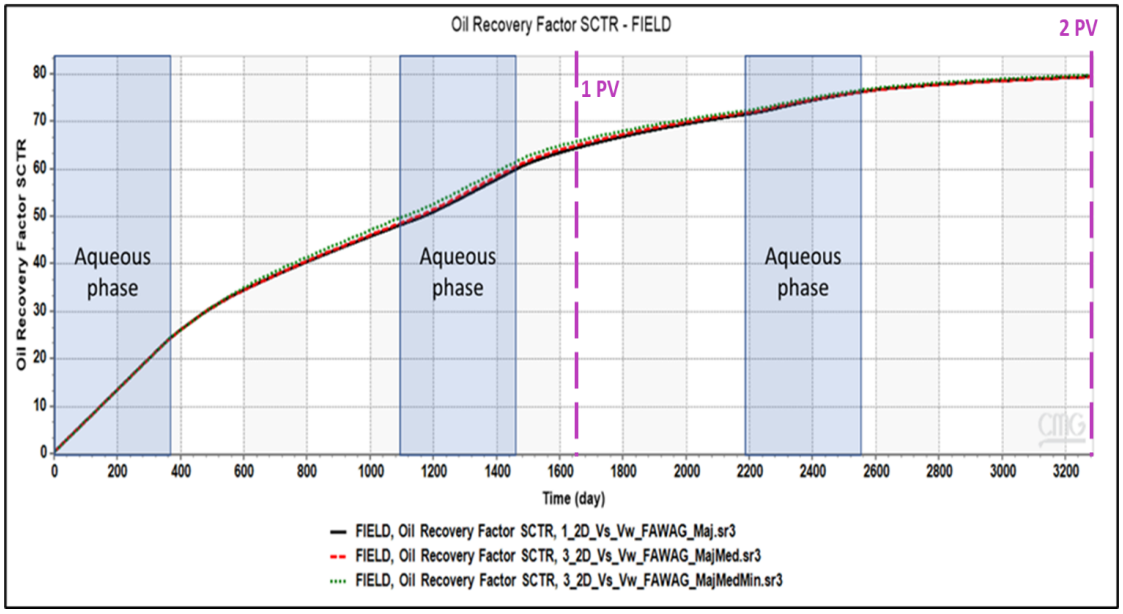

Figure 40: Oil Recovery factor for FAWAG process in the third category of fractures networks (2D model)

The GOR behavior, as can be seen in Figure 41, indicates a very identical behavior in the three cases.

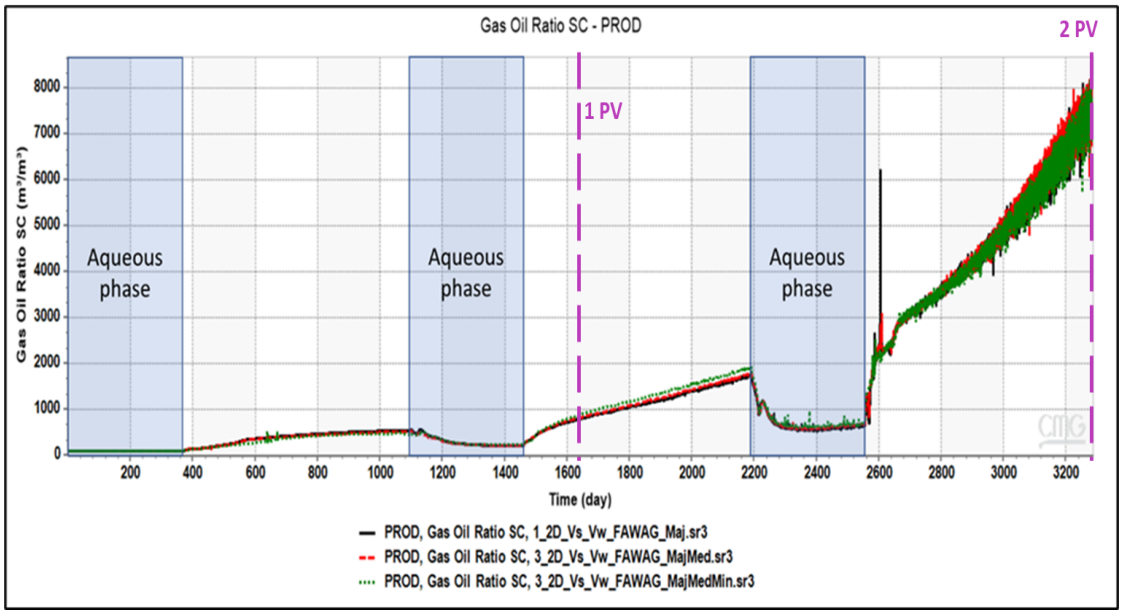

Figure 41: GOR for FAWAG process in the third category of fractures networks (2D model)

Additionally, Figure 42 shows that the water cut behavior demonstrates a similar overall behavior without notable differences.

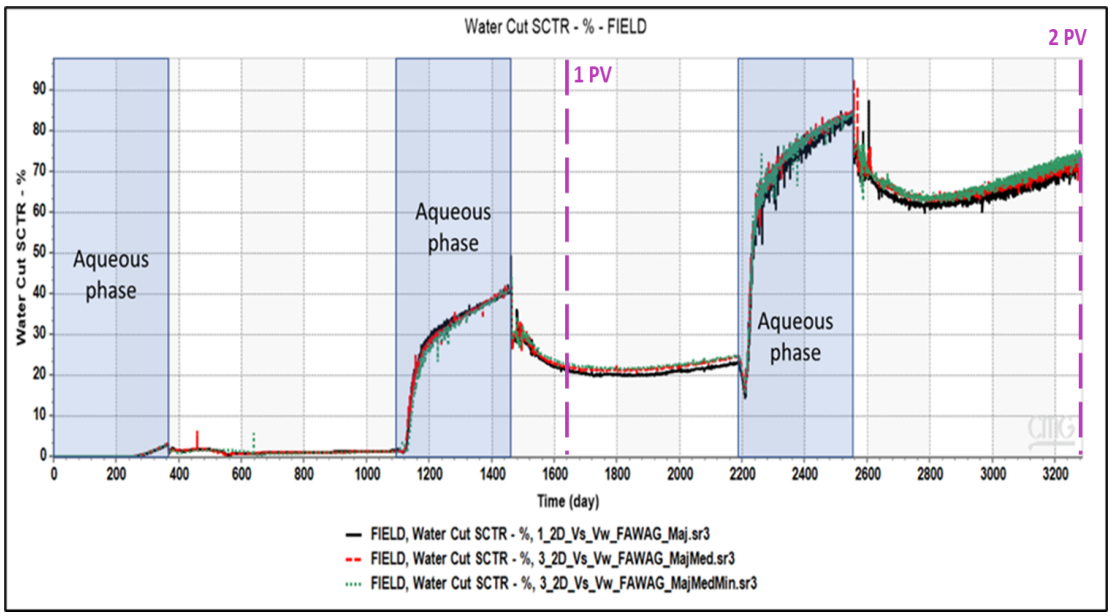

Figure 42: Water cut for FAWAG process in the third category of fractures networks (2D model)

As shown in Figure 43, the gas saturation profile demonstrates that the gas flow behavior in the fracture networks was not affected significantly by including the Medium and Minorfracture networks.

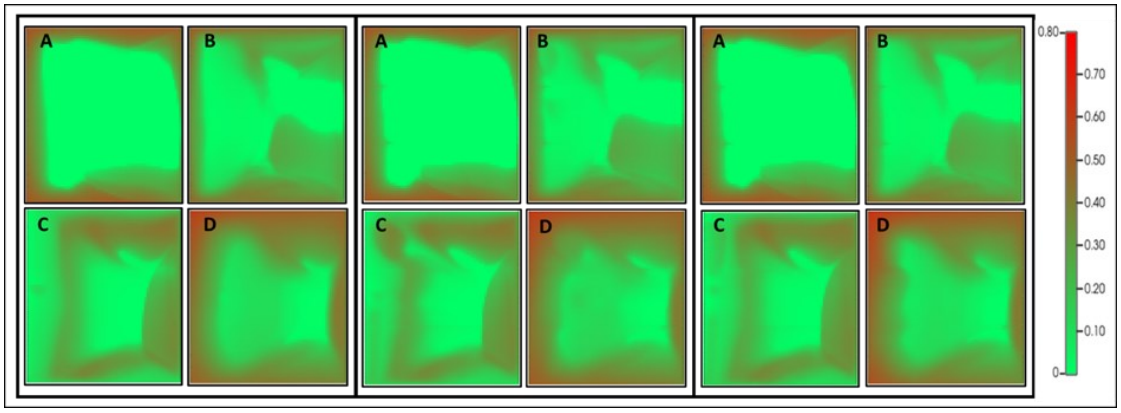

Figure 43: Gas saturation profile (gas in red & oil in green color) for FAWAG process in the third category of fractures networks (2D model) left: Only Major fractures network, Middle: Major & Medium fractures networks, right: Major, Medium & Minor fractures networks, at A:0.5 PV, B:1 PV, C:1.5 PV, D:2 PV

Figure 44 shows that the water phase saturation profile indicates a similar observation to the gas phase.

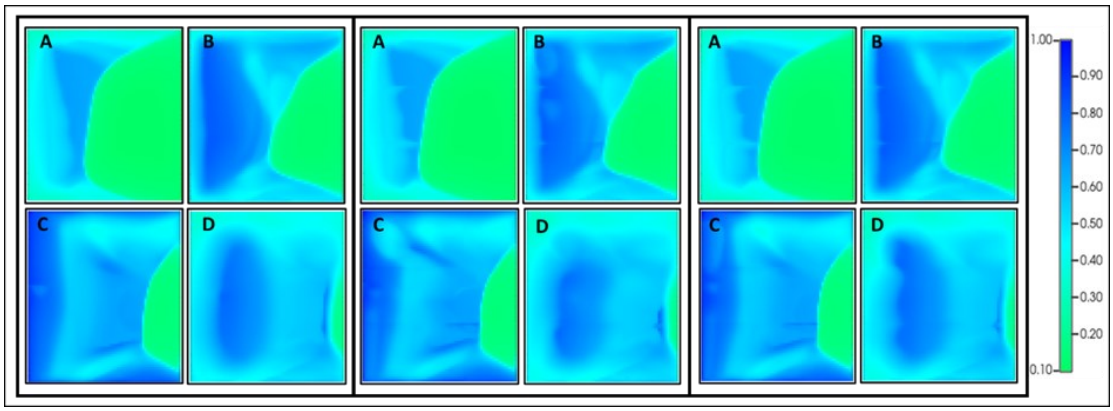

Figure 44: Water saturation profile (water in blue & oil in green color) for FAWAG process in the third category of fractures networks (2D model) left: Only Major fractures network, Middle: Major & Medium fractures networks, right: Major, Medium & Minor fractures networks, at A:0.5 PV, B:1 PV, C:1.5 PV, D:2 PV.

Figure 45 shows that the relative permeability interpolator indicates that including the Medium and the Minor fracture networks does not affect the foam generation behavior.

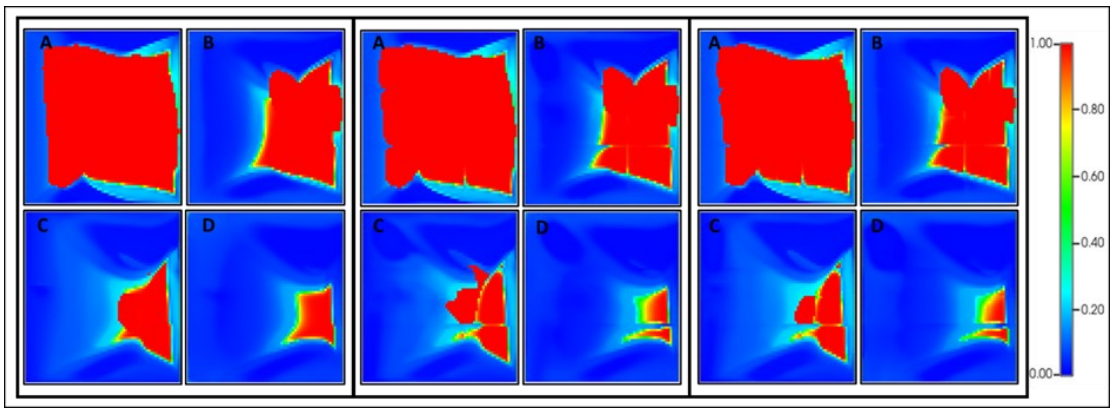

Figure 45: Relative permeability interpolator profile (in blue) for FAWAG process in the third category of fractures networks (2D model) left: Only Major fractures network, Middle: Major & Medium fractures networks, right: Major, Medium & Minor fractures networks, at A:0.5 PV, B:1 PV, C:1.5 PV, D:2 PV

As shown in Figure 46, the dry-out interpolation parameter also indicates that excluding the Medium and the Minor fracture networks will not significantly affect the predicted location for the dry-out. However, a larger dry-out at the upper block can still be observed near the injector. This might be caused by the faster increase in gas saturation supplied through the Medium network.

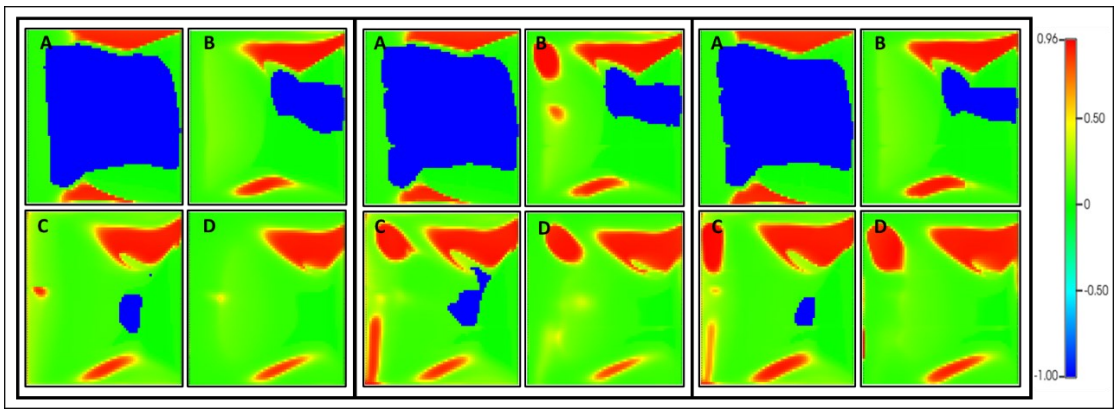

Figure 46: Dry-out interpolation parameter profile (in red) for FAWAG process in the third category of fractures networks (2D model) left: Only Major fractures network, Middle: Major & Medium fractures networks, right: Major, Medium & Minor fractures networks, at A:0.5 PV, B:1 PV, C:1.5 PV, D:2 PV

The demonstrated results have highlighted the relative importance and the impact of excluding and including the fracture networks on the recovery process. However, the behavior and the magnitude of the impact of excluding and including the fracture networks might also be considered as process-dependent. Therefore, in this study, the normal WAG process was compared to the FAWAG, as shown in Figure 47, when different fracture networks were included.

Results indicated that excluding the Medium fractures network results in an underestimation of the positive impact of the foam generation in improving the recovery. The impact can only be observed at the end of injecting the aqueous phase in the second cycle. At the same time, when the Medium fractures network is also included, a positive impact can be observed during the gas injection in the first cycle. However, a very slight difference can be observed when the Minor fractures network is included, which means that the Medium fractures network mainly drives the additional contribution.

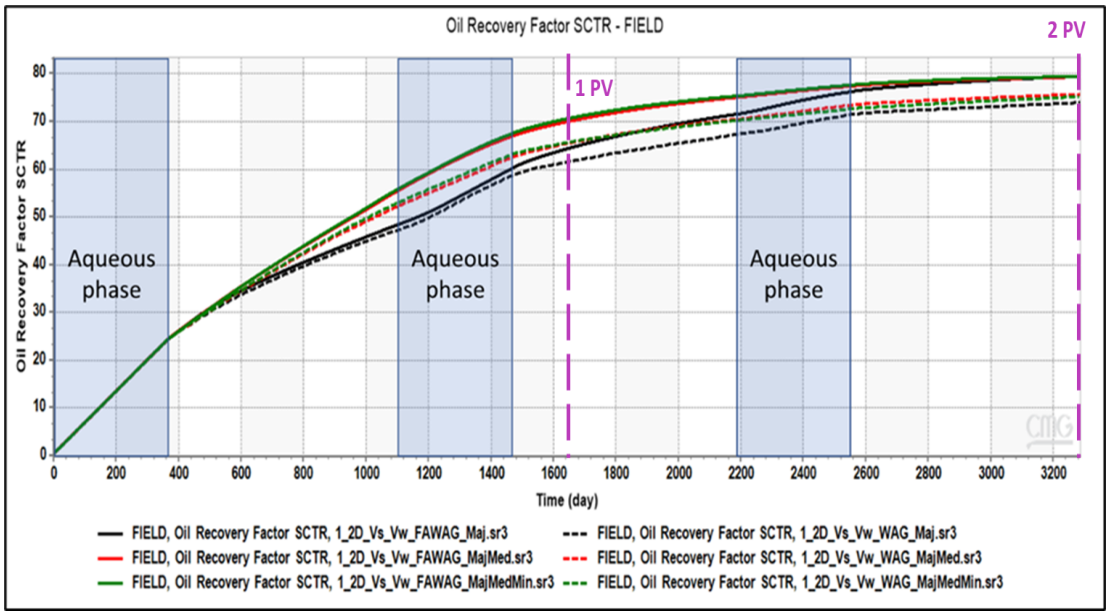

Figure 47: Oil Recovery factor for FAWAG & WAG processes in the first category of fractures networks (2D model)

4.1.3.2 3D Cube

In contrast to the 2D model, the 3D model shows a comparable estimation for the recovery factor in the first category of fracture networks, as shown in Figure 48. which means that excluding the additional fractures network is not affecting the estimation. This observation is mainly related to the differences in the Rn as discussed in the gas injection process.

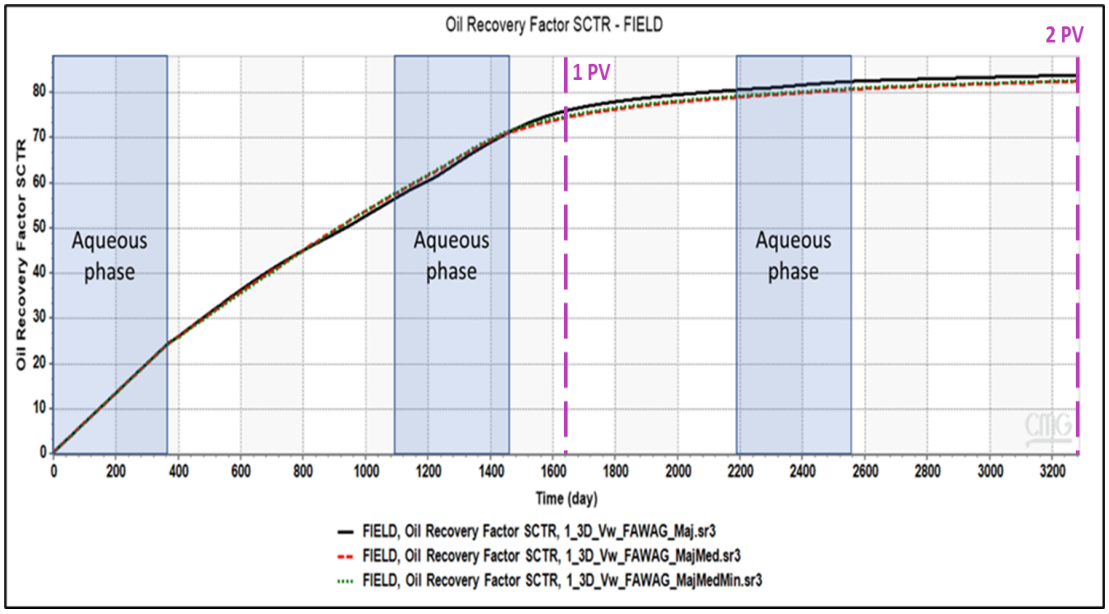

Figure 48: Oil Recovery factor for FAWAG process in the first category of fractures networks (3D Cube model)

The GOR behavior, as shown in Figure 49, indicates that the major differences can be observed at the beginning of the third cycle. Slight differences can also be observed at the beginning of the second cycle of gas-phase injection. However, the observed differences between the 2D and the 3D model in the second cycle might be related to the placement of the wells. In the case of a quarter 5-spot pattern, wells need to be placed in diagonal alignment across the cube.

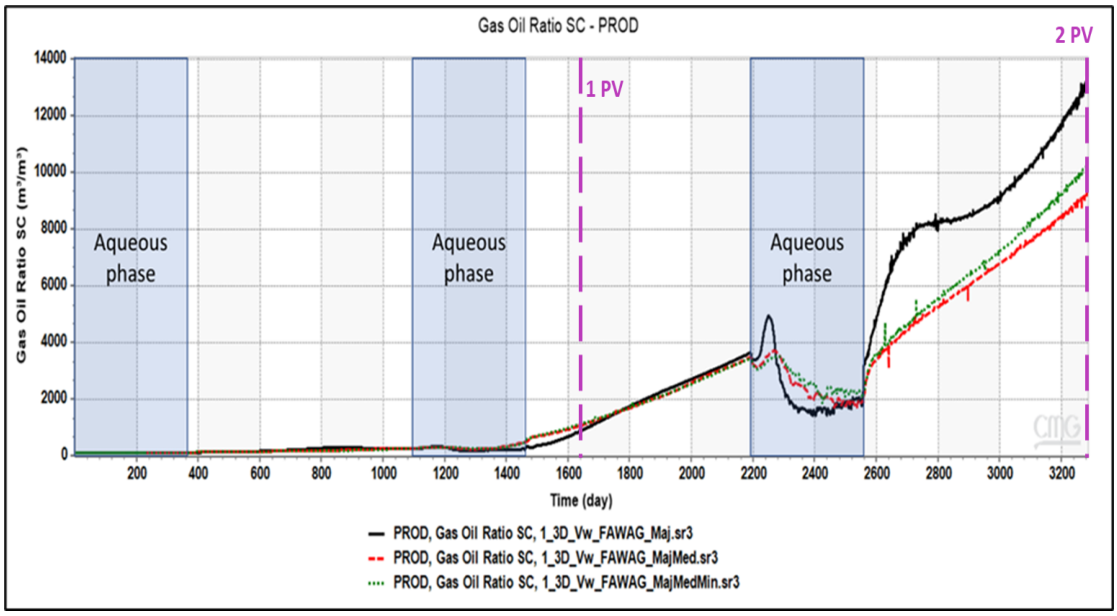

Figure 49: GOR for FAWAG process in the first category of fractures networks (3D Cube model)

The differences in the estimations for the water cut can still be observed in the second cycle, as shown in Figure 50. These observations mean that the effect of excluding the fracture networks can not be completely neglectable, even in the case of high fracture intensity, where it can still impact the estimated produced volumes.

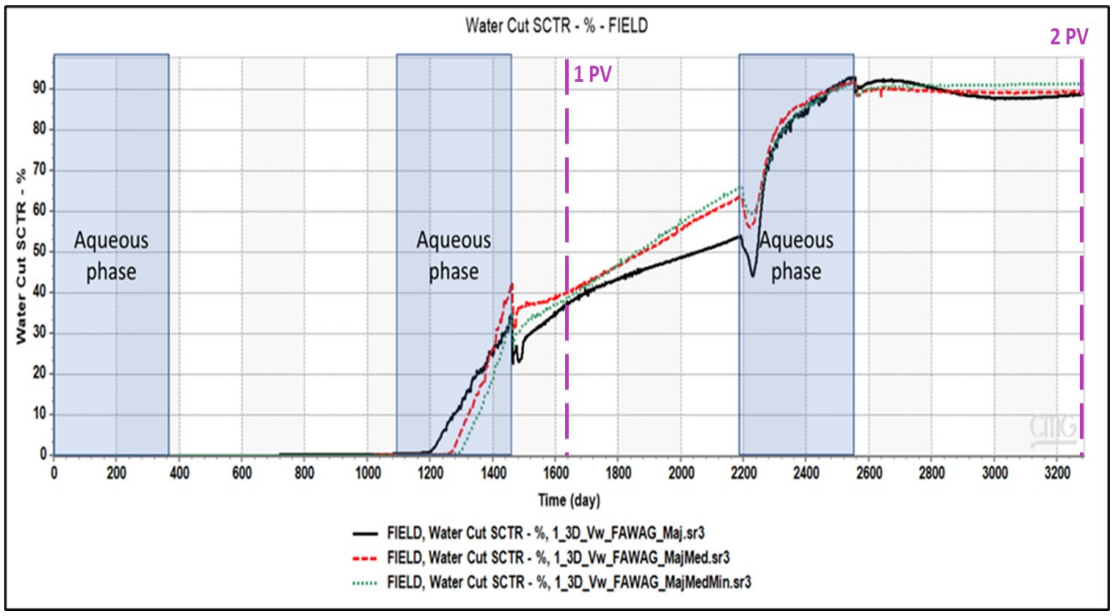

Figure 50: Water cut for FAWAG process in the first category of fractures networks (3D Cube model)

4.2 Sensitivity analysis

4.2.1 Effect on the Recovery Factor

The results section demonstrates that including or excluding the fracture types can significantly impact the estimation of recovery factor and the estimated volumes for the produced phases. In this section, the recovery factor at one pore volume will be used as a comparison point to quantify the effect of the fracture networks on the recovery in the context of the defined dimensionless numbers.

For the gas injection process, results indicated that the increase in the Rd and Rd3 decreases the impact of the additional fractures network on the recovery factor, as shown in Figure 51.

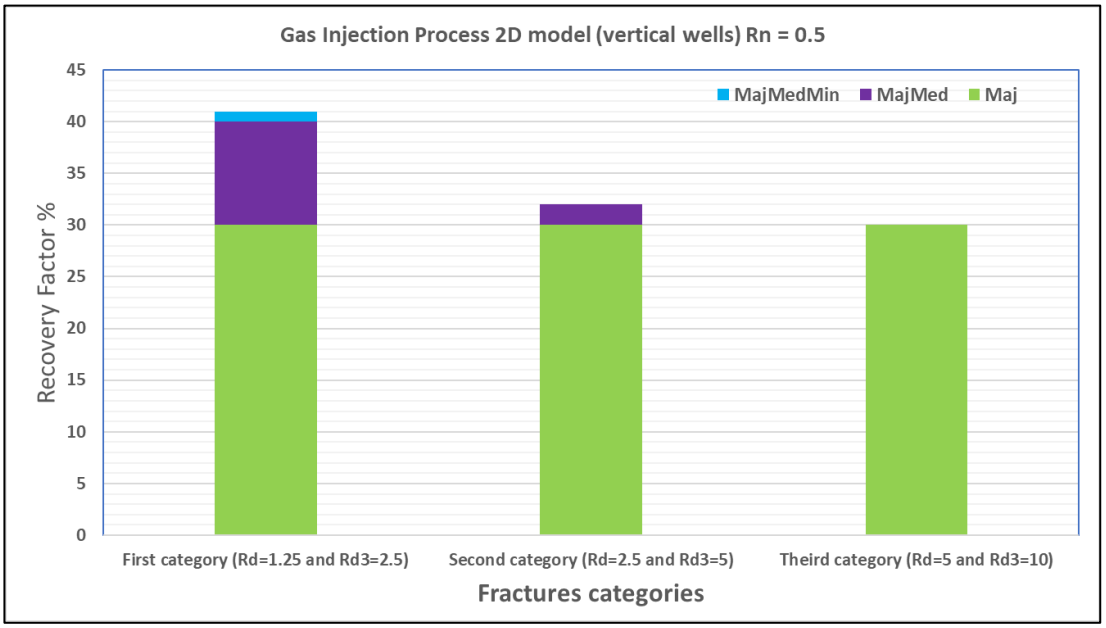

Figure 51: Effect of fractures networks on the recovery factor for the gas injection process

Similar to the gas injection process, results for the FAWAG process indicate that the increase in the Rd and Rd3 decreases the impact on the recovery factor, as can be seen in Figure 52.

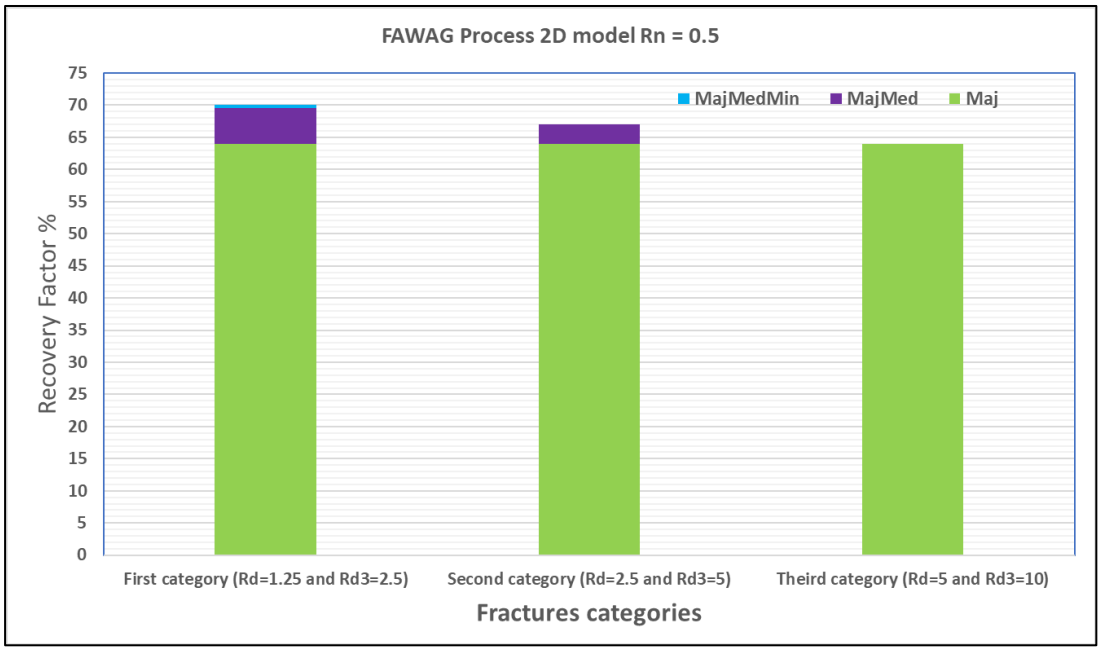

Figure 52: Effect of fractures networks on the recovery factor for FAWAG injection process

Moreover, the decision to include or exclude the fractures networks can also be affected by the Rn, which relates to the intensity of the Major fractures. The gas injection process results indicated that the Rn increase results in decreasing the relative importance of including the other fractures network, as shown in Figure 53.

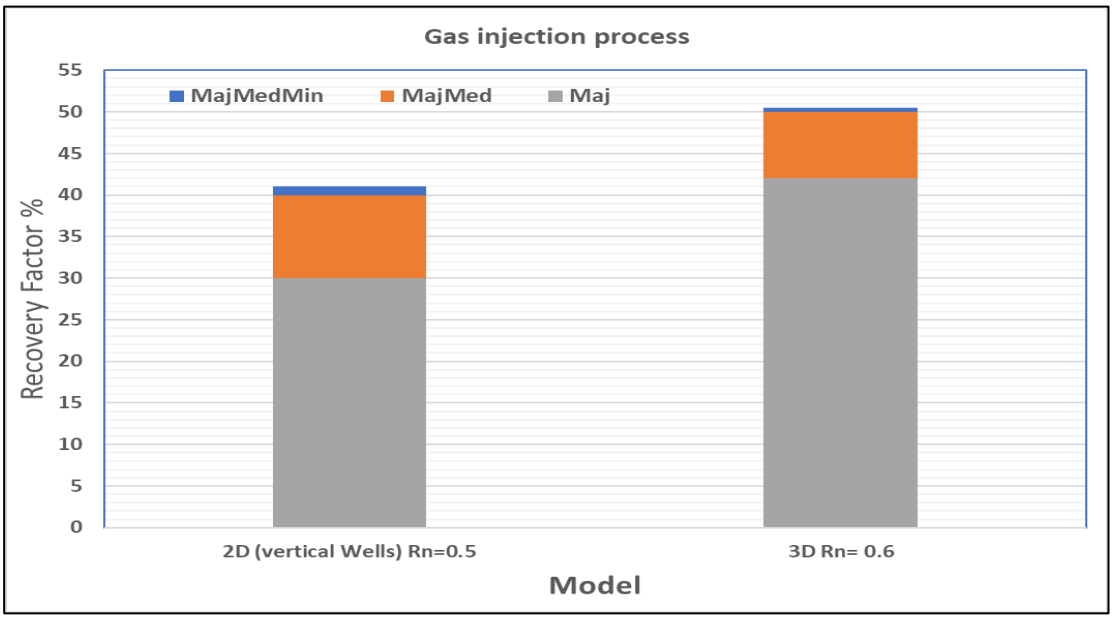

Figure 53: Comparison between the effect of fractures networks on the recovery factor for gas injection process in the 2D and 3D models

Results for the FWAG process indicated that the additional fracture networks could be excluded without any important effect on the estimation of the recovery factor when the Rn number increased to 0.6 in the 3D model, as shown in Figure 54.

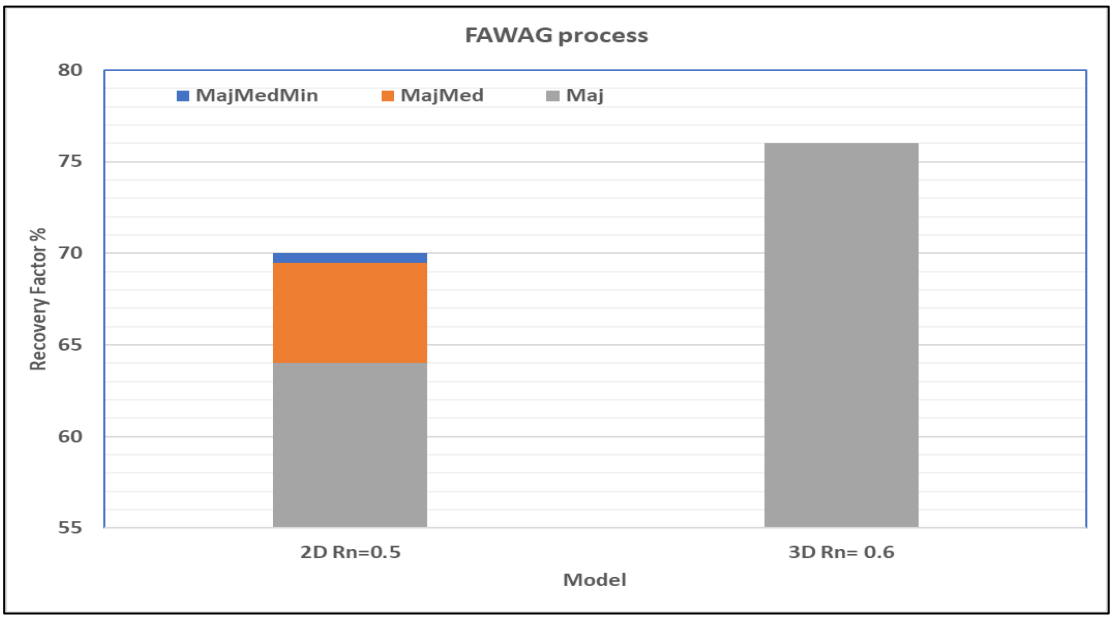

Figure 54: Comparison between the effect of fractures networks on the recovery factor for the FAWAG process in the 2D and 3D models

Using the extended vertical model for the first category has also highlighted that the difference magnitude increases with increasing the reservoir height (Figure 55). Therefore, including or excluding the other fracture networks is important for the assisted gravity drainage processes.

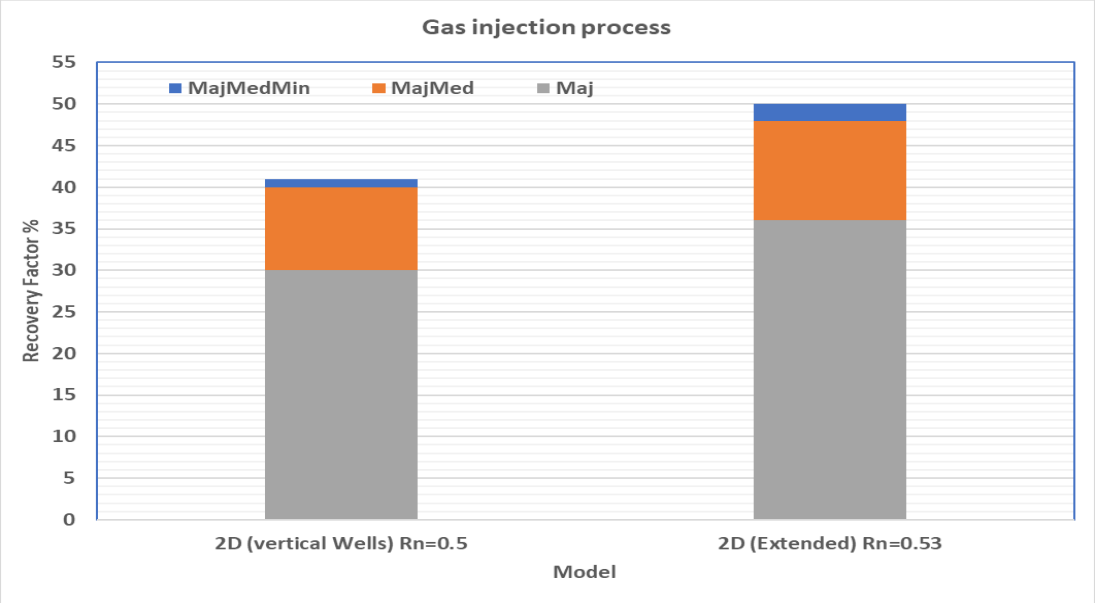

Figure 55: Comparison between the effect of fractures networks on the recovery factor for gas injection process in the 2D and the extended vertical 2D models

Results for the WAG process compared to the FAWAG process have also indicated that the magnitude of impact on the recovery factor can also be a process depending (Figure 56). Continuos gas injection process for the GEM model was also obtained to compare the impact magnitude for the three processes. However, it is important to highlight that the used results in this figure are not comparable to the other results for the gas injection process since different fluid models were used. Moreover, the difference between both results emphasizes the additional impact of the fluid properties on the impact magnitude of the fracture networks.

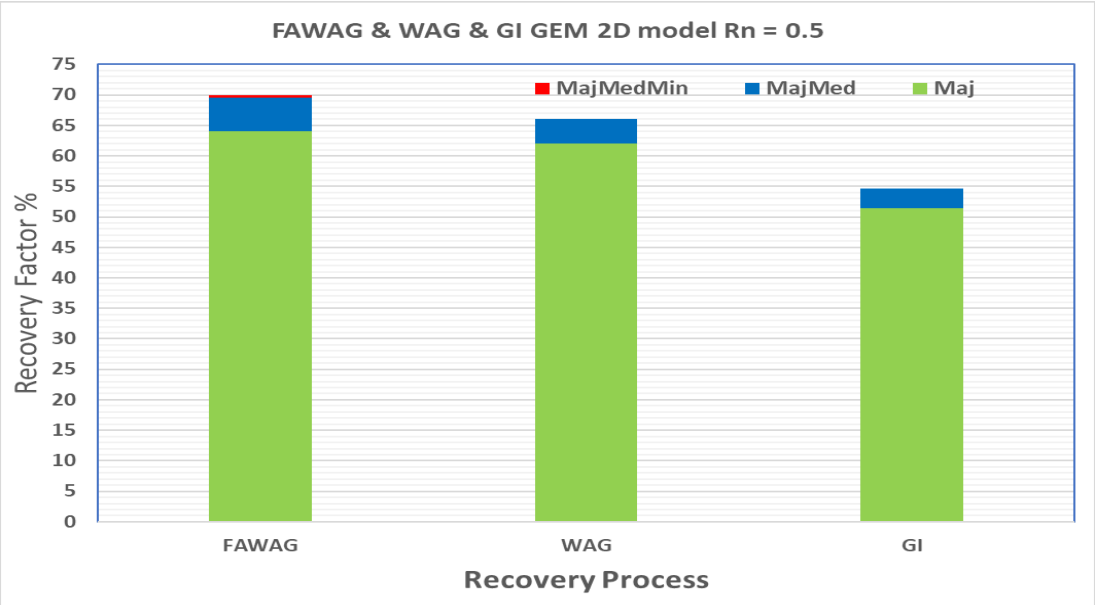

Figure 56: Comparison between the effect of fractures networks on the recovery factor for WAG, FWAG, and GI processes in the 2D GEM model

4.2.2 Homogenization

In the widely used dual continuum models, fracture networks are defined as single fracture sets with averaged properties and spatial spacing in the three dimensions to represent the fracture networks and intensity. The fractures domain will also need defined relative permeability and capillary pressure curves to represent and describe the flow in the fractures. Moreover, a transfer function is needed to describe the interaction between the fractures and matrix domains. These simplifications might not have a remarkable impact on the flow directions and the produced fluid quantities during the primary production. However, this can significantly impact the multi-phase fluid flow behavior and, consequently, the estimated produced fluids volumes for different recovery processes.

Based on the demonstrated results, the highest impact for including or excluding the additional fracture types can be observed in the first category. Hence, the expected impact of the fracture networks homogenization properties is analyzed with three homogenization options. In the first option, all the fractures are considered as a single homogenized set with the same properties as Major, Medium, and Minor. The Minor fractures are excluded in the second option, and the Medium and the Major fractures are Homoginzed into a single set with the same properties in two separate cases. In the third option, the matrix permeability is adjusted to account for the effects of the fracture without the need for explicit representation for the fracture networks, which is also known as pseudo-matrix. The three options results are compared with respect to the original case where all the fracture networks are explicitly represented with the different defined properties for each set.

4.2.2.1 Gas injection

For the first option and where the possibility of considering all the fractures as a single set was investigated, as shown in Figure 57, results have indicated that this homogenization assumption in three cases has overestimated the recovery factor.

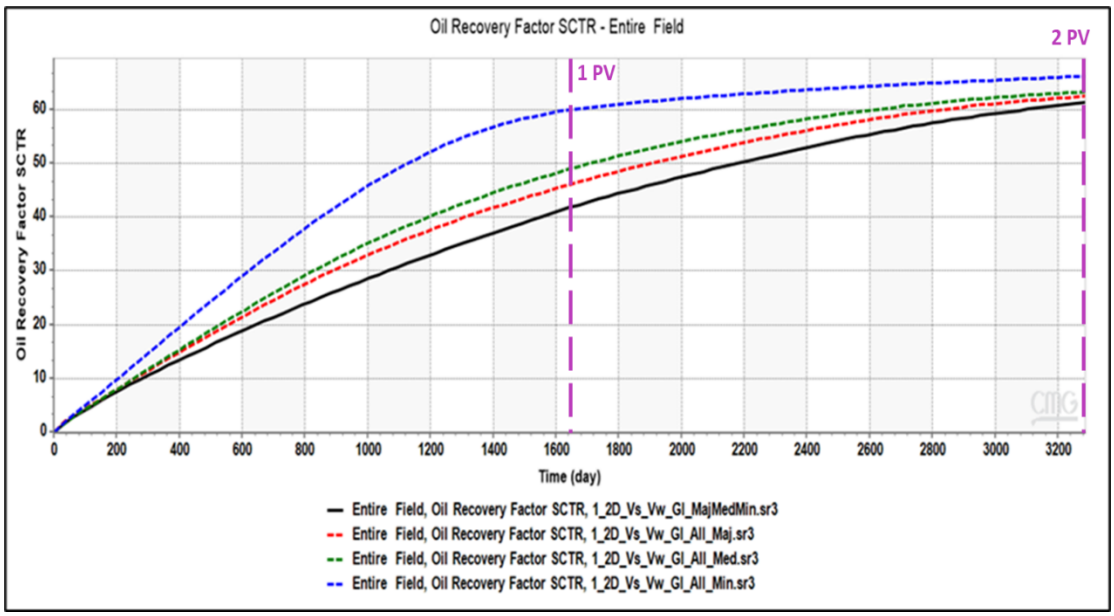

Figure 57: Oil Recovery factor for gas injection process in the first category of fractures networks when all fractures are included in a single set (2D model & Vertical wells)

Moreover, the GOR also indicated that the produced gas volume at the early period before injecting 0.5 pore volumes would be underestimated. In contrast, the GOR will be overestimated in the later period, as shown in Figure 58.

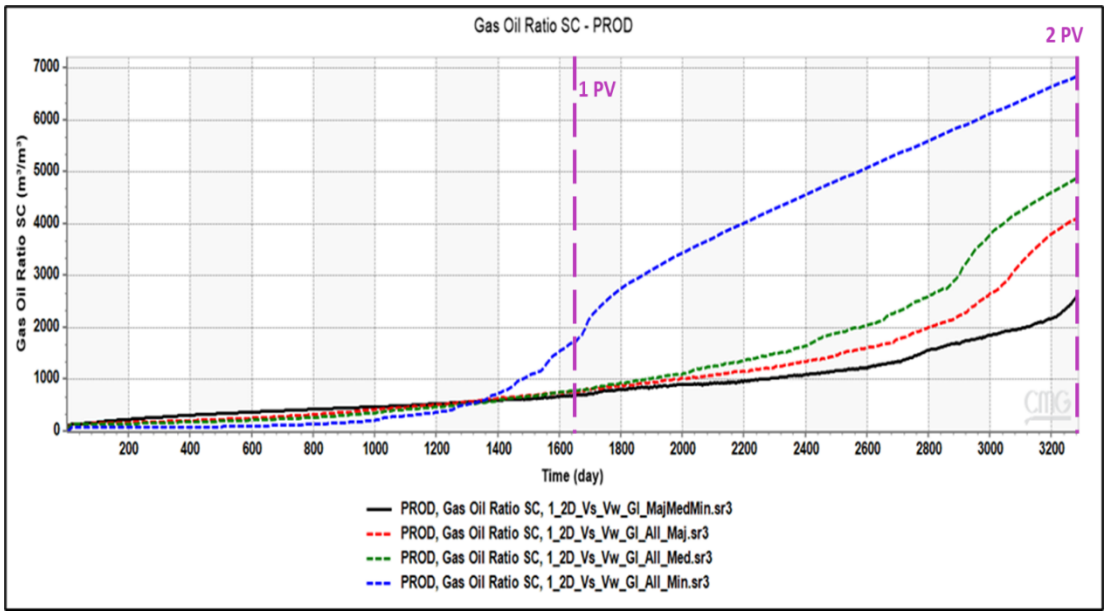

Figure 58: GOR for gas injection process in the first category of fractures networks when all fractures are included in a single set (2D model & Vertical wells)

The differences in oil saturation profile for the homogenized fracture networks are shown in Figure 59.

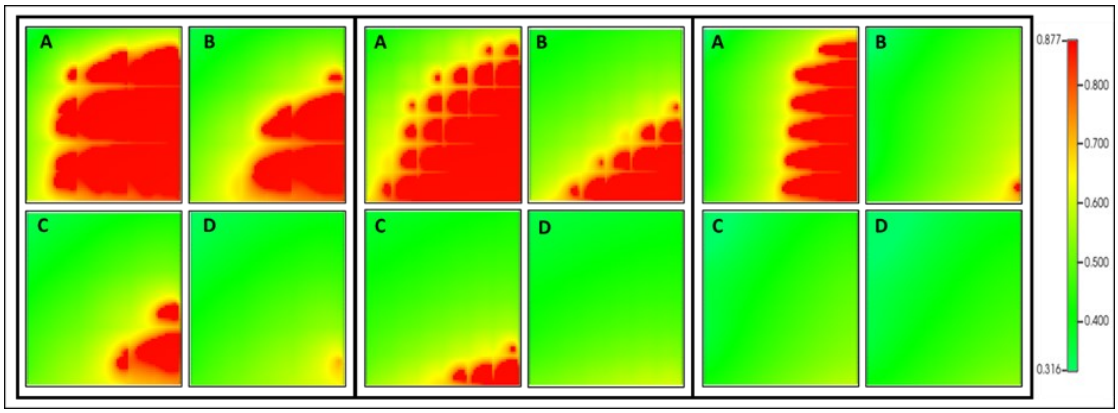

Figure 59: Oil saturation profile (oil in red & gas in green color) for gas injection process in the first category of fractures networks when all fractures are included in a single set (2D model & Vertical wells); left: Major, Medium & Minor fractures network, Middle: all Major fractures networks, right: all Minor fractures networks, at A:0.5 PV, B:1 PV, C:1.5 PV, D:2 PV

In the case of Horizontal wells, similar to the vertical wells, oil recovery was overestimated when all the fractures were homogenized into a single set (Figure 60).

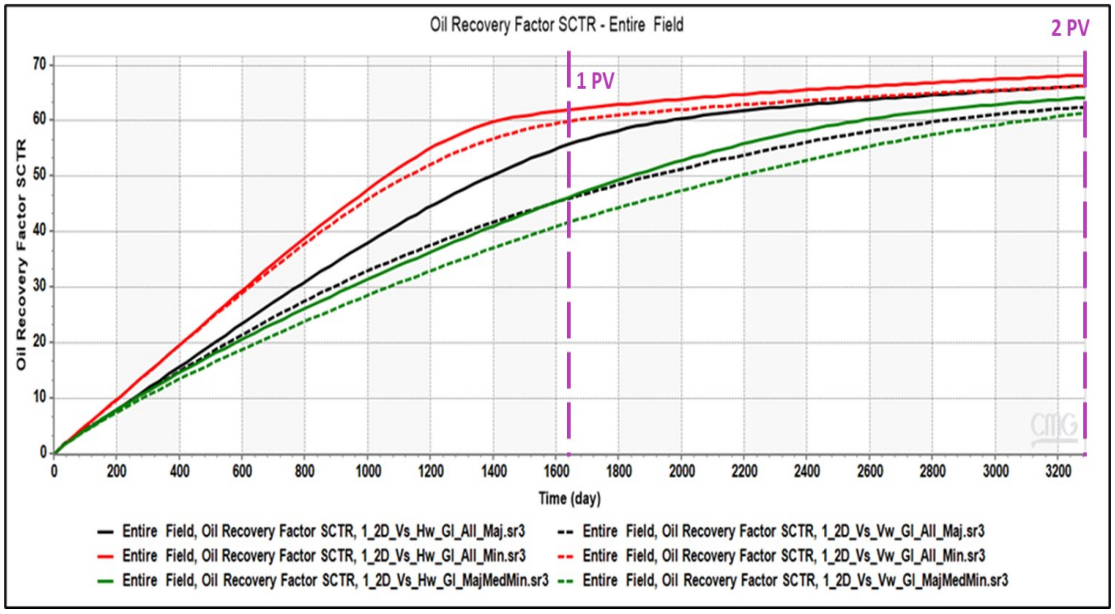

Figure 60: Oil Recovery factor for gas injection process in the first category of fractures networks when all fractures are included in a single set (2D model & Horizontal wells)

As shown in Figure 61, the produced gas volume was overestimated significantly after injecting one pore volume (approximately), while it will be underestimated in the early period.

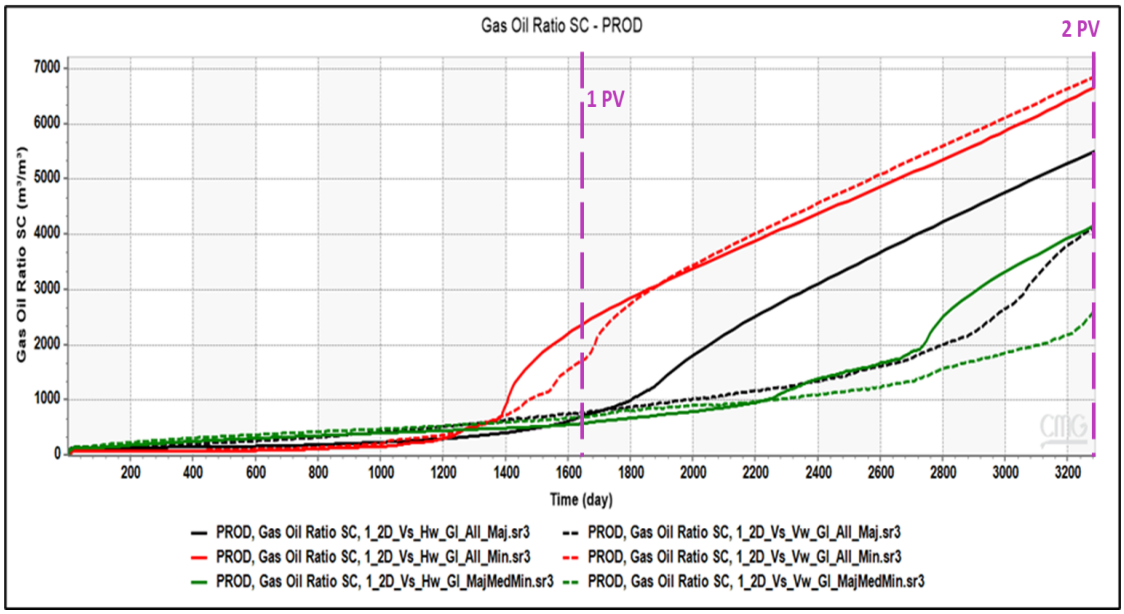

Figure 61: GOR for gas injection process in the first category of fractures networks when all fractures are included in a single set (2D model & Horizontal wells)

Saturation profiles for the Horizontal wells cases are shown in Figure 62. However, the results indicate that homogenization might not be a valid option for simplifying the fracture networks.

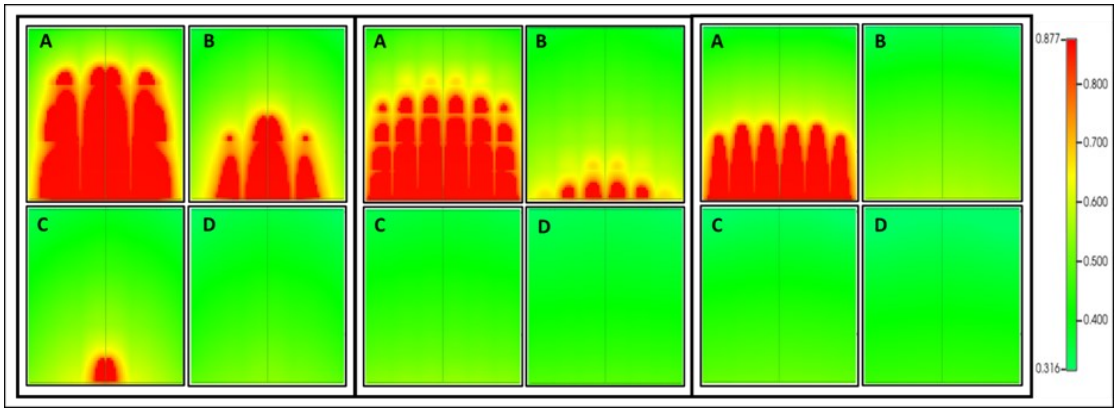

Figure 62: Oil saturation profile (oil in red & gas in green color) for gas injection process in the first category of fractures networks when all fractures are included in a single set (2D model & Horizontal wells); left: Major, Medium & Minor fractures network, Middle: all Major fractures networks, right: all Minor fractures networks, at A:0.5 PV, B:1 PV, C:1.5 PV, D:2 PV

The next tested option excludes the Minor fracture network and considers the Medium fracture network with the same properties as the Major fractures network. Based on this assumption, two additional cases were defined. In the first case, all the fractures were assumed to be Major fractures, while in the other case, all the fractures were assumed to be Medium fractures. In

addition, the option of adjusting the matrix permeability to a pseudo-matrix was also investigated. The pseudo-matrix permeability is introduced to compensate for the effect of the Medium and Minor fracture networks rather than the explicit representation for these fracture types. The matrix permeability is adjusted to be 2 mD which fits the original case when all the fracture networks are included. As shown in Figure 63, the results indicate that the assumption where the Medium fractures network is assumed to have the same properties as the Major fractures shows a good match for the recovery behavior in the original case. Moreover, the case where matrix permeability is adjusted also shows a good match for the recovery behavior.

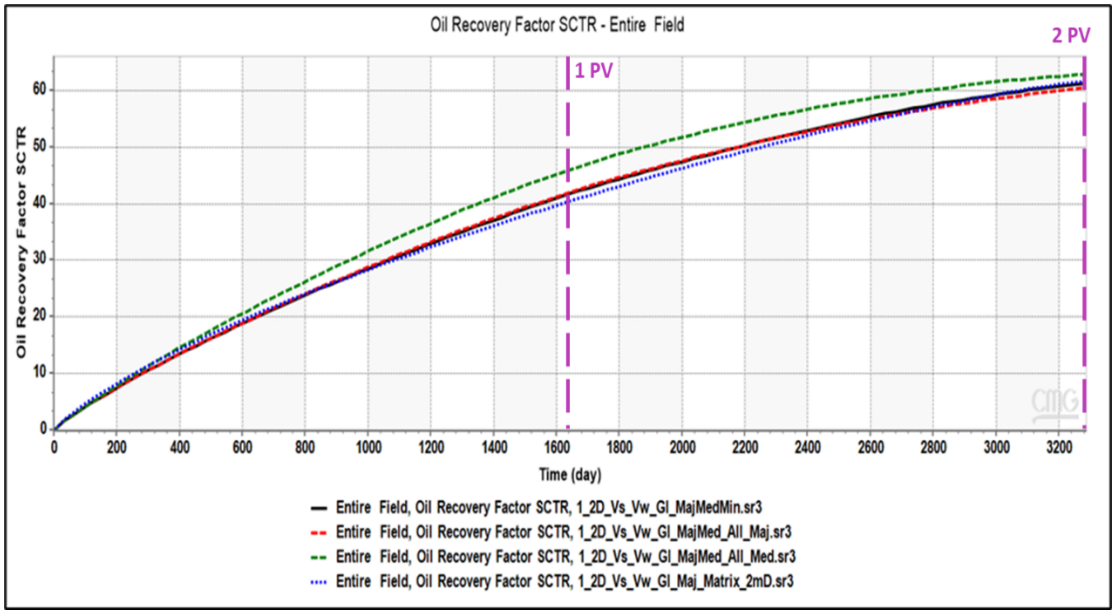

Figure 63: Oil Recovery factor for gas injection process in the first category of fractures networks when a different homogenization option is used (2D model & Vertical wells)

However, the GOR indicates that the case of excluding the Minor fracture type and homogenizing the Medium fracture type into Major fracture properties would result in a better match in comparison to the case of pseudo-matrix. In the pseudo-matrix case, a slight overestimation can still be observed at the early period and before the complete injection of 1 pore volume. After that, the trend is reversed to overestimate the GOR, as shown in Figure 64. General mismatch for the overall behavior can be observed over the injection period.

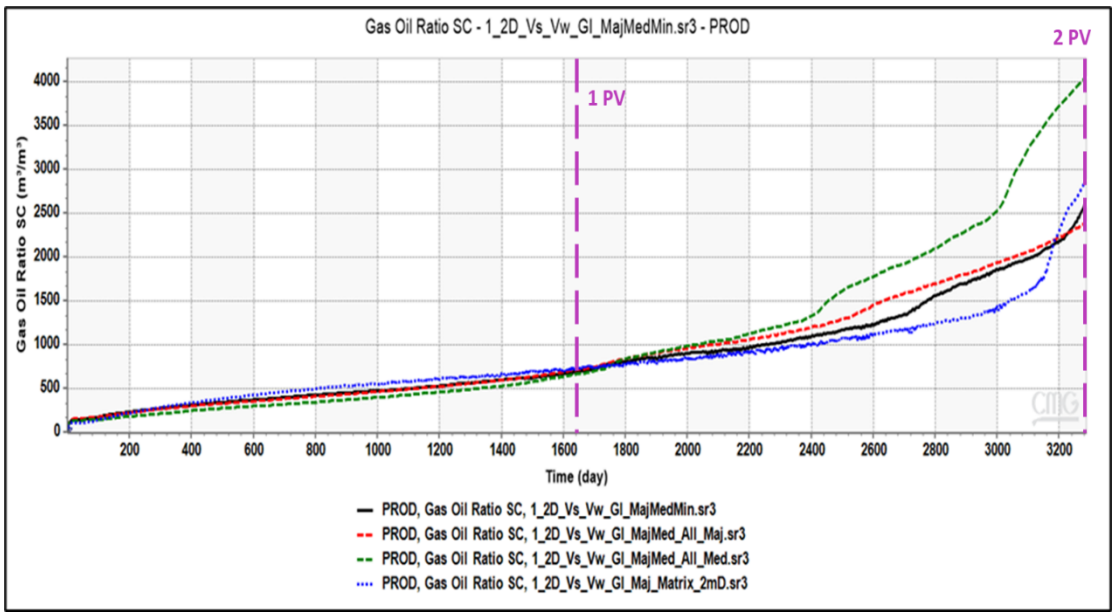

Figure 64: GOR for gas injection process in the first category of fractures networks when a different homogenization option is used (2D model & Vertical wells)

Similar observations were indicated in the extended vertical model. However, the pseudo-matrix option was used with the same value as the standard model. The results have indicated an underestimation of the recovery factor in the medial period between the injection of one pore volume and 1.5 pore volumes, as shown in Figure 65. This observation also supports the previous observation for the impact of non-major fracture networks, where the impact magnitude increases with the increase of the reservoir thickness.

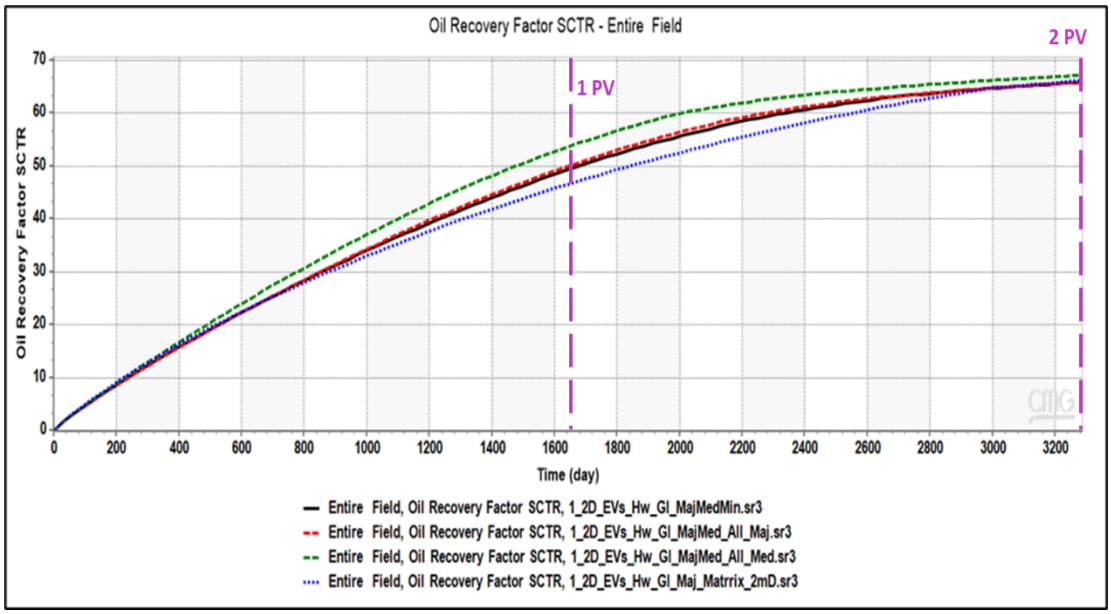

Figure 65: Oil Recovery factor for gas injection process in the first category of fractures networks when a different homogenization option is used (Extended 2D model & Horizontal wells)

Like the recovery factor, the GOR shows a significant mismatch for the overall behavior, especially for the later period after the injection of 1.5 pore volumes, as shown in Figure 66. However, the homogenized case using the Major fractures properties and excluding the Minor fractures shows a better match for the overall behavior and similar observation discussed in the standard model.

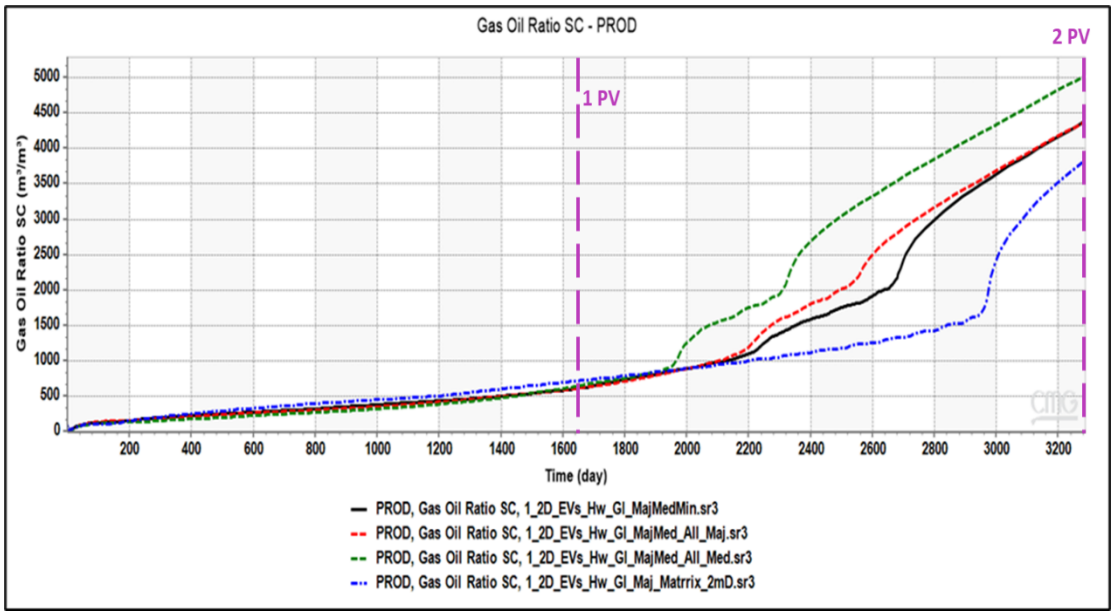

Figure 66: GOR for gas injection process in the first category of fractures networks when a different homogenization option is used (Extended 2D model & Horizontal wells)

After excluding the Minor fractures network, the 3D model indicates that the homogenized fractures network option would slightly underestimate the recovery factor after the complete injection of 0.5 pore volume, as shown in Figure 67. However, this option still demonstrates better results than the pseudo-matrix option.

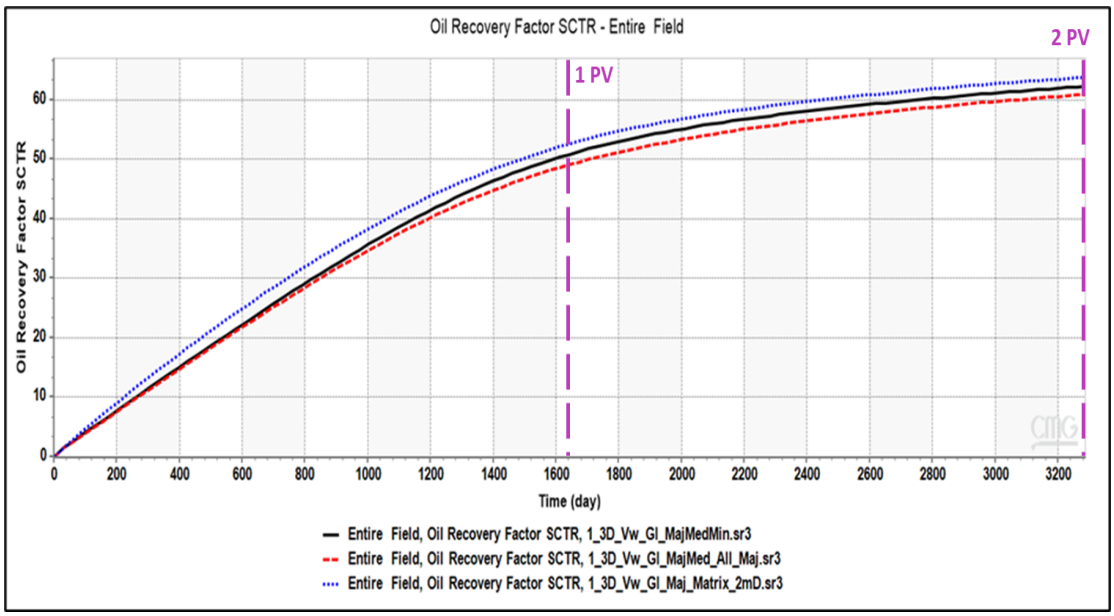

Figure 67: Oil Recovery for gas injection process in the first category of fractures networks when a different homogenization option is used (3D cube model)

The GOR behavior also indicates slight underestimation after the complete injection of 1 pore volume, as shown in Figure 68. This mismatch in the magnitude might be related to the exclusion of the Minor fracture network, indicating that the 2D models have underestimated the effect of the Minor fracture network in the 3D. However, the demonstrated results for the gas injection process indicate that the homogenization option for the fracture networks and excluding the Minor fractures network can provide a good approximation for the early period when less than one pore volume is injected.

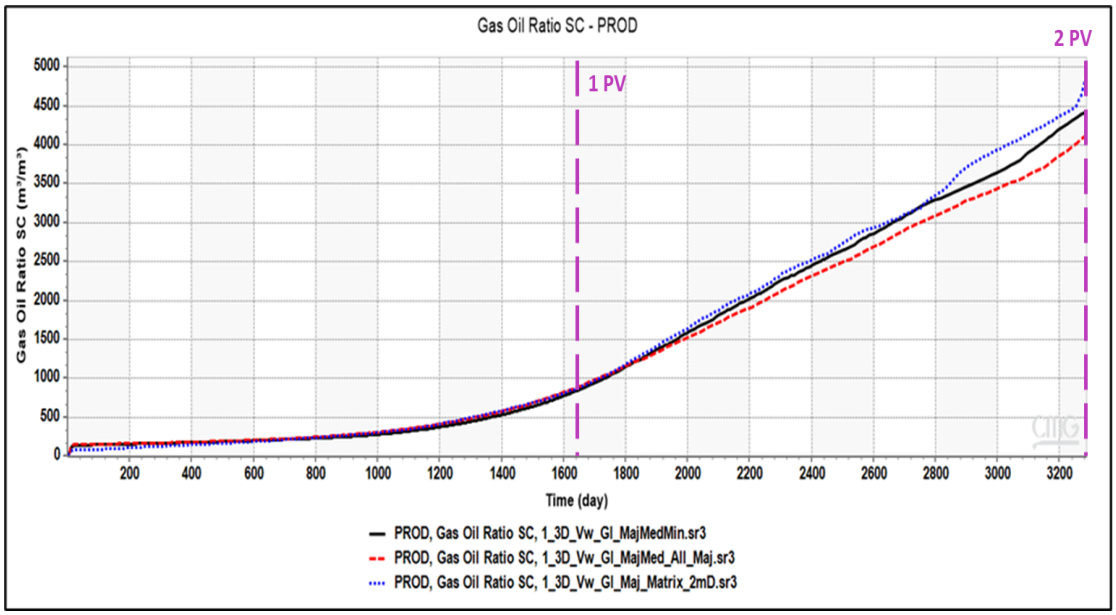

Figure 68: GOR for gas injection process in the first category of fractures networks when a different homogenization option is used (3D cube model)

4.2.2.1.1 Fracture Aperture

Gong & Rossen (2018) have assumed a constant fracture aperture for all the fractures in all the cases to avoid numerical issues. In their study, all the fracture sets in each category have been assumed to have the same major fracture aperture of 2 mm. However, in this study, the impact of this assumption was investigated, and the results as shown in Figure 69.

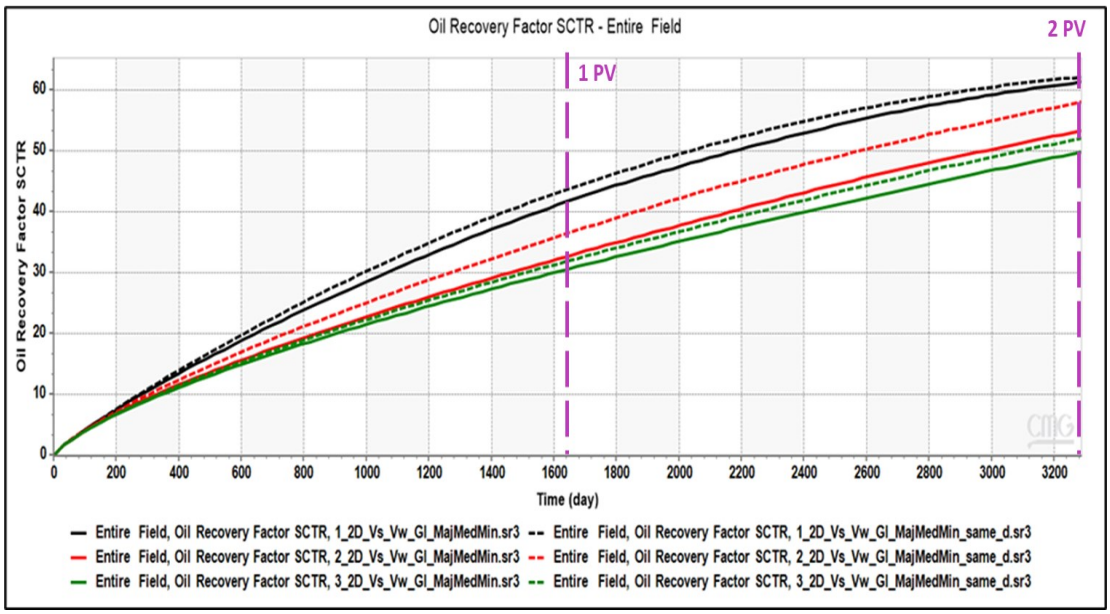

Figure 69: Comparison of oil recovery factor in gas injection process between the first category of fractures networks and when a constant aperture is used (Extended 2D model & Horizontal wells)

Results have indicated that considering a constant fracture aperture rather than changing the fracture aperture with respect to the changes in the permeability of the fracture results in overestimating the recovery factor. Generally, the magnitude in the first and the third fractures categories are fairly similar and result in an overestimation of the recovery factor by 1%. However, the magnitude in the second category is higher and about 5%. This observation is mainly related to the fact that changing fracture aperture also results in changing the fracture volume and fracture capacity while changing the permeability only affects the transmissibility. Similar to the recovery factor, the GOR indicates that the highest difference appears to be in the second category, as shown in Figure 70.

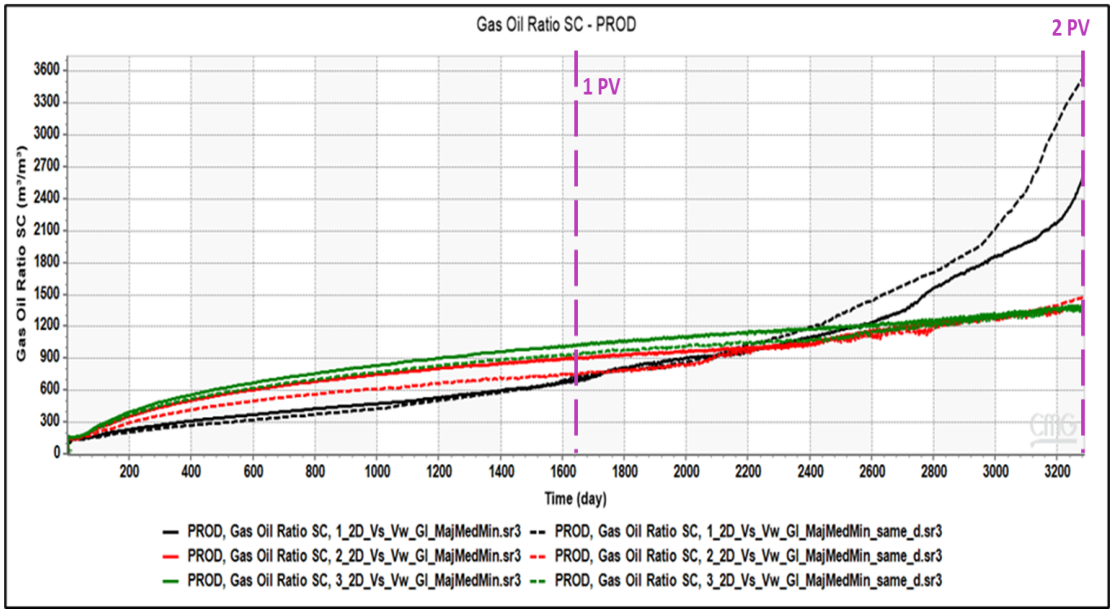

Figure 70: Comparison of GOR in gas injection process between the first category of fractures networks and when a constant aperture is used (Extended 2D model & Horizontal wells)

The comparison of the saturation profile for both cases in the second category indicates that the contribution of the fracture aperture to the fracture transmissibility can be compensated through the change in the fracture permeability. However, the selected constant value for the fracture aperture can blur the effect of liquid bridging and the re-infiltration effect Figure 71. It is also important to highlight that these effects can be spontaneously observed in the embedded discrete fracture models. In contrast, in the dual continuum modeling approach, these effects are mainly subjected to the defined parameters for the shape factor and transfer function in addition to the defined fracture relative permeability and capillary pressure curves.

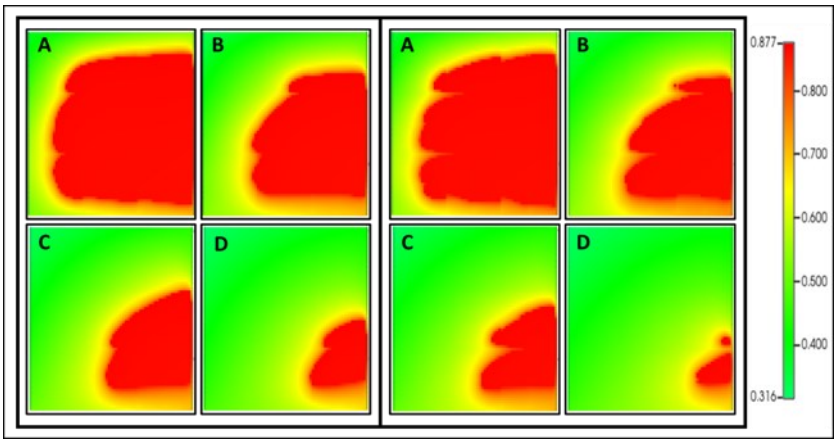

Figure 71: Oil saturation profile (oil in red & gas in green color) for gas injection process in the second category of fractures networks (2D model & Vertical wells) left: Major, Medium & Minor fractures network, right Major, Medium & Minor fractures network with constant fracture aperture, at A:0.5 PV, B:1 PV, C:1.5 PV, D:2 PV

4.2.2.2 Foam-Assisted WAG

Based on the demonstrated results for the gas injection process, the best two options for homogenization were also investigated for the FAWAG process. As shown in Figure 72, both options show a good match for the original case at the early period injection and up to the injection of one pore volume. However, the pseudo-matrix option results in an overestimation of the recovery factor at the later period.

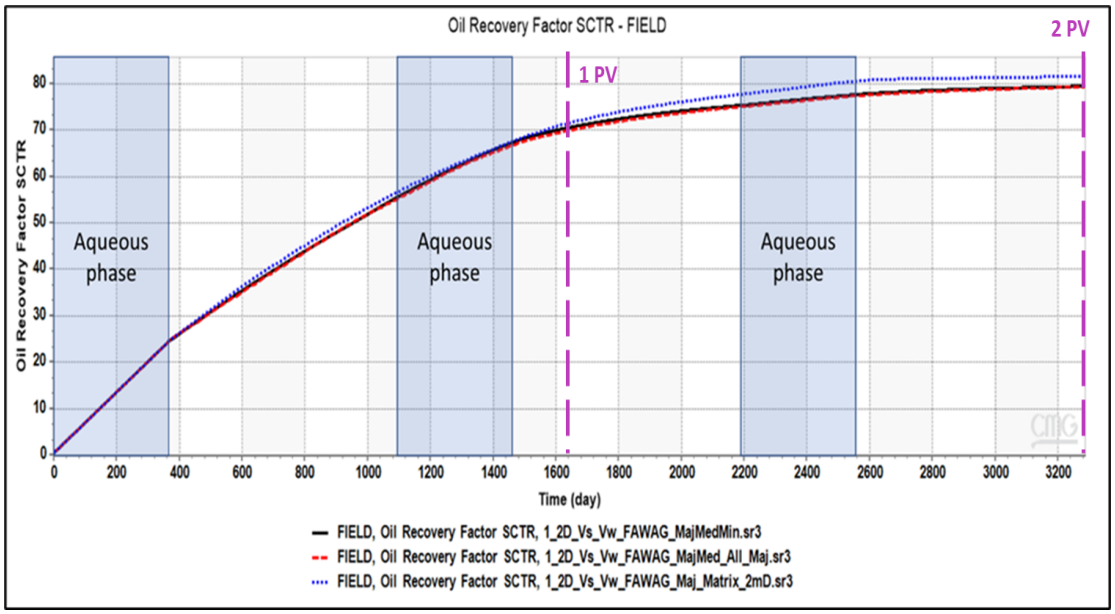

Figure 72: Oil Recovery factor for FAWAG process in the first category of fractures networks when a different homogenization option is used (2D model & Vertical wells)

The GOR behavior, on the other hand, shows a mismatch for the original case in both options, as shown in Figure 73. However, the high GOR for the pseudo-matrix case in the late period hinders the effect in the early period. Therefore, Figure 74 was needed to discuss the early period and injected up to 1.5 pore volumes.

Both homogenization options show a good match for the original case in the early period. However, both cases underestimated the produced gas volume at the start of gas injection in the second cycle. At the end of the second cycle, the original model has a GOR of 3000 m^3/m^3. The GOR for the pseudo-matrix case was about 2130 m^3/m^3, corresponding to a relative error of 29%. The relative error is about 13% for the homogenized fractures option.

In the later period, the pseudo-matrix has a completely different trend and a huge difference in the estimated GOR magnitude.

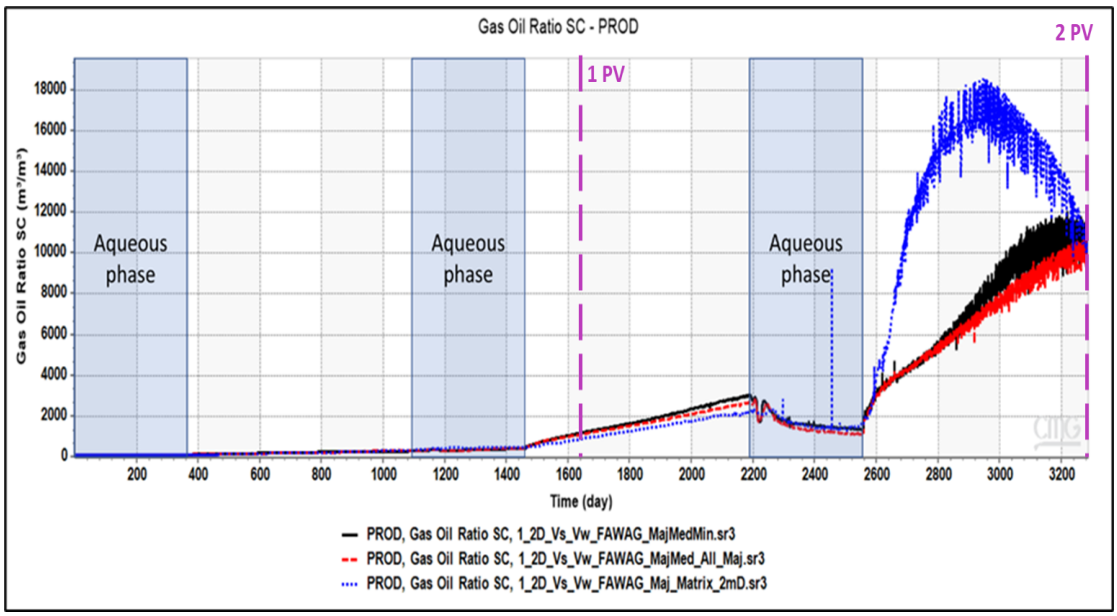

Figure 73: GOR for FAWAG process in the first category of fractures networks when a different homogenization option is used (2D model & Vertical wells) part 1

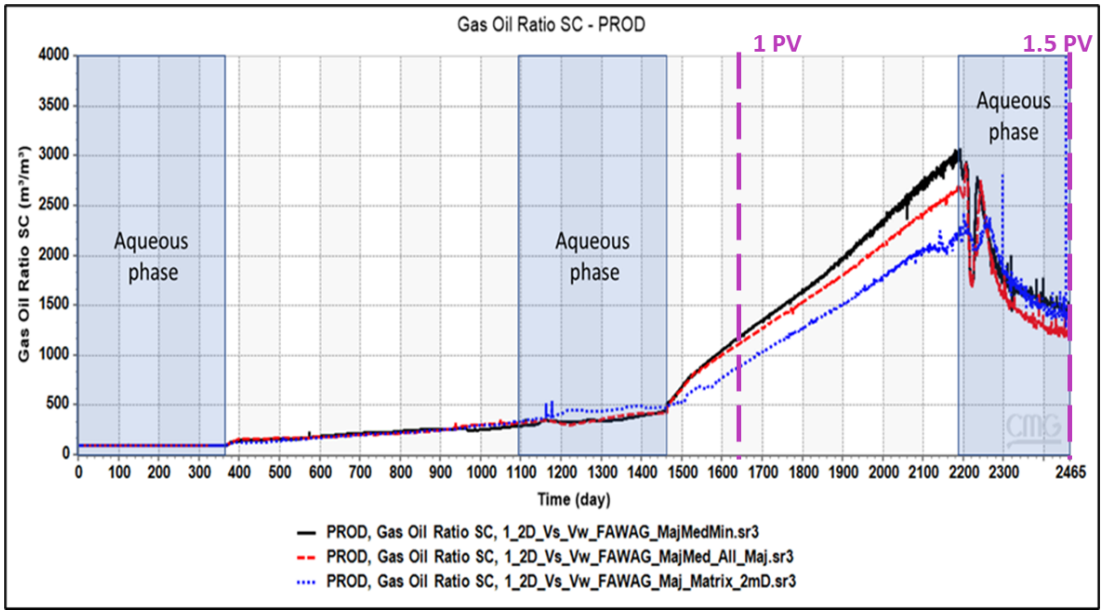

Figure 74: GOR for FAWAG process in the first category of fractures networks when a different homogenization option is used (2D model & Vertical wells) part 2

The water cut behavior also shows a significant mismatch, as shown in Figure 75. The main mismatch starts at the beginning of the second cycle, and the maximum difference can be indicated at the end of the acquis phase injection in this cycle. The homogenized fractures case overestimates the expected water cut by about 8%. The pseudo-matrix case underestimated the water cut by about 14% and continuously underestimated the water cut compared to the original case until the start of gas-phase injection in the second cycle, where it overestimated the water cut.

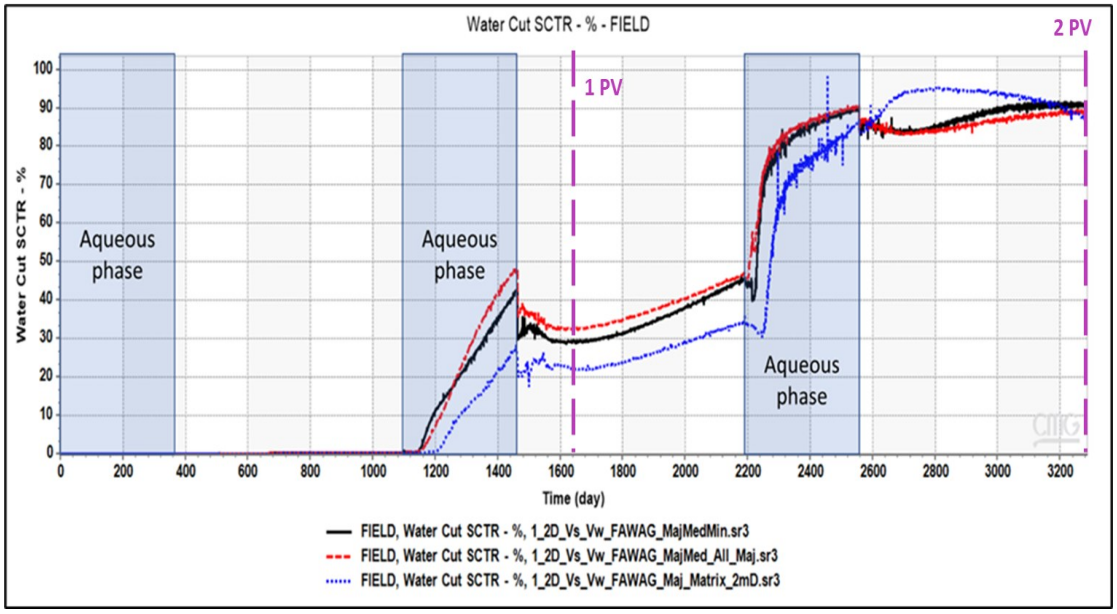

Figure 75: Water cut for FAWAG process in the first category of fractures networks when a different homogenization option is used (2D model & Vertical wells) part 1

Similar to the 2D model, the 3D model shows a good match for the recovery factor in the case of homogenizing the Major and the Medium fractures networks to have the same properties as the Major fractures network. However, a slight difference starts to form after the injection of 0.75 pore volumes to underestimate the recovery factor and continues until the complete injection of 2 pore volumes, as shown in Figure 76.

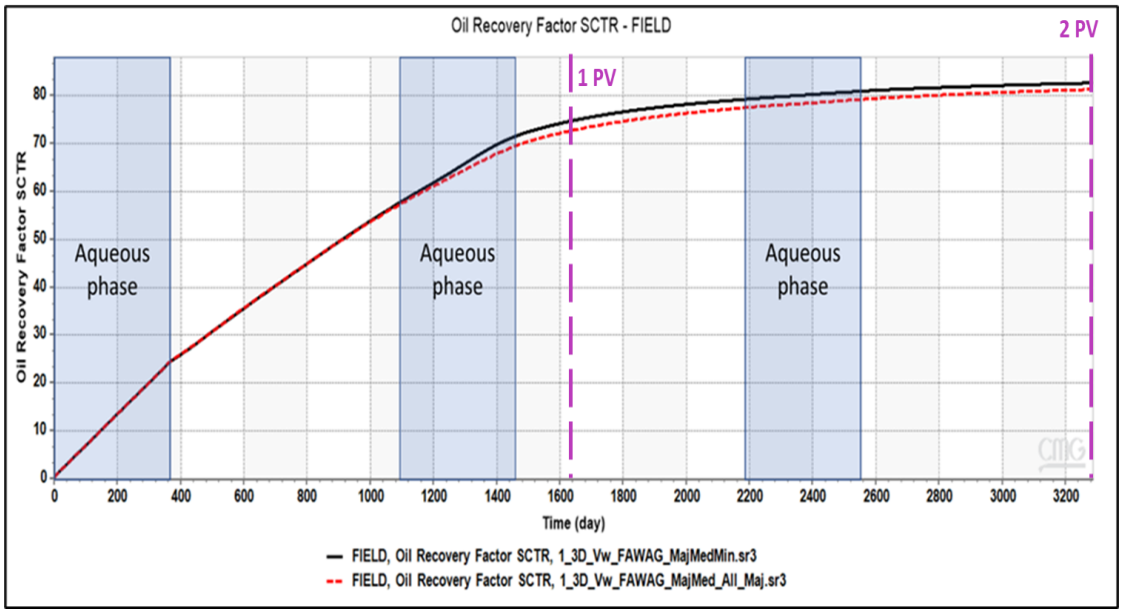

Figure 76: Oil Recovery factor for FAWAG process in the first category of fractures networks when a different homogenization option is used (3D cube model)

The GOR behavior also shows similar trends to the 2D model. However, the underestimation can be observed at the end of the second cycle, 3300 m^3/m^3 in the original model. The

homogenized option indicated a GOR of 3000 m^3/m^3, which corresponds to a relative error of 8%. At the end of the third cycle, the relative error has reached 20%, as shown in Figure 77.

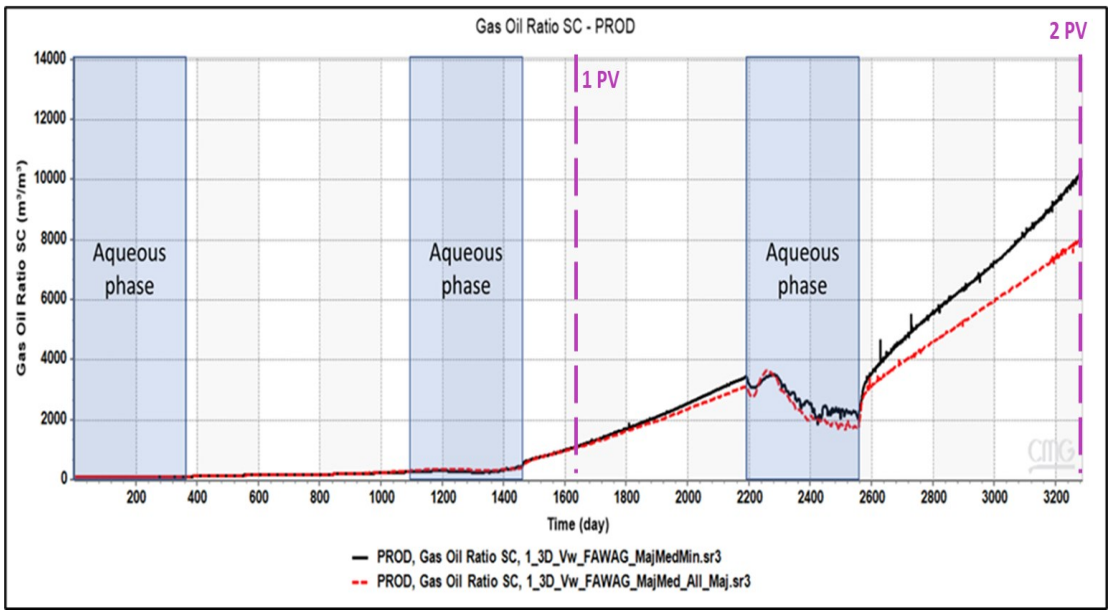

Figure 77: GOR for FAWAG process in the first category of fractures networks when a different homogenization option is used (3D cube model)

As shown in Figure 78, the water cut behavior shows a similar trend to the 2D model to overestimate the produced water volume in the early period and overestimate the water cut at the end of the second cycle of aqueous phase injection by 10%. In contrast to the 2D model, the 3D model demonstrates a change in behavior from overestimation to underestimation for the water cut to reach 9.5%. As discussed in previous sections, these observed differences might be related to the essential difference in the Rn number.

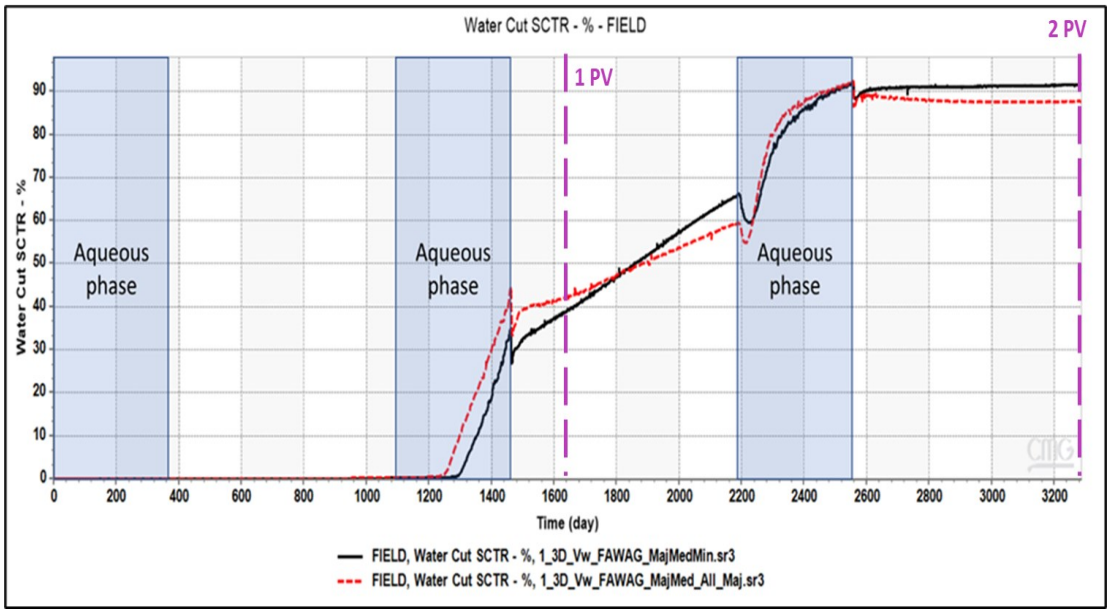

Figure 78: Water cut for FAWAG process in the first category of fractures networks when a different homogenization option is used (3D cube model)

These results indicate that even if objective homogenization techniques were used to simplify the fracture networks, the results suitability of the techniques depends on the recovery process itself. Moreover, the use of hybrid modeling approaches to represent two different fracture sets can be useful to simplify the simulation process for fractured reservoirs and maintain a better accuracy for the estimation of the recovery factor and produced volumes.

The obtained results in this study highlighted the impact of non-major fracture networks on the assessment of the gas-based EOR processes. The impact magnitude for excluding these fracture networks depends on multiple effects that include the recovery process itself and the fluid properties of the reservoir fluids. The use of the defined dimensionless numbers to describe the properties of the fracture networks provides a good description that can be further integrated with force-based dimensionless numbers to evaluate the fractured reservoirs. Moreover, results for the homogenization options indicated that homogenizing the fractures network can provide a good approximation and can be used for the conventional dual continuum approach. However, when the relative error increases above acceptable limits, it can indicate the need to use the hybrid modeling approaches to account for different fracture sets.

Finally, it is important to highlight that the observed spikes in some cases are related to the small grid size used in this model. However, the residual error for material balance calculation was less than 0.5% in all the cases.

Chapter 5

Conclusion

5.1 Summary

Modeling fractured reservoirs have been one of the major challenges in the oil and gas industry in the last decades. The flow behavior in these reservoirs is highly deepening on characteristics of the fractures and matrix blocks. The continuous improvement in the geoscience and detection methods for the fracture networks can significantly improve the understanding of the fracture networks' characteristics. However, the simplification and homogenization process of the fracture networks into a single set of fractures network to use in the conventional dual-porosity and dual-permeability models can underestimate the impact of the fracture networks' recovery process in certain cases.

In this study, a low permeability fractured reservoir with well-connected fracture networks was investigated using the DFN modeling approach provided in the CMG software. Different systematic cases were defined to investigate the impact of including and excluding Medium and Minor fractures networks in addition to the Major fractures network. Dimensionless numbers were used to link the properties of these additional networks to the properties of the major fractures network. The obtained results for the investigated gas-based EOR methods indicated that the magnitude of the impact is process deepening. Generally, the increase in the aperture ratios (Rd and Rd3) decreases the relative importance of considering the additional fracture networks. Moreover, the magnitude of the impact increase with the increase in the reservoir height in the assisted-gravity drainage mode. However, the increase in the major to medium fracture intensity (Rn) decreases the importance of considering the additional fracture networks.

Finally, it is important to highlight that investigating fractured reservoirs on a different scale can be useful for assessing the uncertainty associated with selecting the suitable homogenization technique and modeling approach in the field scale.

5.2 Evaluation

Few studies have discussed the impact of simplifying the fracture networks into a single set of fracture properties to use in the conventional dual-permeability and dual-porosity models. This study has utilized the CMG DFN model to provide insights into the impact of the fracture networks on the gas-based EOR methods. The use of dimensionless numbers can be useful in defining thresholds and performing a quantitative evaluation of the impact of the fracture networks on the recovery. Further studies are needed to compare the results of this study and to investigate the impact on a field scale.

5.3 Future Work

Additional simulation studies are needed to evaluate the effect of Major fracture network properties and their effect on the magnitude of the impact of the Medium and Minor fracture networks on the recovery factor and the estimated produced volumes.

Further experimental studies are needed to observe the impact of fracture networks with different properties on foam generation mechanisms and flow behavior. These results can be further utilized to create a detailed foam model rather than a synthetic and allow the use of population-balance dynamic-texture models, which can provide a more realistic representation of the physical behavior in the FAWAG process or Foam injection process.

Geomechanical models can also be integrated with the flow simulation to investigate the potential changes that can develop over time between the different fracture networks.

Chapter 6

References

Agada, S., Geiger, S., & Doster, F. (2016). Wettability, hysteresis, and fracture–matrix interaction during CO2 EOR and storage in fractured carbonate reservoirs. *International Journal of Greenhouse Gas Control*, *46*, 57–75. https://doi.org/10.1016/j.ijggc.2015.12.035

Aghli, G., Moussavi-Harami, R., & Mohammadian, R. (2020). Reservoir heterogeneity and fracture parameter determination using electrical image logs and petrophysical data (a case study, carbonate Asmari Formation, Zagros Basin, SW Iran). *Petroleum Science*, *17*(1), 51–69. https://doi.org/10.1007/s12182-019-00413-0

Aljuboori, F. A., Lee, J. H., Elraies, K. A., & Stephen, K. D. (2020). Effect of fracture characteristics on history matching in the Qamchuqa reservoir: A case study from Iraq. *Carbonates and Evaporites*, *35*(3), 87. https://doi.org/10.1007/s13146-020-00607-3

Allan, J., & Sun, S. Q. (2003). Controls on Recovery Factor in Fractured Reservoirs: Lessons Learned from 100 Fractured Fields. *SPE Annual Technical Conference and Exhibition*, 18. https://doi.org/10.2118/84590-MS

Bosma, S., Hajibeygi, H., Tene, M., & Tchelepi, H. A. (2017). Multiscale finite volume method for discrete fracture modeling on unstructured grids (MS-DFM). *Journal of Computational Physics*, *351*, 145–164. https://doi.org/10.1016/j.jcp.2017.09.032

Bourbiaux, B. (2010). Fractured Reservoir Simulation: A Challenging and Rewarding Issue. *Oil & Gas Science and Technology – Revue de l'Institut Français Du Pétrole*, *65*(2), 227–238. https://doi.org/10.2516/ogst/2009063

Bratton, T., Canh, D. V., Duc, N. V., Gillespie, P., Hunt, D., Li, B., Marcinew, R., Ray, S., Montaron, B., Nelson, R., Schoderbek, D., & Sonneland, L. (2006). The Nature of Naturally Fractured Reservoirs. *Oilfield Review*, *18*(2), 4–23.

CMG. (2020). *GEM 2020.11 User Guide*. Computer Modelling Group Ltd.

Ghaedi, M., Masihi, M., Heinemann, Z. E., & Ghazanfari, M. H. (2015). History matching of naturally fractured reservoirs based on the recovery curve method. *Journal of Petroleum Science and Engineering*, *126*, 211–221. https://doi.org/10.1016/j.petrol.2014.12.002

Gong, J., & Rossen, W. R. (2017). Modeling flow in naturally fractured reservoirs: Effect of fracture aperture distribution on dominant sub-network for flow. *Petroleum Science*, *14*(1), 138–154. https://doi.org/10.1007/s12182-016-0132-3

Gong, J., & Rossen, W. R. (2018). Characteristic fracture spacing in primary and secondary recovery for naturally fractured reservoirs. *Fuel*, *223*, 470–485. https://doi.org/10.1016/j.fuel.2018.02.046

Guerriero, V., Mazzoli, S., Iannace, A., Vitale, S., Carravetta, A., & Strauss, C. (2013). A permeability model for naturally fractured carbonate reservoirs. *Marine and Petroleum Geology*, *40*, 115–134. https://doi.org/10.1016/j.marpetgeo.2012.11.002

Harimi, B., Masihi, M., & Ghazanfari, M. H. (2019). Characterization of Liquid Bridge in Gas/Oil Gravity Drainage in Fractured Reservoirs. *Iranian Journal of Oil & Gas Science and Technology*, *8*(2), 73–91.

Haugen, A., Fernø, M. A., & Graue, A. (2012). Experimental Study of Foam Flow in Fractured Oil-Wet Limestone for Enhanced Oil Recovery. *SPE Reservoir Evaluation & Engineering*, *15*, 218–228. https://doi.org/10.2118/129763-PA

Heeremans, J. C., Esmaiel, T. E., & Van Kruijsdijk, C. P. J. W. (2006). *Feasibility Study of WAG Injection in Naturally Fractured Reservoirs*. SPE-100034-MS. https://doi.org/10.2118/100034-MS

Kharrat, R., Zallaghi, M., & Ott, H. (2021). Performance Quantification of Enhanced Oil Recovery Methods in Fractured Reservoirs. *Energies*, *14*(16), 4739. https://doi.org/10.3390/en14164739

Lei, Q., Latham, J.-P., & Tsang, C.-F. (2017). The use of discrete fracture networks for modeling coupled geomechanical and hydrological behavior of fractured rocks. *Computers and Geotechnics*, *85*, 151–176. https://doi.org/10.1016/j.compgeo.2016.12.024

Luo, H., & Mohanty, K. K. (2021). Modeling Near-Miscible Gas Foam Injection in Fractured Tight Rocks and Its Challenges. *Energies*, *14*(7), 1998. https://doi.org/10.3390/en14071998

Ma, K., Ren, G., Mateen, K., Morel, D., & Cordelier, P. (2015). Modeling Techniques for Foam Flow in Porous Media. *SPE Journal*, *20*(03), 453–470. https://doi.org/10.2118/169104-PA

Mogensen, K., & Masalmeh, S. (2020). A review of EOR techniques for carbonate reservoirs in challenging geological settings. *Journal of Petroleum Science and Engineering*, *195*, 107889. https://doi.org/10.1016/j.petrol.2020.107889

Silva, R. R., & Maini, B. . (2016). Evaluation of Gas-Assisted Gravity Drainage GAGD in Naturally Fractured Reservoirs NFR. *All Days*, SPE-179585-MS. https://doi.org/10.2118/179585-MS

Talluru, G., & WuMewbourne, X. (2017). Using Data Analytics on Dimensionless Numbers to Predict the Ultimate Recovery Factors for Different Drive Mechanisms of Gulf of Mexico Oil Fields. *Day 3 Wed, October 11, 2017*, D031S030R008. https://doi.org/10.2118/187269-MS

Tohidi Hosseini, S. M., Esfahani, S., Hashemi Doulatabadi, M., Hemmati Sarapardeh, A., & Mohammadi, A. H. (2017). On the evaluation of steam-assisted gravity drainage in naturally fractured oil reservoirs. *Petroleum*, *3*(2), 273–279. https://doi.org/10.1016/j.petlm.2016.01.003

Ukar, E., Laubach, S. E., & Hooker, J. N. (2019). Outcrops as guides to subsurface natural fractures: Example from the Nikanassin Formation tight-gas sandstone, Grande Cache, Alberta foothills, Canada. *Marine and Petroleum Geology*, *103*, 255–275. https://doi.org/10.1016/j.marpetgeo.2019.01.039

Wenli, Y., Sharifzadeh, M., Yang, Z., Xu, G., & Fang, Z. (2019). Assessment of fracture characteristics controlling fluid flow performance in discrete fracture networks (DFN). *Journal of Petroleum Science and Engineering*, *178*, 1104–1111. https://doi.org/10.1016/j.petrol.2019.04.011

Wong, D. L. Y., Doster, F., Geiger, S., Francot, E., & Gouth, F. (2020). Fluid Flow Characterization Framework for Naturally Fractured Reservoirs Using Small-Scale Fully Explicit Models. *Transport in Porous Media*, *134*(2), 399–434. https://doi.org/10.1007/s11242-020-01451-8

Xu, Y., & Sepehrnoori, K. (2019). Development of an Embedded Discrete Fracture Model for Field-Scale Reservoir Simulation With Complex Corner-Point Grids. *SPE Journal*, *24*(04), 1552–1575. https://doi.org/10.2118/195572-PA

Xu, Z.-X., Li, S.-Y., Li, B.-F., Chen, D.-Q., Liu, Z.-Y., & Li, Z.-M. (2020). A review of development methods and EOR technologies for carbonate reservoirs. *Petroleum Science*, *17*(4), 990–1013. https://doi.org/10.1007/s12182-020-00467-5

Yan, X., Huang, Z., Yao, J., Li, Y., & Fan, D. (2016). An efficient embedded discrete fracture model based on mimetic finite difference method. *Journal of Petroleum Science and Engineering*, *145*, 11–21. https://doi.org/10.1016/j.petrol.2016.03.013

Zhou, D., Fayers, F. J., & Orr, F. M. (1997). Scaling of Multiphase Flow in Simple Heterogeneous Porous Media. *SPE Reservoir Engineering*, *12*(03), 173–178. https://doi.org/10.2118/27833-PA.